Biochemical And Biotechnological Approaches As Basis For Structure Determination Of Pigment-Protein Complexes Of Oxygenic Photosynthesis

Dissertation
zur Erlangung des Doktorgrades
der Naturwissenschaften

vorgelegt beim Fachbereich Biowissenschaften
der Johann Wolfgang Goethe – Universität
in Frankfurt am Main

von
Holger Fey
aus Pirmasens

Frankfurt am Main 2006
(D 30)

vom Fachbereich ……...der

Johann Wolfgang Goethe – Universität als Dissertation angenommen.

Dekan: ……

Gutachter: …..……

Datum der Disputation: .....……

"I may not have gone where I intended to go,
but I think I have ended up where I needed to be."

Douglas Adams

Contents

Abbreviations iv
Figure index v
Table index vi

I. Introduction 1

1. Photosynthesis 1

2. Light-harvesting and energy transfer 7

3. Structure and function of photosystem II 11

4. Aims of this work 15

II. Materials and Methods 17

1. Materials 17
1.1 Biological material 17
1.2 Plasmid DNA and primers 18
1.3 Restriction enzymes 19

2. Methods 20
2.1 Plasmid DNA preparation 20
2.2 Mutagenesis through altered primers in PCR 21
2.3 Restriction of DNA 22
2.4 Agarose gel electrophoresis and gel extraction of DNA bands 23
2.5 Polyacrylamide gel electrophoresis for small DNA fragments 24
2.6 Ligation of DNA 25
2.7 Transformation of *Escherichia coli* 25
2.8 Transformation and shoot regeneration of *Nicotiana tabacum* 27
2.9 Growth and culture of tobacco plants 31
2.10 Thylakoid preparation 31
2.11 Photosystem II preparation by solubilisation and centrifugation 33
2.12 Photosystem II preparation by affinity chromatography 33
2.13 Chlorophyll determination (Chl *a* + Chl *b*) 35
2.14 Absorption spectroscopy 35
2.15 Polyacrylamide gel electrophoresis of proteins 35
2.16 Western blot 37
2.17 Oxygen evolution 38
2.18 Pulse amplitude modulated fluorescence measurement (PAM) 38
2.19 Two-dimensional crystallisation of photosystem II 39
2.20 Electron microscopy and sample preparation 39
2.21 FCP preparation from *Cyclotella meneghiniana* 40
2.22 Chlorophyll determination in 90% acetone (Chl *a* + Chl *c*) 41
2.23 Pigment determination by High Performance Liquid Chromatography 42

III. Results 43

1. Transformation of Nicotiana tabacum 43
1.1 Vector preparation (pbKS+SacI$^-$) 44
1.2 Cloning *psbE* (pbKS+SacI$^-$psbE) 46
1.3 Inserting His-tags (pbKS+SacI$^-$psbE-His$_{6/10}$) 47
1.4 Inserting the resistance cassette (pbKS+SacI$^-$psbE-His$_{6/10}$-aadA) 49
1.5 Biolistic transformation of tobacco chloroplasts 50

2. Characterisation of transgenic tobacco 52
2.1 Chlorophyll content of tobacco leafs 52
2.2 Oxygen evolution of tobacco thylakoids 53
2.3 Pulse-amplitude modulated (PAM) fluorometry 54

3. Preparation of photosystem II 55
3.1 Preparation of photosystem II from different tobacco strains 55
3.2 His$_6$-tag facilitated photosystem II preparation 56
3.3 His$_{10}$-tag facilitated photosystem II preparation 58
3.4 Wildtype control photosystem II preparation 59
3.5 Protein composition of different column fractions 60
3.6 Two-dimensional crystallisation of photosystem II 63

4. Characterisation of fucoxanthin-chlorophyll-proteins 64

IV. Discussion 67

1. Photosystem II 67

2. Energy transfer in fucoxanthin-chlorophyll-proteins 74

3. Outlook 79

V. Summary 81

VI. Zusammenfassung 85

VII. References 91

VIII. Appendix 101

1. Equipment and chemicals 101
1.1 Equipment 101
1.2 Chemicals 102

2. Sequences 106
2.1 pbKS+SacI$^-$psbE-His$_6$NC (EH1) 107
2.2 pbKS+SacI$^-$psbE-His$_{10}$NC (EH2) 108
2.3 pbKS+SacI$^-$psbE-His$_6$C (EH3) 109
2.4 pbKS+SacI$^-$psbE-His$_{10}$C (EH4) 110

3. HPLC parameters 111
3.1 HPLC retention times 111
3.2 HPLC calibration factors and calibration limits 111
3.3 Spectral data of FCP pigments 112
3.4 Spectra of FCP pigments 112

Publications 113

Lebenslauf (Curriculum vitae) 115

Acknowledgements 117

Abbreviations

2D	two-dimensional
3D	three-dimensional
AA	acrylamide
aadA	spectinomycin & streptomycin resistance cassette
ADP	adenosin-diphosphate
ATP	adenosin-triphosphate
BA	bis-acrylamide
BBY	Grana thylakoids prepared according to the protocol of Berthold *et al.* (1981)
BChl	bacteriochlorophyll
BPhe	bacteriopheophytin
BSA	bovine serum albumin
CAB	chlorophyll *a*/*b* binding protein
Car	carotenoid(s)
Chl	chlorophyll
cmc	critical micellar concentration
CP24	minor light-harvesting complex (Lhcb6)
CP26	minor light-harvesting complex (Lhcb5)
CP29	minor light-harvesting complex (Lhcb4)
DCBQ	2,6-dichloro-p-benzoquinone
DCMU	dichlorphenyl-dimethylurea
DDM	β-dodecylmaltoside
Ddx	diadinoxanthin
DNA	desoxy-ribonucleic acid
Dtx	diatoxanthin
ε	Extinction coefficient
EPR	electron paramagnetic resonance (spectroscopy)
eV	electron Volt
FCP	fucoxanthin-chlorophyll-protein
FFT	fast Fourier transformation
fs	femtosecond
FT	flow through
Fx	fucoxanthin
$His_{6/10}C$	His-tag with cleavage site
$His_{6/10}NC$	His-tag without cleavage site
HTG	n-heptyl-β-D-thioglucoside
ICT	intra-molecular charge transfer
LB	Luria-Bertani (medium)
LH1	purple bacteria light-harvesting complex 1
LH2	purple bacteria light-harvesting complex 2
LHCIIb	major light-harvesting complex II
MALDI TOF	matrix assisted linear desorption ionisation time of flight (mass spectrometry)
na	not available
NADP	nicotinamid-adenosin-dinucleotide-phosphate
OEC	oxygen evolving complex
PAGE	polyacrylamide gel electrophoresis
PAM	pulse amplitude modulated
pbKS+	pBluescript II KS+ (Stratagene)
PCP	peridinin-chlorophyll *a*-protein
PCR	polymerase chain reaction
Phe	pheophytin
PMF	proton motive force
ps	picosecond
PSI	photosystem I
PSII	photosystem II
RC	reaction centre
S_0	ground state
S_1	singlet excited state 1
S_2	singlet excited state 2
T	triplet state
WOC	water oxidising complex
WT	wildtype

Figure index

Fig. I.1:	Schematic overview of chloroplast built-up	2
Fig. I.2:	Cofactors and electron transport pathway of the *Rhodopseudomonas viridis* (purple bacteria) reaction centre	4
Fig. I.3:	Electron transport chains in photosynthetic organisms	5
Fig. I.4:	The absorption spectra of various photosynthetic pigments.	7
Fig. I.5:	Top view of the modelled structure of the LH1-RC complex of *Rhodobacter sphaeroides*	8
Fig. I.6:	Cartoon of the structure and subunit composition of PSII. (A) Higher plants and green algae. (B) Phycobilisome-containing cyanobacteria	9
Fig. I.7:	LHCIIb monomer as viewed from the side	10
Fig. I.8:	Structural model of the intrinsic protein subunits within the PSII supercomplex	12
Fig. I.9:	Overview of the helix organisation in the PSII core dimer of (a) higher plants and (b) Cyanobacteria	13
Fig. III.1:	Schematic overview of the plasmid DNA used for transformation	44
Fig. III.2:	Restriction analyses of pbKS+SacI$^-$	46
Fig. III.3:	Restriction analyses of pbKS+SacI$^-$psbE (α1)	47
Fig. III.4:	Restriction analyses of pbKS+SacI$^-$psbE-His$_6$NC and -His$_{10}$NC	49
Fig. III.5:	Restriction analyses of different EH1a and EH2a clones to check aadA orientation	50
Fig. III.6:	Regenerated tobacco plants under cell culture conditions on antibiotic-containing medium	50
Fig. III.7:	PAGE of PCR fragments to confirm His-tags in F1 generations of tobacco plants	51
Fig. III.8:	Transgenic (EH2a/34) and WT tobacco plants	52
Fig. III.9:	Oxygen evolution rates of wildtype and mutant (EH2a/34) tobacco thylakoids measured at different light intensities	53
Fig. III.10:	(a) Photochemical and (b) non-photochemical quenching of wildtype and transgenic (EH2a/34) tobacco thylakoids measured at different light intensities	55
Fig. III.11:	Elution profiles of a tobacco strain EH1a/13 (His$_6$) Ni-NTA column PSII preparation	56
Fig. III.12:	Absorption spectra of different Ni-NTA column fractions from a EH1a/13 (His$_6$) PSII preparation	57
Fig. III.13:	Elution profiles of a tobacco strain EH2a/34 (His$_{10}$) Ni-NTA column PSII preparation	58
Fig. III.14:	Absorption spectra of different Ni-NTA column fractions from a EH2a/34 (His$_{10}$) PSII preparation	58
Fig. III.15:	Elution profiles of a wildtype tobacco Ni-NTA column PSII preparation	59
Fig. III.16:	Absorption spectra of different Ni-NTA column fractions from a wildtype tobacco PSII preparation	60
Fig. III.17:	SDS-PAGE of Ni-NTA column fractions of an EH2a/34 PSII preparation and a WT control preparation	60
Fig. III.18:	SDS-PAGE of Ni-NTA column fractions of an EH1a/13 PSII preparation and a WT control preparation	61
Fig. III.19:	Western blot of a SDS-PAGE (Fig. III.18) of Ni-NTA column fractions of a EH1a/13 PSII preparation and a WT control preparation, treated with an antibody against D1	62

Fig. III.20: Overlay of Western blot (anti-D1) and SDS-PAGE of Ni-NTA column fractions of an EH1a/13 (His_6) PSII preparation and a WT control preparation 62
Fig. III.21: (a) Electron micrograph of a RC-CP47 2D crystal after negative staining (53 000x magnification); (b) Fast Fourier Transformation of the electron micrograph 64

Fig. IV.1: View of the PSII dimer perpendicular to the membrane normal 68
Fig. IV.2: The compartmental scheme that was used to model the energy transfer network in FCP 77
Fig. IV.3: Hypothetical FCP structure model 78

Fig. VIII.1: Normalised spectra of FCP pigments in organic solvents 112

Table index

Tab. I.1: *psb* genes and gene products 14

Tab. III.1: Chlorophyll content of wildtype and transgenic tobacco leafs 52
Tab. III.2: Salt conditions during 2D crystallisation of spinach RC-CP47 complexes 63
Tab. III.3: Pigment-pigment stoichiometries of sucrose gradient bands of solubilised *C. meneghiniana* thylakoids normalised to 1 Chl *a* molecule 65
Tab. III.4: Lifetimes and the energy transfer efficiencies determined by target analysis 66

Tab. IV.1: Overview of LHC pigment stoichiometries 75

Tab. VIII.1: HPLC retention times of FCP pigments in minutes 111
Tab. VIII.2: HPLC calibration factors 111
Tab. VIII.3: HPLC calibration limits 111
Tab. VIII.4: Extinction coefficients of pigments in the respective solvent, which were used for HPLC calibration 112

I. Introduction

1. Photosynthesis

The process, in which light energy is converted to chemical energy by plants, algae and certain bacteria, is called photosynthesis, which is the main source of energy for life in earth's biosphere. Before the accumulation of oxygen began around 3.5 billion years ago, photosynthesis was limited to anoxygenic bacteria, which used inorganic (e.g. H_2S, Fe^{2+}) or organic compounds as electron and proton donors to synthesise reduced carbohydrates out of carbon dioxide. A major step in evolution occurred when cyanobacteria started to utilise water as their primary electron donor and molecular oxygen was released as a by-product. The net reaction of oxygenic photosynthesis can be summarised as:

$$6\ CO_2 + 12\ H_2O \xrightarrow{h\nu} C_6H_{12}O_6 + 6\ O_2 + 6\ H_20 \qquad \Delta G^{0'} = 2872\ kJ/mol$$

Today, cyanobacteria are classified as the most primordial organisms capable of oxygenic photosynthesis. So far *Gloebacter violaceus* PCC 7421, a primal member of the order of cyanobacteria, was found to be the only cyanobacterium whose photosynthesis apparatus is not organised in a thylakoid membrane, but in the cytoplasma membrane instead (Nakamura *et al.*, 2003; Rivas *et al.*, 2004). In higher plants and algae the components of the photosynthetic apparatus are located in the thylakoid membranes of chloroplasts (Fig. I.1). Chloroplasts are cellular organelles with limited genetic independence, which contain, among other components, soluble proteins for the enzymatic reactions of CO_2 fixation (Calvin Cycle), replication and gene expression in the stroma. According to the endosymbiont theory, the chloroplasts of higher plants and algae are evolutionary related to cyanobacteria that have been engulfed by a host cell and domesticated to form a symbiotic life form. It is assumed that chloroplasts are of monophyletic origin (van den Hoek *et al.*, 1993), a finding which has been confirmed by 16 S-rRNA and 18 S-rRNA analyses. The primary

endosymbiosis event is considered to go back to a member of the glaucophytes that acquired a cyanobacterium by phagocytosis. In the course of evolution the endosymbiont was transformed and the rhodophytes (red algae) and chlorophytes (green algae) developed. Apart from the glaucophytes, rhodophytes are the only eukaryotic organisms employing phycobilisomes for light-harvesting, which are otherwise typical components of cyanobacteria. The event of a subsequent round of endosymbiosis, in which a red or green alga was engulfed and retained by a eukaryotic host, is defined as secondary endosymbiosis. The resulting plastids classically have three or four envelope membranes (McFadden, 2001). Plastids derived by secondary endosymbiosis are a common trait of eukaryotic phytoplankton, such as dinoflagellates, coccolithophores and diatoms (Falkowski *et al.*, 2004).

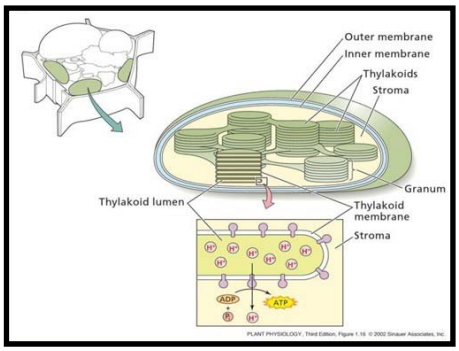

Fig. I.1: Schematic overview of chloroplast organisation (Taiz & Zeiger, 2002)

In principle, photosynthesis can be divided into light reactions and dark reactions. The light reactions are a sequence of reactions that lead to the formation of energy equivalents and reducing equivalents, which are carried out by membrane integral protein complexes in the thylakoid membrane. The most important complexes are photosystem I, photosystem II, the cytochrome b_6/f complex and the ATP-synthase complex. Thylakoids are flat membrane vesicles, which form structurally distinguishable areas in the chloroplasts of higher plants. A distinction can be drawn between areas of stacked membranes (grana thylakoids) and un-stacked membranes (stroma thylakoids). However, at large the thylakoids of a chloroplast form one closed membrane system with a continuous internal compartment, the thylakoid lumen (Schönknecht *et al.*, 1990).

In the catalytic reaction centres of the photosystems, the absorption of light leads to a primary separation of charges and a sequential release of electrons, which are then transported along a chain of cofactors to specific acceptors (Buchanan *et al.*, 2000). According to their terminal electron acceptors, photosystems can be divided into two groups: type I and type II. If electrons are ultimately transported to an iron sulphur cluster, the reaction centre is classified as type I, whereas type II reaction centres use quinones as electron acceptors (Heathcote, 2001). Anoxygenic photosynthetic bacteria have only one reaction centre, whereas cyanobacteria, red algae, green algae and higher plants employ two photosystems, with both types of reaction centres present. Two sequential photosystems are necessary to bridge the gap in redoxpotential between water and $NADPH+H^+$. Photosystem I of plants, algae and cyanobacteria is a type I reaction centre and other type I reaction centres are found in green sulphur bacteria and heliobacteria. The splitting of water into molecular oxygen and protons is carried out by photosystem II, a reaction centre of type II.

Both types of photosystems absorb light radiation and use this energy to transport electrons along a sequence of cofactors across the photosynthetic membrane. In higher plants, these electrons are used to produce reducing equivalents in the form of $NADPH+H^+$ and to transport protons across the thylakoid membrane, in order to form a pH gradient, which in turn provides the driving force (*proton motive force*, PMF) for the formation of ATP out of ADP and inorganic phosphate P_i. In the consecutive dark reactions, ATP and $NADPH+H^+$ are needed to fuel the biochemical reactions, which convert CO_2 into carbohydrates (Mitchell, 1976).

The first structure of a photosynthetic reaction centre was solved by recording X-ray diffraction patterns of 3D crystals of the type II reaction centre of *Rhodopseudomonas viridis*, a purple bacterium (Deisenhofer *et al.*, 1985). In purple bacteria, three major protein subunits (L, M and H) provide the scaffold for the binding of the cofactors of the reaction centre. The purple bacteria reaction centre was found to share considerable homology with the proteins of the photosystem II reaction centre, with the sequence identity of D1/D2 to the L/M subunits being around 20 % (Svensson et al., 1996). The cofactors of the reaction centre are: one carotenoid, four bacteriochlorophylls (BChl *a* and BChl *b*), two bacteriopheophytins (BPhe *a* and BPhe *b*), two quinones (Q_A and Q_B) and one non-heme iron. Some reaction centres of purple bacteria contain a fourth

protein subunit, a cytochrome c with four covalently bound heme groups (Ermler *et al.*, 1994). In the case of the homologous photosystem II the bacteriochlorophylls and bacteriopheophytins are replaced by chlorophylls and pheophytin. In purple bacteria the quinones are either one menaquinone (Q_A) and one ubiquinone (Q_B) (*Rhodopseudomonas viridis*) (Deisenhofer & Michel, 1991) or two ubiquinones (*Rhodobacter sphaeroides*) (Ermler *et al.*, 1994), whereas in higher plants and cyanobacteria Q_A and Q_B are both plastoquinones (Buchannan *et al.*, 2000).

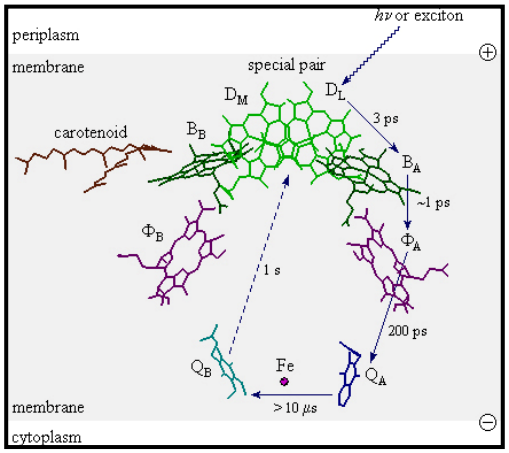

Fig. I.2: Cofactors and electron transport pathway of the *Rhodopseudomonas viridis* (purple bacteria) reaction centre. D_M / D_L: special BChl pair, B_A/B_B: accessory BChls, Φ_A/Φ_B: BPhe, Q_A/Q_B: Quinones (Deisenhofer & Michel, 1991).

Although the cofactors are arranged almost symmetrically, one side of the reaction centre is heavily favoured for the pathway of electron transport. The nomenclature of the special chlorophyll pair follows the respective light absorption wavelength that leads to charge separation, namely P_{870} for purple bacteria and filamentous green bacteria, P_{680} for photosystem II and P_{700} for photosystem I of higher plants, algae and cyanobacteria (Fig. I.3). After the primary charge separation in the special chlorophyll pair the electron is first transported to another chlorophyll, then to a pheophytin and finally to Q_B via Q_A (Fig. I.2). The first stable electron acceptor is pheophytin and the state $P_{870}^{+}Phe^{-}$ (or $P_{680}^{+}Phe^{-}$, respectively) is referred to as the primary radical pair. For example, the radical pair $P_{680}^{+}Phe^{-}$ has an electrochemical potential of 1.7 eV (Fig. I.3), which represents an efficient conversion of the photon energy available on excitation at 680 nm, which amounts to 1.8 eV (Barber *et al.*, 1997).

It has to be pointed out though that the picture of a special chlorophyll pair for P_{680} is slowly changing to that of an arrangement of four chlorophyll molecules (Chl_{D1}, P_{D1}, P_{D2}, Chl_{D2}; nomenclature as in Zouni *et al.*, 2001), which are responsible for primary charge separation (Barber, 2002; Barter *et al.*, 2003; Dismukes, 2001). Of the two quinones Q_A and Q_B, Q_A is more strongly bound to the protein and is only a one electron acceptor, whereas Q_B can dissociate into the membrane phase as a hydro-quinone after the uptake of two electrons and two protons and is consequently replaced by a non-hydrated quinone. This basic built-up can be found in all reaction centres of the pheophytin-quinone type (type II).

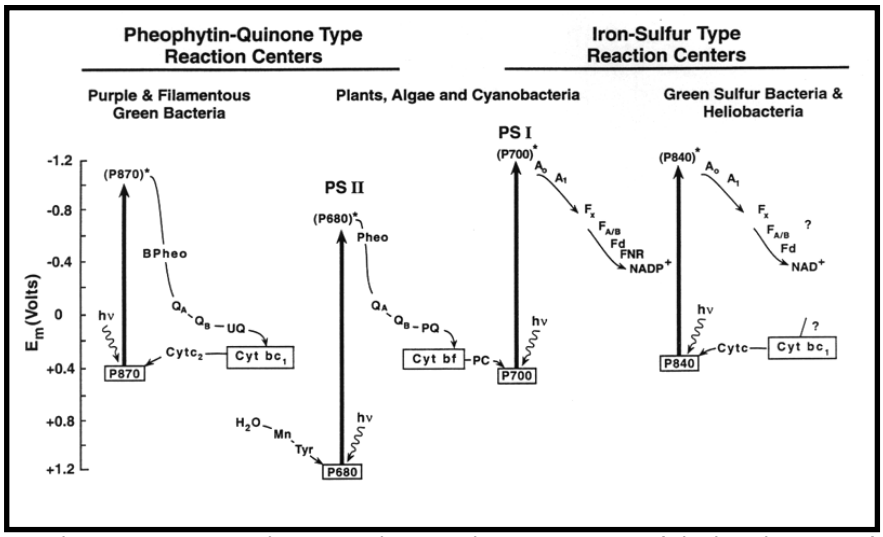

Fig. I.3: Electron transport chains in photosynthetic organisms (Blankenship, 1992). h*v*: Light energy; P870/P680/P700/P840: "special chlorophyll pairs" (*see also text*); $(P870)^*/(P680)^*/(P700)^*/(P840)^*$: excited states; Cyt: Cytochrome; Q_A/Q_B/UQ/PQ: (hydro)quinones; PC: Plastocyanin; A_0/A_1: accessory Chls; $F_X/F_{A/B}$: Iron-sulphur centres; Fd: Ferredoxin; FNR: Ferredoxin-$NADP^+$-Oxidoreductase

In higher plants, algae and cyanobacteria, the electrons to re-reduce photosystem II are ultimately provided by water, which is oxidised to molecular oxygen. This splitting of water is facilitated by a cluster of metal ions consisting of four manganese and one calcium ion (Siegbahn, 2002; Loll *et al.*, 2005). The manganese-calcium cluster is mechanistically linked to P_{680}, via a tyrosine residue called Y_Z, which is located on the D1 protein of the reaction centre. After excitation by light and the release of an electron, the P_{680}-cation returns to its uncharged state by subtracting an electron from Y_Z, which in turn oxidises the manganese-calcium cluster. In total the manganese-calcium cluster has to go through four photochemical turnovers to accumulate enough

oxidising potential to be able to perform the water splitting reaction (Kok *et al.*, 1970; Tommos & Babcock, 2000). The different oxidation levels are called S-states (S_0-S_4) and in the dark the manganese calcium cluster resides in the S_1 state.

From the acceptor side of PSII the hydroquinone diffuses to the lumenal part of the cytochrome b_6/f complex, which catalyses the electron transfer from the hydroquinone to plastocyanin, a soluble carrier protein, while simultaneously pumping protons across the thylakoid membrane. Plastocyanin serves also as the primary electron donor for photosystem I. By directing one of the two electrons of the incoming hydroquinone to a quinone on the stromal side of the complex, the cytochrome b_6/f complex is able to pump double the number of protons per electron transported, because after a second electron and a second proton are accepted by the stromal quinone it can be re-oxidised to a quinone on the lumenal side of the complex (Q-cycle).

In P_{700}, the absorption of light also leads to the release of electrons, which are then transported to $NADP^+$ via accessory chlorophylls, iron-sulphur clusters and ferredoxin (Fig. I.3). On the stromal side of the thylakoid membrane, the ferredoxin-$NADP^+$-oxidoreductase (FNR) catalyses the reduction of $NADP^+$ to $NADPH+H^+$, which leads to an enhancement of the pH gradient across the membrane, since this process actively removes H^+ on the stromal side. The resulting pH gradient drives the formation of ATP out of ADP and inorganic phosphate by the ATP-synthase complex, utilising a chemi-osmotic mechanism of energy conversion (Wang, 1969).

In addition to the linear electron flow, electrons may also participate in cyclic transport pathways, which provide a control mechanism for the ratio of reduction equivalents ($NADPH+H^+$) to energy equivalents (ATP). Ferredoxin is a soluble carrier protein on the stromal side of the thylakoid membrane and instead of relaying electrons to the FNR, ferredoxin has the additional ability to transport electrons back to the cytochrome b_6/f complex, which subsequently leads to an increased transport of protons across the thylakoid membrane (Richter, 1988), thus resulting in a higher pH gradient across the membrane, the prerequisite for ATP formation by the ATP-synthase complex.

2. Light-harvesting and energy transfer

In contrast to the high degree of conservation between the reaction centres of varying photosynthetic organisms, the respective light antennae differ greatly. The light-harvesting antennae are an important tool for adaptations to different habitats and ecological niches, as they carry the pigments to collect and utilise light in spectral regions, where the reaction centres themselves do not show a significant light absorption (Fig. I.4).

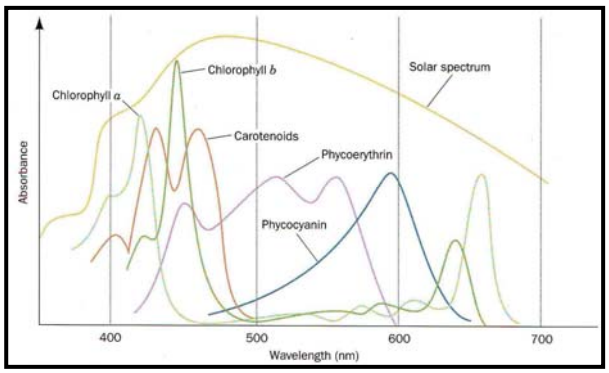

Fig. I.4: The absorption spectra of various photosynthetic pigments. The chlorophylls have two absorption bands, one in the red and one in the blue. Phycoerythrin absorbs blue and green light, whereas phycocyanin absorbs yellow light. Together these pigments absorb most of the visible light in the solar spectrum (Voet & Voet, 1995).

In green filamentous and green sulphur bacteria the light-harvesting function is carried out by structures called chlorosomes, which lie on the cytoplasmatic side of the plasmamembrane and stand out for their very high chlorophyll to protein ratio (*for a review on the subject see* Olson, 1998). The chlorophylls of green bacteria can be divided into two groups; the chlorosome-chlorophylls (BChl *c*, *d* or *e*) and bacteriochlorophyll *a*. The photosynthetic unit of a typical green filamentous bacterium holds between 100 and 200 molecules of bacteriochlorophyll *c* in one chlorosome and around ten molecules bacteriochlorophyll *a*, which together transfer excitation to a single reaction centre of the quinone type (type II). The photosynthetic units of green sulphur bacteria encompass up to 1000 to 2000 chlorosome-chlorophylls and around 100 bacteriochlorophyll *a* molecules that harvest light for a single reaction centre of the iron-sulphur type (type I).

In purple bacteria, the light-harvesting complexes LH1 and LH2 form membrane integral circular structures, with the reaction centre located inside the LH1 ring (Fig. I.5). Energy transfer between LH1 and the reaction centre involves predominantly the near-infrared, the so-called Q_y excitations, of bacteriochlorophylls. Since the transfer time of excitation energy from LH1 to the reaction centre is an order of magnitude slower than the initial electron transfer step, the reaction centre constitutes an effective excitation energy sink. In a series of excitation energy transfer steps, the transfer from LH1 to the reaction centre is the rate limiting step, proceeding an order of magnitude slower than transfers between different LHs, which occur on a picosecond timescale. One ring of LH1 contains 32 molecules of bacteriochlorophyll and 16 carotenoids (Damjanović *et al.*, 2000).

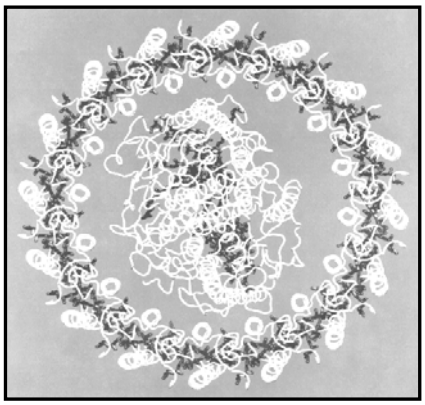

Fig. I.5: Top view of the modelled structure of the LH1-RC complex of *Rhodobacter sphaeroides*. RC structure encompassed by the LH1 ring. Protein components of LH1 and RC are shown in white; BChls, BPhes and carotenoids are in black (Damjanović *et al.*, 2000)

Phycobilisomes, the light-harvesting apparatus of cyanobacteria and red algae, are, unlike most light-harvesting antenna complexes, not integral membrane complexes, but instead they are attached to the surface of the photosynthetic membranes (Fig. I.6). They are composed of both the pigmented phycobiliproteins and the non-pigmented linker polypeptides; the former are important for absorbing light energy, while the latter are important for stability and assembly of the complex. The pigments bound by phycobilisomes are phycoerythrin, phycocyanin and allophycoyanin. The composition of the phycobilisome is very sensitive to a number of different environmental factors. Some of the filamentous cyanobacteria can alter the composition of the phycobilisome in response to the prevalent wavelengths of light in the environment. This process,

called complementary chromatic adaptation, allows these organisms to make efficient use of the available light energy needed to drive photosynthetic electron transport and CO_2 fixation. Under conditions of macronutrient limitation, many cyanobacteria degrade their phycobilisomes in a rapid and orderly fashion. Since the phycobilisome is an abundant component of the cell, its degradation may provide a substantial amount of nitrogen to nitrogen-limited cells. Furthermore, degradation of the phycobilisome during nutrient-limited growth may prevent photodamage that would occur if the cells were to absorb light under conditions of metabolic arrest (Grossman *et al.*, 1993).

Photosynthetic eukaryotes are traditionally divided into three major groups, largely on the basis of their light-harvesting pigments. The chlorophytes (green algae and higher plants) have Chl *a/b* antennae, the chromophytes have Chl *a/c* antennae and the rhodophytes (red algae) have only chlorophyll *a* and rely on phycobilisomes (*see above*) as their major photosystem II antenna (Green & Durnford, 1996).

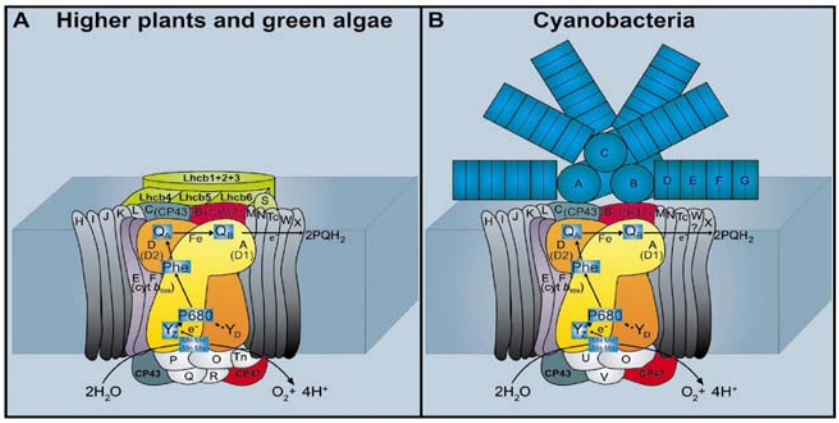

Fig. I.6: Cartoon of the structure and subunit composition of PSII. (A) Higher plants and green algae. (B) Phycobilisome-containing cyanobacteria. The proteins of the core complex including the extrinsic proteins of the oxygen evolving complex are labelled according to the gene nomenclature (e.g. PsbA=A) with common designations given for the major subunits (e.g. A=D1 protein). The outer light-harvesting proteins are coloured light green for the plant systems (intrinsic Lhcb proteins) and blue-green for the cyanobacterial systems (extrinsic phycobiliproteins forming a phycobilisome where A, B and C are allophycocyanin rods) and D, E, F and G are discs of other phycobiliproteins (e.g. C-phycocyanin). The electron transfer pathway from water oxidation to plastoquinone reduction (PQH_2) is shown (Hankamer *et al.*, 2001b).

The most prominent chlorophyll *a/b* (CAB) protein of higher plants is the major light-harvesting complex II (LHCIIb), which is organized as trimers *in vivo* (mixture of Lhcb1, 2 and 3) and mostly captures light for photosystem II. Under certain conditions LHCIIb can dissociate from photosystem II and migrate to photosystem I as a means of

regulation of excitation energy distribution (Allen, 1995). Each monomer of LHCIIb binds eight molecules chlorophyll *a*, six chlorophyll *b*, two lutein, one neoxanthin and one violaxanthin or antheraxanthin (Liu *et al.*, 2004). Additionally, photosystem II binds the minor antenna complexes CP29 (Lhcb4), CP26 (Lhcb5) and CP24 (Lhcb6), which also belong to the CAB gene family. The same is true for the two Light-harvesting complexes associated with photosystem I, which are called LHCI-680 (Lhca2 + Lhca3) and LHCI-730 (Lhca1 + Lhca4), according to their fluorescence emission maxima.

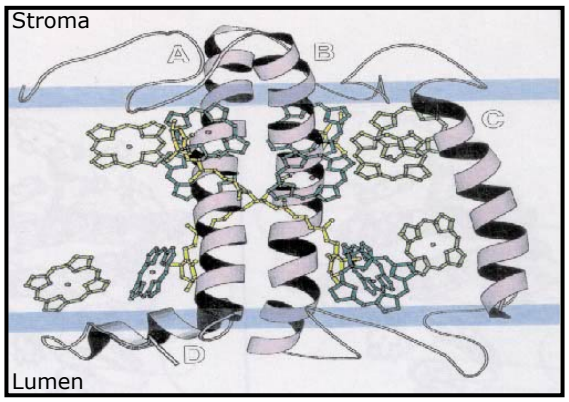

Fig. I.7: LHCIIb monomer as viewed from the side (Kühlbrandt *et al.*, 1994). *Helix nomenclature see text*.

The peripheral light-harvesting antennas of all eukaryotes are encoded by a large nuclear gene family that also includes a group of eukaryotic stress-response genes and related prokaryotic genes. The respective apoproteins are synthesised in the cytosol and need to be transported to the chloroplast and post-translationally inserted into the thylakoid membrane (Jansson, 1994). All members of the extended family of proteins, which also includes the fucoxanthin-chlorophyll *a/c*-binding-proteins (FCPs) of diatoms and brown algae and early light inducible proteins (ELIPs), are predicted to have the same overall fold as LHCIIb (Green & Durnford, 1996). The LHCIIb polypeptide folds into three membrane-spanning helices, with an additional amphi-pathic helix near the C-terminal end (Helix D). The first (B) and third helix (A) cross each other at an angle of about 30° to the membrane normal and are held together by reciprocal ion pairs involving an arginine on one helix and a glutamate on the other (Fig. I.7). Despite the considerable homologies of eukaryotic light-harvesting complexes (Green & Kühlbrandt, 1995), their pigmentation varies greatly and there is

also great diversity in the oligomeric states of the CAB proteins. In higher plants alone, there are functional monomers (CP24, CP26, CP29), dimers (LHCI-680, LHCI-730) and trimers (LHCIIb). The oligomeric state of fucoxanthin-chlorophyll-proteins *in vivo* remains unclear, but in *in vitro* experiments trimers and higher oligomeric states could be isolated, with a characteristic pattern of isoforms (Büchel, 2003). Overall, the light-harvesting antenna of diatoms is composed of at least eight different isoforms of FCP (fcp1-fcp7 and fcp12) (Eppard & Rhiel, 1998; Eppard *et al.*, 2000; Eppard & Rhiel, 2000).

Compared to LHCIIb with 14 chlorophylls and 4 carotenoids, CP29 binds only eight chlorophylls (6 Chl *a*, 2 Chl *b*) and two carotenoids (Bassi *et al.*, 1999), although the apoprotein is larger (28 kDa vs. 25 kDa). The antenna of photosystem I bind 18 chlorophylls and 3.5 carotenoids in the LHCI-680 heterodimer and 22.8 chlorophylls and 3.9 carotenoids in the LHCI-730 heterodimer, respectively (Schmid *et al.*, 2002). For the pigmentation of the FCPs, in which the more common accessory chlorophyll *b* is replaced by chlorophyll *c*, a chlorophyll type which lacks the phytolester, see Table III.3 (p. 64). The homologies between FCP and the light-harvesting complexes are most pronounced in helices A and B. In contrast to this, the N- and C-terminus as well as the loop regions are considerably shorter in FCPs and render the protein more hydrophobic compared to the LHCs of higher plants. Overall, this also accounts for the considerably smaller size of the FCPs (fcp1, fcp2, fcp3, fcp4 = ~18 kDa; fcp5, fcp6, fcp7 = ~19 kDa; fcp12 = ~22 kDa).

3. Structure and function of photosystem II

Photosystem II functions as a water-plastoquinone oxidoreductase and is located in the thylakoid membranes of higher plants, algae and cyanobacteria. It is a multisubunit complex which comprises more than 25 different proteins. At the heart of the complex is the reaction centre consisting of the D1 and D2 proteins. Together these two related reaction centre subunits bind all the cofactors which give rise to primary and secondary electron flow (*see also I.1*).

Two chlorophyll binding proteins, CP43 and CP47, are closely associated with D1 and D2 (Barber *et al.*, 1997). One of their functions is to act as an inner light-harvesting antenna system, but both are characterised by an unusual structural feature; they have very large hydrophilic loops exposed on the lumenal surface (Bricker, 1990), which are expected to play an important role in stabilising the oxygen evolving complex (OEC). The structural similarity of D1 and D2 to the L and M subunits of the purple bacteria reaction centre was confirmed by electron crystallography studies of a subcomplex of photosystem II. Both the D1 and the D2 subunits consist of five transmembrane helices related by a pseudo-twofold axis (Rhee *et al.*, 1997; Rhee *et al.* 1998). Following this pseudo-twofold symmetry, the reaction centre proteins are accompanied by the two subunits CP47 and CP43 with six transmembrane helices each, with CP47 adjacent to D2 and CP43 adjacent to D1 (Fig. I.8) (Nield *et al.*, 2000).

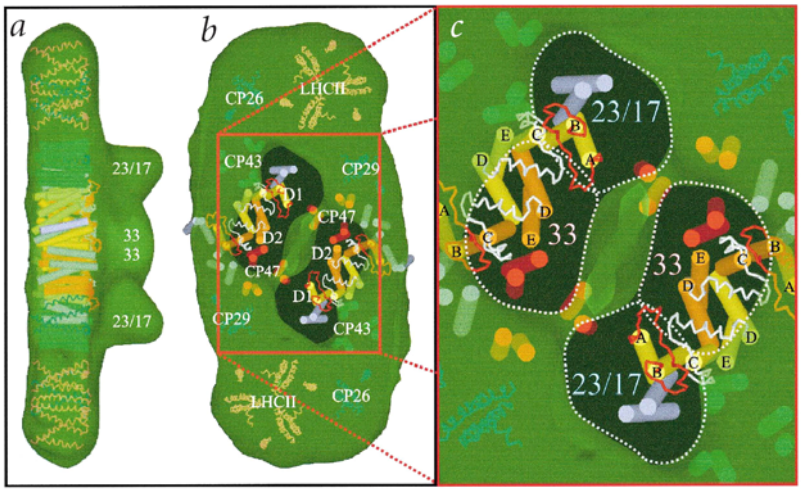

Fig. I.8: Structural model of the intrinsic protein subunits within the PSII super-complex. (a) & (b): Semi-transparent surface representation of the structural model, viewed from the side and lumenal surface, respectively, containing helices of the protein subunits. (c): A magnification of the docking sites for the extrinsic OEC proteins emphasising the underlying helices of the core dimer. Helices attributed to the D1 and D2 proteins in yellow and orange, respectively (Nield *et al.*, 2000)

The spatial organisation of CP43-D1-D2-CP47 was observed to be similar to the arrangement of the transmembrane helices of the photosystem I reaction centre, despite little sequence homology of the proteins (Krauss et al., 1996), indicating either a distant common evolutionary ancestor for both photosystems or a functional necessity requiring a particular helix arrangement. Based on a structure derived from cyanobacterial photosystem II, two additional helices close to the reaction centre are

attributed to the α- and β-subunits of cytochrome b_{559} (Fig. I.9) (Zouni *et al.*, 2001). It is an indispensable constituent of photosystem II, but its function is not clearly defined, yet. Cytochrome b_{559} is a redox-active protein, and both photooxidation and photoreduction of its heme iron have been observed. Because these reactions are very slow and characterised by low quantum yields, it is generally assumed that cytochrome b_{559} takes no active part in the primary electron transfer reactions (Bondarava *et al.*, 2003).

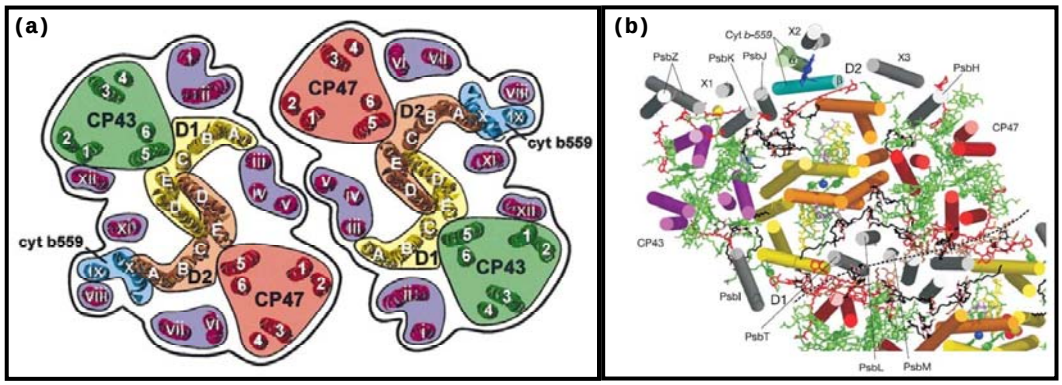

Fig. I.9: Overview of the helix organisation in the PSII core dimer of (a) higher plants (Hankamer et al., 2001b) and (b) Cyanobacteria (Loll *et al.*, 2005)

In the last years, several medium to high resolution structures of cyanobacterial photosystem II have been published, which enabled an almost complete cofactor assignment (Zouni *et al.*, 2001; Kamiya & Shen, 2003; Ferreira *et al.*, 2004; Loll *et al.*, 2005). For higher plants, no such high resolution structure is available, yet. Hankamer *et al.* (2001a) reached a resolution of ~10 Å parallel to the membrane plane and ~23.8 Å perpendicular to the membrane plane with two-dimensional crystals of the complete reaction centre of spinach PSII. The partial PSII complexes, which were crystallised by Rhee *et al.* (1997; 1998), resulted in a model with a resolution of ~8 Å. For *Thermosynechococcus elongatus* the locations of 35 molecules chlorophyll *a*, 11 β-carotene, two pheophytin, two plastoquinone, two heme, one bicarbonate, 14 lipid, three β-dodecylmaltoside, the Mn_4Ca cluster, one Fe^{2+} and one putative Ca^{2+} ion could be determined in each monomer (Loll *et al.*, 2005). A belt of lipids surrounds the reaction centre, separating it from the antenna complexes and smaller subunits (Loll *et al.*, 2005). The unusually high lipid content provides structural flexibility that might be required for increasing the local mobility of the subunits. As D1 is most prone to photodamage, it needs to be replaced continuously by newly synthesized D1 (Baena-

Gonzales & Aro, 2002). A flexible environment, such as that provided by the belt of lipids, might be essential in facilitating this high turnover of D1 (Loll *et al.*, 2005). In total, cyanobacterial photosystem II is made up of at least 20 protein subunits (Tab. I.1). The photosystem II dimers of cyanobacteria are 205 Å long, 110 Å wide and 105 Å thick (45 Å inside the membrane) (Ferreira *et al.*, 2004). The molecular weight depends on the respective photosystem II preparation and varies between 460 and 650 kDa (Ferreira et al., 2004; Kashino *et al.*, 2002; Kuhl *et al.*, 1999; Kuhl *et al.*, 2000; Shen & Kamiya, 2000). In general the photosystem II supercomplexes of higher plants and green algae are significantly larger than PSII of cyanobacteria, due to the membrane intrinsic light-harvesting complexes LHCIIb, CP29, CP26 and CP24 (Fig. I.8).

Gene	Protein	Mass [kDa]	transmembrane Helices
psbA (c)	D1	38 (Sp)	5
psbB (c)	CP47	56 (Sp)	6
psbC (c)	CP43	50 (Sp)	6
psbD (c)	D2	39 (Sp)	5
psbE (c)	Cyt b_{559} (α)	9 (Sp)	1
psbF (c)	Cyt b_{559} (β)	4 (Sp)	1
psbH (c)	H-protein	8 (Sp)	1
psbI (c)	I-protein	4 (Pe)	1
psbJ (c)	J-protein	4 (Sp)	1
psbK (c)	K-protein	4 (Sp)	1
psbL (c)	L-protein	4 (Pe)	1
psbM (c)	M-protein	4 (To)	1
psbN (c)	N-protein	5 (Sp)	0
*psbO (n)**	extrinsic (OEC)	27 (Sp)	0
*psbP (n)**	extrinsic (OEC)	20 (Sp)	0
*psbQ (n)**	extrinsic (OEC)	16 (Sp)	0
*psbR (n)**	R-protein	10 (Sp)	4
*psbS (n)**	LHC-like protein	22 (Sp)	1
psbT (c)	T-protein	3 (Sp)	0
*psbT (n)**	T-protein	10 (Sy)	0
*psbU***	U-protein	15 (Sy)	0
*psbV***	Cyt c_{550}	6 (Sy)	1
*psbW (n)**	W-protein	6 (Sp)	1
psbX (n)	X-protein	4 (Sp)	(na)
psbZ (n)	ORF 62 / ycf9	7 (To)	(na)

Tab. I.1: *psb* genes and gene products. The *psbA* to *psbX* genes occur in all types of oxygenic organisms except for those found exclusively in higher plants and algae (*) or cyanobacteria (**). In eukaryotic organisms the *psb* genes are located in either the chloroplast (c) or the nuclear (n) genomes. The molecular masses of the mature PsbA to PsbX proteins, except PsbU, are calculated from the protein sequences reported in the SWISSPROT database using the MacBioSpec (Sciex Corp., Thornhill, Ontario, Canada) for spinach (Sp), pea (Pe), tobacco (To) and Synechococcus sp. (Sy). The number of predicted transmembrane helices is based on hydropathy analyses of primary sequence; these are not available (na) for *psbX* and *psbZ*. Adapted from Barber *et al.* (1997).

The structures of cyanobacterial and plant photosystem II cores are overall very similar, but show some distinctive features. The greatest differences lie in the subunit compositions of the two complexes (Tab. I.1) and here especially in the extrinsic proteins of the oxygen evolving complex. The 23 kDa (PsbP) and 17 kDa (PsbQ) proteins are only found in higher plants, where as PsbU and PsbV are exclusive for cyanobacteria. The PsbV protein of cyanobacteria, which is also called cytochrome c_{550}, is important for stabilising the oxygen evolving complex and, according to EPR measurements (Lakshmi *et al.*, 2002), shares a functional homology to the PsbP and PsbQ proteins of higher plants. Apart from this, there are also some additional differences in the locations of cytochrome b_{559} and the core antenna CP47 in relation to the D1 and D2 reaction centre proteins. Although the two helices of the α- and β-chain (PsbE & PsbF) of cytochrome b_{559} in higher plants have the same relative orientation to one another and the membrane plane, the cytochrome is about four Ångstrom removed from its position in the cyanobacterial photosystem II. Within the D1 and D2 proteins there are significant structural differences at the stromal ends of transmembrane helices between higher plants and cyanobacteria, even though these proteins are highly homologous (85 % identical residues). This could be due to the fact that the respective light-harvesting antennas differ so greatly; membrane intrinsic CAB proteins in higher plants and phycobilisomes in cyanobacteria (Fig. I.6). Despite the discrepancies in the spatial arrangement of the protein backbone, the positions of the crucial cofactors are precisely conserved (Büchel & Kühlbrandt, 2005).

4. Aims of this work

One of the major problems when working with higher plant photosystem II is its relative instability during isolation. Together with the antenna proteins and several other proteins, some of which still have an unclear function, photosystem II forms a huge multi-protein-complex, which tends to fall apart during classical preparation methods. This problem is more pronounced when working with higher plants, than it is the case when working with thermophilic organisms. In order to achieve a faster and

less stringent method of purification for photosystem II, one possible strategy is to add a His-tag to one of the subunits of photosystem II, namely the α-chain of cytochrome b_{559} (PsbE). A His-tag is a sequence of six or ten consecutive histidine residues, which can be exploited to perform affinity chromatography with columns containing Ni-NTA as the matrix material. Since PsbE is encoded in the chloroplast genome, the biolistic transformation ("*gene gun*") is the method of choice for producing transgenic plants. After the generation of transgenic tobacco plants, these need to be tested if the addition of the His-tag has any detrimental effects on the growth of the plants or their photosynthesis. The possibility to purify photosystem II quickly with the His-tag system is supposed to yield material of improved quality for spectroscopic applications, crystallisation trials and structural studies of PSII in general.

In order to effectively study the structure and function of the light-harvesting complexes of diatoms, the FCPs, the pigment-stoichiometry is an important prerequisite for the interpretation of many spectroscopic measurements. Therefore FCPs are to be purified by sucrose density ultra centrifugation, the pigments extracted and quantified with HPLC.

II. Materials and Methods

1. Materials

Equipment and chemicals see Appendix (VIII.1)

1.1 Biological material

- XL1 blue competent cells (*Escherichia coli*), Stratagene, La Jolla, CA (USA)
- XL10 gold ultra competent cells (*Escherichia coli*), Stratagene, La Jolla, CA (USA)
- *Nicotiana tabacum* cv. Petit Havana (wildtype); Solanaceae; Solanales
- *Spinachia oleracea*; Amaranthaceae; Caryophyllales
- *Cyclotella meneghiniana*; Bacillariophyceae; Heterokontophyta

Constructed during this work:

- *Nicotiana tabacum* EH1a/13 (His_6 non-cleavable)
- *Nicotiana tabacum* EH2a/20 (His_{10} non-cleavable)
- *Nicotiana tabacum* EH2a/22 (His_{10} non-cleavable)
- *Nicotiana tabacum* EH2a/34 (His_{10} non-cleavable)
- *Nicotiana tabacum* EH3a/3 (His_6 cleavable)
- *Nicotiana tabacum* EH4a/21 (His_{10} cleavable, sterile)
- *Nicotiana tabacum* EH4a/26 (His_{10} cleavable, sterile)
- *Nicotiana tabacum* EH4a/28 (His_{10} cleavable, fertile)
- *Nicotiana tabacum* EH1a/30 (no His-tag, aadA positive)
- *Nicotiana tabacum* EH2a/33 (no His-tag, aadA positive)

1.2 Plasmid DNA and primers

Plasmids:

– pBR322Sal9 (kindly provided by R. Bock, Münster)

– pBluescript II KS+ , Stratagene, La Jolla, CA (USA)

Constructed during this work:

– pbKS+SacI$^-$

– pbKS+SacI$^-$psbE

– pbKS+SacI$^-$psbE-His$_6$NC

– pbKS+SacI$^-$psbE-His$_{10}$NC

– pbKS+SacI$^-$psbE-His$_6$NC-aadA

– pbKS+SacI$^-$psbE-His$_{10}$NC-aadA

– pbKS+SacI$^-$psbE-His$_6$C

– pbKS+SacI$^-$psbE-His$_{10}$C

– pbKS+SacI$^-$psbE-His$_6$C-aadA

– pbKS+SacI$^-$psbE-His$_{10}$C-aadA

Primers:

All oligonucleotides were ordered online from MWG (Ebersberg, Germany) and purified to HPSF quality (= High Purity Salt Free) before delivery.

pbKS+SacI$^-$:

$P_{forward}$ (mut1): `5′ – GCG AAT TGG AGA TCC ACC G – 3′`

$P_{reverse}$ (mut2): `5′ – CGG TGG ATC TCC AAT TCG C – 3′`

His-Tags:

$P_{reverse}$ (P7652): `5′ - CCG AAT GAG CTA AGA GAA TCT T - 3′`

$P_{forward}$ (PsbE – His):

a) EH1 = His_6, non cleavable (H6NC): 5′ - T TTT GAG CTC AGC ATG CAT CAT CAC CAT CAC CAT TCT GGA AGC ACA GGA GAA CGT - 3′

b) EH2 = His_{10}, non cleavable (H10NC): 5′ - T TTT GAG CTC AGC ATG CAT CAT CAC CAT CAC CAT CAC CAT CAC CAT TCT GGA AGC ACA GGA GAA CGT - 3′

c) EH3 = His_6, cleavable (H6C): 5′ - T TTT GAG CTC AGC ATG CAT CAT CAC CAT CAC CAT ATT GAT GGA CGA TCT GGA AGC ACA GGA GAA CGT - 3′

d) EH4 = His_{10}, cleavable (H10C): 5′ - T TTT GAG CTC AGC ATG CAT CAT CAC CAT CAC CAT CAC CAT CAC CAT ATT GAT GGA CGA TCT GGA AGC ACA GGA GAA CGT - 3′

1.3 Restriction enzymes

All restriction endonucleases used in this work were commercially obtained from New England Biolabs (Ipswich, MA, USA) or Fermentas (Burlington, Ontario, Canada).

- AgeI (NEB)
- BamHI (NEB)
- BglII (NEB)
- DpnI (NEB)
- DraI (Fermentas)
- Ecl136II (Fermentas)
- EcoRV (NEB)
- HindIII (NEB)
- PvuI (NEB)
- SacI (NEB)
- SalI (NEB)
- ScaI (NEB)
- SpeI (NEB)

2. Methods

2.1 Plasmid DNA preparation

a) QIAprep Spin Miniprep Plasmid DNA purification

The QIAprep Miniprep procedure is based on alkaline lysis of bacterial cells followed by adsorption of DNA onto silica in the presence of high salt. Subsequently the DNA can be washed and eluted in purified form. The preparation was carried out as described in the *QIAprep Miniprep Handbook* by *QIAgen.*

b) QIAfilter Midiprep Plasmid DNA purification

This protocol is designed for preparation of up to 100 µg of high- or low-copy plasmid or cosmid DNA using the QIAfilter Plasmid Midi Kit. In this protocol, QIAfilter Cartridges are used instead of conventional centrifugation to clear bacterial lysates. The preparation was carried out as described in the *Plasmid Purification Handbook* by *QIAgen.*

c) Plasmid DNA preparation ("1, 2, 3 Miniprep")

Alternatively to using purification kits, plasmid DNA was isolated by centrifuging the bacterial culture for 1 min at 10 000 rpm in a table top centrifuge. The pellet was resuspended with 100 µl ice cold Sol-1, without vortexing. After the addition of 200 µl Sol-2 and careful mixing, the cells were lysed during 5 min incubation at room temperature. Subsequently, the solution was neutralised with 150 µl ice cold Sol-3 and incubated for 10 min on ice. Cell debris was removed by centrifuging 15 min at 12 000 rpm in a table top centrifuge at 4°C. The purity of the plasmid DNA was enhanced by precipitating the sample with 100 % isopropanol, centrifugation for

30 min at 12 000 rpm and washing the pellet with 70 % ethanol. After washing, the plasmid DNA can either be resuspended in H_2O or buffer.

Stock solutions:

Sol-1
50 mM Glucose
10 mM EDTA
25 mM Tris/HCl, pH 8.0
Add:
5 µL RNase A per ml Sol-1
1 spatula tip Lysozyme per ml Sol-1

Sol-2
0.2 N NaOH
1 % SDS

Sol-3
3 M KAc, pH 4.8

2.2 Mutagenesis through altered primers in PCR

The polymerase chain reaction (PCR) is a method to amplify strands of DNA in an *in vitro* system with a DNA polymerase. The DNA polymerase needs small pieces of DNA to start the extension of a sequence. These oligonucleotides are called primers and need to be complementary to a specific part of the template DNA. The longer the chosen primer, the higher its specificity of binding to the template. Although primers bind with a higher affinity to actual complementary sites on the template DNA, mismatches and partial binding can occur, without fully inhibiting the reaction. This

opens up the possibility to generate mutated DNA amplificates through the use of purposefully altered primers during the PCR.

Reactions were carried out as 50 µl assays, with 10 ng of template DNA and 100 ng of each primer. ThermalAce DNA polymerase, dNTPs and buffers were commercially obtained from Invitrogen (Paisley, UK).

The PCR-mix was set up on ice and cycled 30 times with denaturation at 95°C for 30 s, annealing at 55°C for 30 s and an extension time of 4 min at 74°C. Before the cycling, an initial denaturation was carried out for 3 min at 95°C and after the cycling, 10 min at 74°C allowed for final chain extensions.

After the reaction, PCR products were purified with the QIAquick PCR product purification kit (QIAgen), which uses a silica gel column to bind the DNA, while impurities are washed away (*see respective documentation*).

After purification, the residual template DNA in the sample was digested with DpnI, a restriction endonuclease that only cleaves methylated DNA.

2.3 Restriction of DNA

DNA endonuclease reactions were setup according to the description in the NEB catalogue (New England Biolabs, 2005/2006 edition).

Typically, restrictions were set up as 20 µl or 50 µl reactions, using a specific buffer for the respective endonuclease or endonucleases. For restrictions intended for analytical gel electrophoresis, DNA amounts from 200 ng to 750 ng were sufficient. For preparative restrictions, DNA amounts from 0.75 µg up to 5 µg were used. If possible, endonucleases were heat inactivated after the reaction (*see respective documentation*). Very long incubation times (more than 2 hrs) were avoided, even with high amounts of DNA in the reaction, especially when fragments of the digest were submitted to ligation experiments later on.

2.4 Agarose gel electrophoresis and gel extraction of DNA bands

DNA molecules of different sizes can be separated by electrophoresis in agarose gels. Due to their negative charge, DNA molecules wander in an electric field. In the gel molecules of different sizes wander at different speeds, because of the molecular sieve properties of the gel.

The density of the gel was adjusted between 0.7 % and 2.5 % to optimise the electrophoresis for different sizes of DNA molecules (higher percentage for smaller bands). To prepare the gel, the agarose was suspended in the same buffer that was used as running buffer (usually TBE or TAE) and heated in a microwave oven, until the suspension had reached its boiling point and the agarose was completely dissolved. DNA bands were stained with ethidium bromide, either by adding ethidium bromide directly to the gel before pouring, by bathing the gel after the run in an ethidium bromide solution or by adding the ethidium bromide to the loading dye.

Stock solutions:

10x TBE
1 M Tris/HCl, pH 8.3
0.83 M Boric acid
10 mM EDTA

10x TAE
40 mM Tris acetate, pH 8.2
20 mM Sodium acetate
1 mM EDTA

10x DNA loading dye
2 mg Xylene cyanol
3 mg Bromphenole blue
add 1 ml 1x TAE (or TBE)

1x DNA loading dye

100 µl 10x loading dye (*see above*)
10 µl Ethidium bromide (10 mg/ml) (optional)
490 µl 1x TAE (or TBE)
ad 1000 µl with 100 % Glycerol
(store in the dark, if ethidium bromide is used)

2.5 Polyacrylamide gel electrophoresis for small DNA fragments

When very small DNA fragments needed to be resolved with electrophoresis, vertical polyacrylamide gels were used instead of the horizontal agarose gels.

Electrophoresis was carried out in 10 % polyacrylamide/urea gels, with TBE as the gel and running buffer. To facilitate the entry of the DNA molecules into the gel, a 4 % polyacrylamide stacking gel was used. Gels were run over night at 60 V in the cold room (4°C). After the run, the DNA was stained in an ethidium bromide bath.

Stock solutions:

Acrylamide/Bisacrylamide

40 % Acrylamide
1.25 % Bisacrylamide

10x TBE

1 M Tris/HCl, pH 8.3
0.83 M Boric acid
10 mM EDTA

2.6 Ligation of DNA

In a ligation reaction, homologous cohesive ("sticky") or blunt ends of DNA molecules can be fused together. The DNA ligase is an important repair enzyme in eukaryotic cells, which restores broken phosphodiester bonds in DNA molecules. This function can be used in *in vitro* cloning experiments to insert a DNA fragment into a vector molecule. Most commonly the T4 DNA ligase is used in these experiments, which can be isolated from bacteriophage T4 infected *E. coli* cells. The ratio of vector DNA to insert DNA is critical for the ligation and the ideal ratio can be calculated with the following formula:

(size of vector / 2) • (1 / size of insert) = ng vector to be used for 1 ng insert

The ligation reactions were set up in small volumes (10 to 20 µl) to keep the overall concentration high. If the DNA samples were too diluted, the total volume was reduced with a vacuum evaporation system (SpeedVac). The reaction mix was either incubated for 1 h at 16°C or overnight at 4°C. After successful ligation the DNA could be used, for example, for the transformation of bacteria.

2.7 Transformation of *Escherichia coli*

Competent *E. coli* cells can be genetically transformed by the introduction of circular DNA molecules (plasmids) with various methods. Competent cells, like the XL1-blue or XL10-gold strains (Stratagene), are commercially available, but competent cells can also be prepared in the lab.

a) Heat shock transformation

After the competent cells were thawed on ice, β-mercaptoethanol (25 mM final concentration) was added and the cells aliquoted in 100 µl steps to falcon tubes.

Depending on the source, 0.1 to 50 ng of DNA were used for the transformation. Transformation efficiency with purified plasmid DNA is very high and thus low amounts were sufficient, whereas the transformation efficiency with ligation products was rather low. The cells were then heat shocked for 45 s at 42°C in a water bath, in order to make the membranes penetrable for the plasmid DNA. Prior to plating on LB-agar medium, transformed cells were grown for 60 to 90 min in 0.9 ml preheated SOC medium at 37°C with shaking at 225 to 250 rpm.

SOC medium:
(for 1 litre)

20.0 g Tryptone
5.0 g Yeast extract
0.5 g NaCl
- autoclave -
add:
10 ml of 1 M $MgCl_2$
10 ml of 1 M $MgSO_4$
1 ml of a 2 M filter-sterilised glucose solution OR 2 ml of 20 % (w/v) glucose
prior to use
- filter sterilise -

b) Electroporation

Competent cells were thawed on ice and made penetrable for DNA by electroporating them at 2500 V in a 0.2 cm cuvette with a time constant of 5 ms in an Eppendorf Multiporator. Immediately after electroporation, 1 ml of preheated LB medium was added, the cells grown for 60 to 90 min at 37°C with shaking at 225 to 250 rpm and plated on LB-agar medium.

2.8 Transformation and shoot regeneration of *Nicotiana tabacum*

The so-called biolistic transformation method ("*particle*" or "*gene*" *gun*) can be used to introduce genetically engineered plasmid DNA to chloroplasts of higher plants, like for example *Nicotiana tabacum*. Through the process of homologous recombination, the plastid encoded wildtype *psbE* gene can be replaced by a His-tagged version of the same gene. Along with the His-tag a second gene is incorporated in the chloroplast genome, which confers resistance to certain antibiotics and thus allows for selective growth of successfully transformed plants.

Biolistic transformation was carried out according to the procedure of Ye *et al.* (1990), with modifications as in Bock *et al.* (1994) and below.

Gold particles (1–1.1 mg, 0.6 μm, Bio-Rad) were cleaned with 100 % ethanol and coated with DNA by precipitation with ethanol. DNA coated gold particles were resuspended in ethanol and loaded on macrocarrier discs. These were inserted in a heptacarrier, which was sealed with a rupture disc that breaks at a helium pressure of ca. 1100 to 1350 psi. Gold particles were shot at leafs of tobacco plants cultivated under sterile conditions. Leaves were placed with their abaxial side facing up. After the shooting, the tobacco leafs were cut into smaller pieces (~5 mm x ~5 mm) and laid out in petri dishes on regenerative RMOP medium, containing 0.5 mg/ml spectinomycin. The leaf pieces were then incubated for 4 to 5 weeks with 16 hrs light at 25°C and 8 hrs darkness at 20°C per day, with a light intensity of ca. 50 $\mu E/(s \cdot m^2)$.

After several rounds of regeneration on antibiotic-containing medium, successful transformation was confirmed through PCR methods. Seeds were then produced from homoplasmic tobacco strains by self fertilisation of the fully regenerated plants. The presence of the His-tag needed to be confirmed again with PCR methods in the resulting F1 generation.

Plant cell and tissue culture stock solutions

RM Macro	**10x**	
$CaCl_2$ x 2 H_2O	4.40 g	
KH_2PO_4	1.70 g	
KNO_3	19.00 g	
$MgSO_4$ x 7 H_2O	3.70 g	
NH_4NO_3	16.50 g	
	H_2O ad 1000 ml	(autoclave, store at 4°C)

RM Micro	**100x**	
$MnSO_4$ x 1 H_2O	1690.0 mg	
$ZnSO_4$ x 7 H_2O	860.0 mg	
H_3BO_3	620.0 mg	
KJ	83.0 mg	
Na_2MoO_4 x 2 H_2O	25.0 mg	
$CuSO_4$ x 5 H_2O	2.5 mg	
$CoCl_2$ x 6 H_2O	2.5 mg	
	H_2O ad 1000 ml	(autoclave, store at 4°C)

FeNaEDTA (Sigma E6760)	1 %	(filter sterilise, store at 4°C in the dark)

Vitamins		
Glycine	1 mg/ml	(filter sterilise, store at 4°C)
Nicotinic acid	1 mg/ml	(filter sterilise, store at 4°C)
Pyridoxine•HCl	1 mg/ml	(filter sterilise, store at 4°C in the dark)
Thiamine•HCl	1 mg/ml	(filter sterilise, store at 4°C in the dark)

Hormones

Auxins:

1-Naphthaleneacetic acid (NAA)	1 mg/ml in 0.1 M NaOH (filter sterilise, 4°C)
Indole-3-acetic acid (IAA)	1 mg/ml in 0.1 M NaOH (filter sterilise, -20°C)
2,4-Dichlorophenoxyacetic acid (2,4 D)	2.2 mg/ml dissolve in 5 ml EtOH add H_2O adjust pH 5.0 with KOH (2 M) adjust the volume filter sterilise and store at 4°C

Cytokinins:

6-Benzylaminopurine (BAP)	1 mg/ml	in 0.1 M HCl (filter sterilise, 4°C)
Zeatin (Zea)	1 mg/ml	in 0.1 M NaOH (filter sterilise, -20°C, do not autoclave!)
Zeatinriboside (ZeaR)	1 mg/ml	in H_2O (= pH ~5) (filter sterilise, -20°C, do not autoclave!)

Miscellaneous:

Gibberellic acid (GA_3)	0.1 mg/ml	(filter sterilise, 4°C, do not autoclave!)

Other components

$AgNO_3$	1 %	(filter sterilise, store at 4°C in the dark)

Antibiotics

Spectinomycin (Spec)	100 mg/ml
Streptomycin (Strep)	100 mg/ml
Kanamycin (Kan)	100 mg/ml
Hygromycin B	416 mg/ml

RMOP Medium for shoot regeneration (thick plates) (for 1 litre)

10x RM Macro	100 ml	
100x RM Micro	10 ml	
1 % FeNaEDTA	5 ml	
Sucrose	30 g	
myo-Inositol	100 mg	
Thiamine•HCl (1 mg/ml)	1.0 ml	
NAA (1 mg/ml)	0.1 ml	
BAP (1 mg/ml)	1.0 ml	
	H_2O ad 1000 ml	
	adjust pH 5.8 with 2 M KOH / HCl	
Agar (Duchefa M1002)	7.4 g	(3.7 g / 500 ml)
	autoclave	
Spectinomycin (100 mg/ml)	5 ml	(2.5 ml / 500 ml)

Thin RMOP plates

- Prepare medium like above, but pour in normal bacteria growth petri dishes
- Pour only a very thin layer. Spread medium by swirling the petri dish. The layer would be too thick, if the medium would spread equally by itself.
- Pack and store plates as soon as possible to prevent drying out

RM Medium for plant maintenance in sterile environment

10x RM Macro	100 ml	
100x RM Micro	10 ml	
1 % FeNaEDTA	5 ml	
Sucrose	30 g	
	H_2O ad 1000 ml	
	adjust pH 5.75 with 2 M KOH	
Agar (Duchefa M1002)	~7.1 g	(~3.55 g / 500 ml)
	autoclave	

2.9 Growth and culture of tobacco plants

Tobacco plants (*Nicotiana tabacum*) were grown for 8 to 10 weeks under a light regime of 8 hours light and 16 hours darkness per day, with a light intensity of 100 to 150 µE/(s·m^2). Before the seeds can be planted, they need to be incubated for 2 to 3 days at 4°C and then soaked for another 1 or 2 days in H_2O. The plants were kept under a controlled environment at a constant temperature of 25°C and 50 % relative air humidity. The plants were fertilised once per week with Wuxal Top N (1:1000).

2.10 Thylakoid preparation

Thylakoid membranes were isolated as described in Burke *et al.* (1978) with the following modifications.

Spinach or tobacco leaves were ground in a Waring blender in 150 ml or 200 ml Grinding Buffer per 100 g of fresh weight, respectively. The leave extract was filtered through 4 layers of muslin and one layer of cotton and then centrifuged (10 min, 7500 rpm/8600 g, 4°C in a Hermle AS4.13 rotor). The pellets, consisting of chloroplasts and cell debris, were resuspended in about half the initial volume in Resuspension Buffer and washed by a second centrifugation (10 min, 7500 rpm/8600 g, 4°C in a Hermle AS4.13 rotor). Depending on the subsequent purification steps, the pellet was either resuspended in Homogenisation Buffer ("classical" PSII preparation, *see II.2.11*) or in Ni-NTA E&W Buffer w/o DDM (affinity chromatography, *see also II.2.12*). In both cases, as little buffer as possible was used. After homogenisation and a chlorophyll determination in 80% acetone (Porra *et al.*, 1989) (*see II.2.13*), the thylakoids were either flash frozen in liquid nitrogen and stored at -80°C or submitted directly to the "classical" PSII preparation (*see II.2.11*).

Buffers:

Grinding Buffer

50 mM HEPES, pH 7.5

400 mM NaCl

10 mM $MgCl_2$ 6x H_2O

2 g/l BSA

0.5 g/l Ascorbate

Resuspension Buffer

50 mM Mes-NaOH, pH 6.0

150 mM NaCl

5 mM $MgCl_2$ 6x H_2O

1 g/l BSA

0.5 g/l Ascorbate

Homogenisation Buffer

50 mM Mes-NaOH, pH 6.0

150 mM NaCl

5 mM $MgCl_2$ 6x H_2O

Ni-NTA E&W Buffer w/o DDM

20 mM Mes-NaOH, pH 6.8

15 mM NaCl

5 mM $MgCl_2$ 6x H_2O

10 % (v/v) Glycerol

2.11 Photosystem II preparation by solubilisation and centrifugation

By partial solubilisation of the thylakoid membranes and subsequent centrifugation, grana thylakoids, which contain mostly PSII, can be separated from stroma thylakoids, which contain mostly PSI.

After solubilisation of the thylakoid membranes with Triton X-100 (Berthold *et al*., 1981), grana particles were sedimented by centrifugation (30 min, 19 000 rpm/ 40 000 g, 4°C in a Beckman JA30.50 rotor), resuspended in Buffer 1 and washed by centrifugation (30 min, 19 000 rpm/40 000 g, 4°C in a Beckman JA30.50 rotor). After homogenisation the grana particles were solubilised with 2.7 % HTG (n-heptyl-β-D-thioglucoside) at a total chlorophyll concentration of 3 mg/ml for 20 min on ice. After dilution of the sample below the cmc of HTG by adding two volumes of buffer, the unsolubilised membrane fractions were removed by centrifugation (20 min, 17 000 rpm/35 000 g, 4°C in a Beckman JA-20 rotor). PSII is found in the supernatant.

Buffer 1

40 mM Mes-NaOH, pH 6.5

20 mM NaCl

1 mM $CaCl_2$ 2x H_2O

5 mM $MgCl_2$ 6x H_2O

2.12 Photosystem II preparation by affinity chromatography

Nickel-nitrilotriacetic acid (Ni-NTA) metal affinity chromatography can be used to isolate proteins, which carry tags with, for example, six or ten consecutive histidine residues (His_6-tag or His_{10}-tag). In its unprotonated form, histidine is able to form complex bonds with the immobilized nickel ions of the matrix material. While the desired proteins are bound to the column, all other components can be washed away and finally the protein eluted in high purity. Elution can be achieved either competitively by adding high amounts of imidazole to the column or by decreasing the

pH to a level, where histidine is protonated and thus cannot form any complexes with nickel anymore.

After solubilisation of the thylakoid membranes with 25 mM DDM (β-dodecyl-maltoside) at a total chlorophyll concentration of 1 mg/ml for 20 min on ice, all unsolubilised material was removed by centrifugation (10 min, 13 000 rpm, 4°C in a Hermle A8.24 rotor) and the supernatant applied to the Ni-NTA column, which was equilibrated with two column volumes of Ni-NTA E&W buffer w/ DDM before loading the sample. After the column had been washed with 3 column volumes of Ni-NTA E&W buffer w/ DDM, photosystem II could be eluted by adding two column volumes of imidazole containing Ni-NTA Elution buffer.

Buffers:

Ni-NTA E&W Buffer w/ DDM

20 mM Mes-NaOH, pH 6.8
15 mM NaCl
5 mM $MgCl_2$ 6x H_2O
10 % (v/v) Glycerol
0.03 % (w/v) β-dodecylmaltoside

Ni-NTA Elution Buffer

20 mM Mes-NaOH, pH 6.0
15 mM NaCl
5 mM $MgCl_2$ 6x H_2O
10 % (v/v) Glycerol
0.03 % (w/v) β-dodecylmaltoside
150 mM Imidazole

2.13 Chlorophyll determination (Chl *a* + Chl *b*)

Concentrations of chlorophyll *a* and chlorophyll *b* were measured photometrically with a Pharmacia Biotech *Ultrospec 4000* UV/visible spectrophotometer (Pfizer Pharma, Germany) in 80 % acetone and calculated with the following formula (Porra *et al.*, 1989):

$$c\,(\text{Chl } a) = 12.3 \cdot A_{663.6} - 2.55 \cdot A_{646.6} \quad [\mu g/ml]$$

$$c\,(\text{Chl } b) = 20.3 \cdot A_{646.6} - 4.9 \cdot A_{663.6} \quad [\mu g/ml]$$

2.14 Absorption spectroscopy

Absorption spectra were recorded between 370 and 750 nm with a Pharmacia Biotech *Ultrospec 4000* UV/visible spectrophotometer (Pfizer Pharma, Germany) with an optical path length of 1 cm and a band-pass of 2 nm.

2.15 Polyacrylamide gel electrophoresis of proteins

SDS polyacrylamide gel electrophoresis (SDS-PAGE) is a separation method for proteins, where proteins are resolved according to their apparent molecular mass.

Based on the protocol of Schägger & v. Jagow (1987), protein samples were loaded on 10 % separating polyacrylamide/urea gels, with a 4 % stacking gel, using the Biometra gel casting system. Samples were loaded in Rotiload (Roth) and the gels run for 30 min at 60 V and then switched to 90 V until the bromphenole blue band reached the bottom of the gel.

After the run, the protein bands in the gel were stained with Coomassie brilliant blue, a triphenylmethane dye that selectively binds to proteins.

Stock solutions:

3x Gelbuffer

3 M Tris/HCl, pH 8.45

0.3 % (w/v) SDS

Anodebuffer

0.2 M Tris/HCl, pH 8.9

Cathodebuffer

0.1 M Tris

0.1 M Tricine

0.1 % (w/v) SDS

(just add components, no adjustment of pH necessary!)

Acrylamide/Bisacrylamide

40 % Rotiphorese 40	38.96 % AA	1.039 % BA
Rotiphorese Gel B	---	2.0 % BA

Staining solution (100 ml)

175 mg	Coomassie Brilliant Blue G-250
50 ml	100 % Ethanol
7 ml	100 % Acetic acid
43 ml	H_2O

Destain solution

10 % Ethanol

7 % Acetic acid

2.16 Western blot

After electrophoresis, proteins can be transferred to a nitrocellulose or PVDF membrane, in order to make them accessible to reactions with antibodies. This technique is called western blotting. It is used to detect proteins with high specificity.

After the run, gels were equilibrated in Cathodebuffer and then proteins were blotted for 30 to 60 min, at a current of 1.5 mA/cm^2 of the gel, onto the membrane. For this transfer, the membrane and gel were surrounded by filter papers soaked in Anodebuffer and Cathodebuffer, respectively.

The membranes were then treated with peroxidase coupled antibodies binding to the D1 protein of photosystem II. Bands were visualised by ECL and recorded on X-ray film.

Anodebuffer I

0.3 M Tris/HCl, pH 10.4

10 % Methanol

Anodebuffer II

25 mM Tris/HCl, pH 10.4

10 % Methanol

Cathodebuffer

25 mM Tris/HCl, pH 9.4

40 mM Glycine

10 % Methanol

PBS

137 mM NaCl

2.7 mM KCl

4.3 mM Na_2HPO_4 7x H_2O

1.4 mM KH_2PO_4

Western Blocking Solution

5 % Milk powder
(0.05 % Tween 20) (optional)
in PBS

ECL detection solution (Peroxidase coupled antibodies)

200 µl Luminol (250 mM in DMSO) (store in the dark)
89 µl p-Coumaric acid (90 mM in DMSO) (store in the dark)
2 ml Tris/HCl, pH 8.5 (1 M)
fill up to 20 ml with H_2O
add 6.1 µl 30 % H_2O_2

2.17 Oxygen evolution

Oxygen evolution was measured with a Clark-type electrode (electrode setup: Perkeo Soft slide projector, Zeiss Ikon; Servogor 310 recorder, BBC Goerz; Bachofer control unit and measuring cell) at 20°C with 1 mM DCBQ and 1 mM ferricyanide as electron acceptors in the reaction mix. The measurements were carried out in Ni-NTA E&W Buffer w/o DDM at a total chlorophyll concentration of 50 µg/ml.

2.18 Pulse amplitude modulated fluorescence measurement (PAM)

Fluorescence measurements were carried out at 20°C, using a Mini-PAM photosynthesis yield analyzer (Walz, Germany). Plants were dark adapted for 5 min before each measurement. For determining the photosynthetic yield and the values for photochemical and non-photochemical quenching, the parameters F_0 (ground fluorescence), F_M (maximum fluorescence), F (steady state fluorescence), F_0' (ground

fluorescence in steady state) and F_M' (maximum fluorescence in steady state) were recorded in situ on intact tobacco leaves.

2.19 Two-dimensional crystallisation of photosystem II

Photosystem II was crystallised by solubilisation with n-heptyl-β-D-thioglucoside (HTG) at a total chlorophyll concentration of 1 mg/ml and dialysis against 25 ml dialysis buffer for 4 days at 30°C in the dark. According to the respective experiments, the dialysis buffer also contained different salts as additives (*see III.3.6*).

Dialysis buffer

40 mM Mes-NaOH, pH 6.5
1 µg/ml Butylated hydroxytoluene
1 mM Sodium azide
1 mM Sodium ascorbate
30 % Glycerol

2.20 Electron microscopy and sample preparation

Electron microscopy specimens were prepared on carbon films of around 100 Å thickness, which were supported by copper grids (3.05 mm diameter/400 mesh, Plano). Carbon was evaporated onto freshly cleaved mica (75 x 25 mm, Plano), using an Edwards Auto 306 Turbo carbon evaporator system at $1.0 \bullet 10^{-7}$ torr (Butt *et al.*, 1991). Copper grids were washed in 100 % acetone, sonicated in 100 % ethanol and dried on filter paper (Whatman No. 4). Carbon films were transferred onto the grids by floating the carbon on a water surface, with the grids arranged in the water below. On removal of the water the carbon film sinks onto the grids and the carbon covered grids can be recovered.

To visualise structures in the electron microscope, samples were contrasted with uranyl acetate. 1.5 µl of the sample were pipetted on a carbon coated grid and the residual liquid removed by carefully applying a piece of filter paper to the side of the grid. After washing the grid with H_2O and subsequent removal of the liquid with filter paper, one drop of uranyl acetate was applied to the grid and then dried in the same way. The grid was left exposed to air until it was dry, before storage.

Specimens were scanned and images recorded, using a Philips CM12 transmission electron microscope (120 kV) equipped with a Gatan CCD camera.

2.21 FCP preparation from *Cyclotella meneghiniana*

The diatom *C. meneghiniana* (culture collection Göttingen, strain 1020-1a) was grown in batch cultures in ASP-2 medium (Provasoli *et al.*, 1957) supplemented with 1 mM silica at 20°C under a 16 h light (40 µE/(s·m^2)) to an 8 h dark cycle.

Thylakoid membranes of *C. meneghiniana* were isolated according to the method described by Büchel and Wilhelm (1993) with slight modifications to reduce chlorophyllase activity. Cells were harvested by centrifugation, resuspended in Buffer A and silica crystals removed by slow centrifugation. All following steps were carried out in dim light and at 4°C. Cells were broken using a cell disrupter (Constant Cell systems) at 250 kPa. Cell debris and unbroken cells were removed during a slow spin (1000 g for 10 min) and membranes were pelleted by 1 h of centrifugation at 75 000 g. The membrane fraction was then washed using Buffer B in a further centrifugation step (20 min, 40 000 g), resuspended in a little amount of Buffer C, and frozen until use. Thylakoids were solubilised at 0.125 mg Chl *a*/ml with 10 mM β-dodecylmaltoside (DDM/Chl a 41:1, w/w) for 20 min on ice and loaded on top of a continuous sucrose gradient achieved by a freeze-thaw cycle of a solution of 19 % (w/v) sucrose in Buffer C. Separation was carried out by centrifugation using a swing-out rotor at 200 000 g for 16 h, which was shown to be sufficient to reach equilibrium. Bands of brown colour were harvested and concentrated using Amicon filtrating devices with a cut-off of 30 kDa.

Buffer A

10 mM Mes-NaOH, pH 6.5

2 mM KCl

5 mM EDTA

1 M Sorbitol

Buffer B

10 mM Mes-NaOH, pH 6.5

2 mM KCl

5 mM EDTA

Buffer C

10 mM Mes-NaOH, pH 6.5

2 mM KCl

2.22 Chlorophyll determination in 90% acetone (Chl *a* + Chl *c*)

Solutions containing chlorophyll *a* and chlorophyll *c* were measured photometrically with a Pharmacia Biotech *Ultrospec 4000* UV/visible spectrophotometer (Pfizer Pharma, Germany) and concentrations were calculated using the following formula (Jeffrey and Humphrey, 1975):

$$c\ (\text{Chl } a) = 11.78 \cdot A_{663} - 2.29 \cdot A_{630} \quad [\mu g/ml]$$

$$c\ (\text{Chl } c) = 24.36 \cdot A_{630} - 3.73 \cdot A_{663} \quad [\mu g/ml]$$

2.23 Pigment determination by High Performance Liquid Chromatography

High Performance Liquid Chromatography (HPLC) is a very precise and sensitive method for determining pigment concentrations in solution. The samples are injected into a high pressure system, which transports the pigments through a column with a flow of solvents. Due to the different strengths of interaction between the individual pigments and the combination of column material and eluents, some pigments move faster through the column than others. A diode array detector (DAD) then measures the eluate of the column and thus spectra of the solution can be recorded online. If the system has been calibrated with pigment solutions of known concentrations, a quantification of the samples can be performed.

Pigment stoichiometries of isolated FCP sucrose density gradient bands were determined by analytical HPLC, after precipitation of the proteins and extraction of the pigments in 90 % acetone (final concentration). Pigment species were separated on a reversed-phase column (Lichrosorb RP-18, 7 µm, 250 mm x 4 mm), using a two-step linear gradient from 80 % methanol/20 % H_2O to 60 % methanol/40 % acetone. Pigments were identified by their absorption spectra in solution (online diode array detector). For quantification, calibration curves measured on the same HPLC system were obtained using pure chlorophyll *a*, chlorophyll *c*, fucoxanthin (Fx) and diadinoxanthin (Ddx). Pure pigments (Chl *a* was a kind gift by S. Hobe, Mainz; Chl *c*, Fx and Ddx were purchased from DHI Water and Environment, Denmark) were first quantified photometrically, using their extinction coefficients and then injected on the HPLC system and the respective peak areas were recorded. Chl *a* was quantified in 80 % acetone at 431 nm using an extinction coefficient (ε) of 95.82 $lg^{-1}cm^{-1}$ (Lichtenthaler, 1987). Chl *c* was measured in 90 % acetone at 444 nm ($\varepsilon = 374\ lg^{-1}cm^{-1}$) (Jeffrey, 1972). Fucoxanthin and diadinoxanthin concentrations were determined in 100 % acetone at 448 nm ($\varepsilon = 166\ lg^{-1}cm^{-1}$ and $223\ lg^{-1}cm^{-1}$, respectively) (Haugan *et al.*, 1992; Johansen *et al.*, 1974). For an overview of the extinction coefficients, HPLC retention times, HPLC calibration factors and spectra of the related pigments see VIII.3 (pp. 111-112).

III. Results

1. Transformation of Nicotiana tabacum

Before starting to add a His-tag to one of the subunits of photosystem II, a good position has to be elucidated. Since the lumenal space of the chloroplasts is very crowded with the extrinsic proteins of the water oxidising complex (WOC) and the extended loops of CP47 and CP43, which most likely play a role in stabilising the water oxidising complex (Bricker, 1990), difficulties may arise, when trying to introduce a poly-histidine sequence in that particular region. Either the His-tag could be shielded by other proteins, which would render the purification procedures inefficient or the high density of charged residues could prove detrimental to the photosynthetic processes and thus impair the growth of the plants and also reduce the comparability of transgenic to wildtype tobacco plants. Therefore, subunits with both termini on the lumenal side were discarded as possible candidates for mutagenesis. Another important criterion is the proximity to the reaction centre proteins D1 and D2. In order to have the possibility to isolate different subpopulations of photosystem II (super)complexes, the His-tag should be as close to the reaction centre as possible. At the same time, this would guarantee that not only a distal subunit is purified with the His-tag, but that the reaction centre is present in the preparation with high probability. Unfortunately, this excludes any of the nuclear encoded subunits of photosystem II. Due to the small size of the chloroplast genome, it occurs that different genes are encoded on both strands simultaneously. If this is the case, the mutation of one gene is impossible without disrupting the gene on the second strand; hence these genes could not be used for this work, either.

According to these criteria, cytochrome b_{559} is a good candidate for carrying a His-tag. The α-chain, which is encoded by the *psbE* gene, has its N-terminus on the stromal side of the thylakoid membrane and additionally it is very centrally located to the reaction centre. For example in the sub-complexes of photosystem II that were used in the crystallisation experiments of Rhee *et al.*, which had lost the inner antenna protein CP43, the cytochrome b_{559} complex was still present (Rhee *et al.*, 1997; Rhee *et al.*

1998). The major disadvantage of PsbE is that it is encoded by the chloroplast genome, thus making it much less accessible to transformation methods, compared to nuclear encoded genes.

The method of choice for directed mutations in chloroplast encoded genes, is the so called biolistic transformation ("*gene gun*"), which utilises the homologous recombination machinery of the chloroplast to exchange the original sequence with the engineered sequence of interest, after it has been shot into the chloroplast (*see also III.1.5*). Large stretches of identical sequences on the original and engineered DNA increase the probability of homologous recombination (Bock & Hagemann, 2000). Therefore large flanking regions are needed up- and downstream of the gene of interest, leading to final DNA constructs, which are much bigger than the coding sequence of the gene might suggest (Fig. III.1).

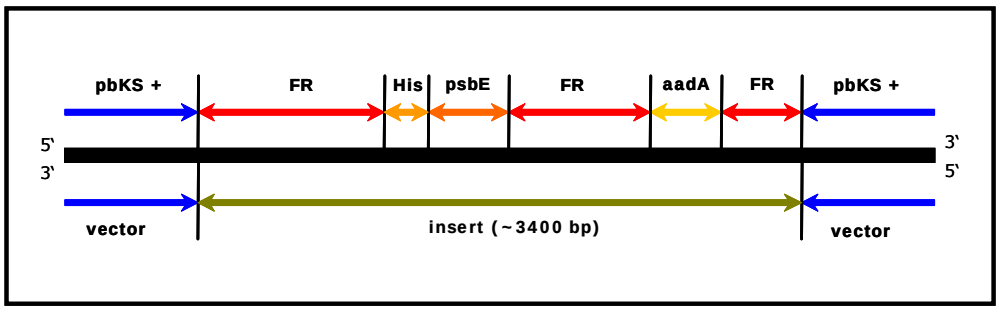

Fig. III.1: Schematic overview of the plasmid DNA used for transformation. pbKS+ = pBluescript II vector (~3.0 kbp); FR = Flanking regions of psbE (~2.1 kbp), His = His-tag (~33 bp), psbE = Cyt b_{559} α-chain (~120 bp), aadA = resistance cassette

1.1 Vector preparation (pbKS+SacI$^-$)

For the biolistic transformation method, large amounts of circular DNA molecules, so called plasmids, are needed to introduce new DNA to chloroplasts. Plasmids have the advantage of being easily modified and amplified in bacterial systems. In order to integrate new pieces of DNA into a plasmid, it is cut with one or more restriction endonucleases, which open the ring-like structure of the molecule. These restriction enzymes recognise specific sequences on DNA strands and cleave them in defined ways. Therefore the sequence of the plasmid should not contain recognition sites for

restriction enzymes, which are used in later modification steps, since this would lead to unwanted cutting of the construct. For the same reasons, the insert has to be checked carefully for any possible recognition sites, which might interfere with the construction of the desired plasmid.

In this case, the SacI restriction site of the pbKS+ bluescript plasmid (commercially available from Stratagene) needed to be eliminated. To this end, copies of the plasmid were produced with the polymerase chain reaction (PCR), but the primers for the reaction were not exactly complementary to the original sequence and thus generated a point mutation at a defined position. After this mutation the SacI restriction endonuclease will no longer recognise the site and cannot cut the molecule anymore. The recognition site for the cleavage by SacI is GAGCTC.

(Template) 5′ - GCC GCC ACC GCG GTG GAG CTC CAA TTC GCC C - 3′
3′ - CGG CGG TGG CGC CAC CTC GAG GTT AAG CGG G - 5′
(Primer) 5′ - GCC GCC ACC GCG GTG GAT CTC CAA TTC GCC C - 3′

(Template) 5′ - GGG CGA ATT GGA GCT CCA CCG CGG TGG CGG C - 3′
3′ - CCC GCT TAA CCT CGA GGT GGC GCC ACC GCC G - 5′
(Primer) 5′ - GGG CGA ATT GGA GAT CCA CCG CGG TGG CGG C - 3′

After the PCR, template DNA is digested with the restriction endonuclease DpnI, which only cleaves methylated DNA. The PCR only produces linear DNA strands, so in order to restore the ring-like structure of the plasmid, the ends of the newly produced DNA strands need to be ligated, before *E. coli* can be transformed with the construct. After successful transformation, clones can be picked, their plasmid DNA isolated and checked with restriction analyses.

Plasmid DNA isolated from several different mutant and control (wildtype/original pbKS+) clones, was subjected to single and double digests with the restriction endonucleases ScaI and SacI. When cutting pbKS+ with both enzymes, two bands appear on the gel, because a big section of the plasmid is cut out (Fig. III.2, lanes 7, 8, 9 and 10). Using only one of the two enzymes with the original plasmid only leads to its linearisation (Fig. III.2, lanes 13, 17 and 18). If the elimination of the SacI cleavage site

was successful, there should only be one band in the double digests of these samples (Fig. III.2, lanes 3, 5 and 6). This shows that the mutation worked for clones M4, M7 and M8. From this point on, clone M7 was used as the basis for the next modification steps.

Lanes:

1) 1 kbp ladder
2) M2 double digest (SacI & ScaI)
3) M4 double digest (SacI & ScaI)
4) M6 double digest (SacI & ScaI)
5) M7 double digest (SacI & ScaI)
6) M8 double digest (SacI & ScaI)
7) WT2 double digest (SacI & ScaI)
8) WT3 double digest (SacI & ScaI)
9) WT4 double digest (SacI & ScaI)
10) pbKS+ double digest (SacI & ScaI)
11) M6 single digest (SacI)
12) M7 single digest (SacI)
13) WT3 single digest (SacI)
14) pbKS+ single digest (SacI)
15) M6 single digest (ScaI)
16) M7 single digest (ScaI)
17) WT3 single digest (ScaI)
18) pbKS+ single digest (ScaI)
19) pbKS+ undigested
20) 1 kbp ladder

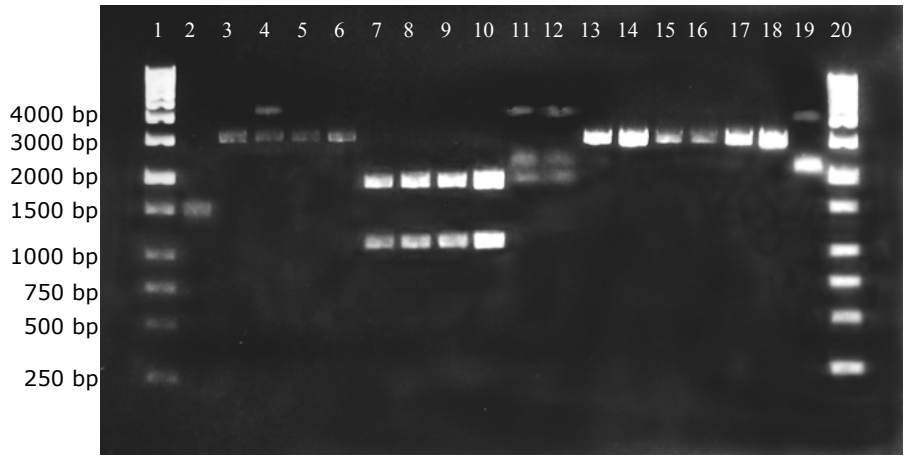

Fig. III.2: Restriction analyses of pbKS+SacI$^-$

1.2 Cloning *psbE* (pbKS+SacI$^-$psbE)

The next step in the preparation of the plasmid for the transformation of tobacco chloroplasts is to insert the gene for the cytochrome b_{559} α-chain (*psbE*) along with large flanking regions into the vector plasmid. The *psbE* gene was cut out as a fragment of 2.3 kbp of the pBR322Sal9 plasmid, using the restriction endonucleases SalI and SpeI. The resulting fragments were separated on a 0.75 % agarose gel, the bands cut out and the DNA extracted. These DNA fragments were then used in ligation experiments

with the vector pbKS+SacI$^-$ (M7), which needed to be cut with SalI and SpeI and dephosphorylised with Shrimp Alkaline Phosphatase, prior to the ligation reaction. XL10 gold competent *E. coli* cells (commercially available from Stratagene) could be transformed with the ligation product, yielding a number of positive clones. The restriction analysis of one of these positive clones (α1) can be seen in Figure III.3. Several single and double digests were carried out and all the required bands appear on the gel, even though some samples were not fully digested (e.g. R5).

R1: pbKS+SacI$^-$psbE single digest (SalI)	1 band, 5.3 kbp
R2: pbKS+SacI$^-$psbE single digest (SacI)	1 band, 5.3 kbp
R3: pbKS+SacI$^-$psbE single digest (EcoRV)	1 band, 5.3 kbp
R4: pbKS+SacI$^-$psbE single digest (SpeI)	1 band, 5.3 kbp
R5: pbKS+SacI$^-$psbE double digest (SpeI, SalI)	2 bands, 3.0 + 2.3 kbp
R6: pbKS+SacI$^-$psbE double digest (SpeI, SacI)	2 bands, 4.7 + 0.6 kbp
R7: pbKS+SacI$^-$psbE double digest (SpeI, EcoRV)	2 bands, 3.6 + 1.6 kbp
M: size marker (HindIII)	

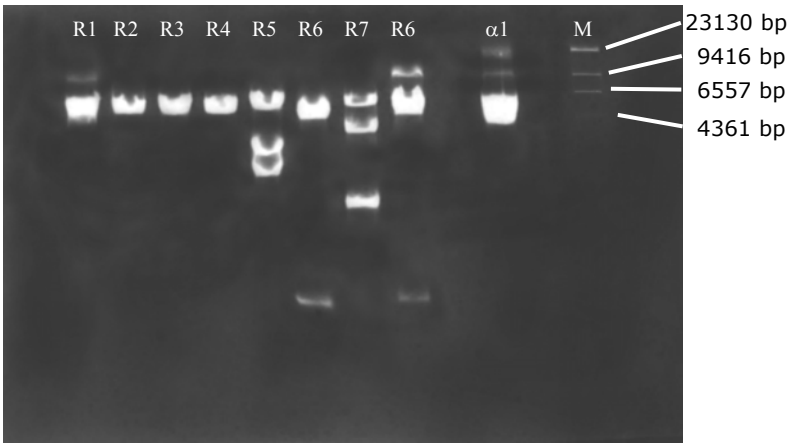

Fig. III.3: Restriction analyses of pbKS+SacI$^-$psbE (α1)

1.3 Inserting His-tags (pbKS+SacI$^-$psbE-His$_{6/10}$)

Using pbKS+SacI$^-$psbE (α1) as a template and altered primers (*see also III.1.1*), DNA fragments were polymerised that contained an additional poly-His coding sequence on the N-terminal side of the *psbE* gene, as compared to the original. These DNA fragments were cut with the restriction enzymes AgeI and SacI and inserted into the

equally cut vector plasmid (α1), yielding four different final constructs: EH1 (pbKS+SacI⁻psbE-His_6NC), EH2 (pbKS+SacI⁻psbE-His_{10}NC), EH3 (pbKS+SacI⁻psbE-His_6C) and EH4 (pbKS+SacI⁻psbE-His_{10}C). These four constructs were used to transform XLI Blue *E. coli* cells and the plasmid DNA, which was prepared from these cells, submitted to sequencing (performed by Seqlab, Göttingen; sequences *see VIII.2*) and checked with restriction analyses, in order to confirm the correctness of the achieved DNA constructs (Fig. III.4).

Reverse primer (P7652): `5′ - CCG AAT GAG CTA AGA GAA TCT T - 3′`

Forward primers (PsbE – His):

a) EH1 = His_6, non cleavable [H_6NC]

`5′ - T TTT GAG CTC AGC ATG CAT CAT CAC CAT CAC CAT TCT GGA AGC ACA GGA GAA CGT - 3′`

b) EH2 = His_{10}, non cleavable [H_{10}NC]

`5′ - T TTT GAG CTC AGC ATG CAT CAT CAC CAT CAC CAT CAC CAT CAC CAT TCT GGA AGC ACA GGA GAA CGT - 3′`

c) EH3 = His_6, cleavable [H_6C]

`5′ - T TTT GAG CTC AGC ATG CAT CAT CAC CAT CAC CAT ATT GAT GGA CGA TCT GGA AGC ACA GGA GAA CGT - 3′`

d) EH4 = His_{10}, cleavable [H_{10}C]

`5′ - T TTT GAG CTC AGC ATG CAT CAT CAC CAT CAC CAT CAC CAT CAC CAT ATT GAT GGA CGA TCT GGA AGC ACA GGA GAA CGT - 3′`

`GAG CTC` – SacI restriction site; `ATG` – Start codon; `CAT`/`CAC` – His codons

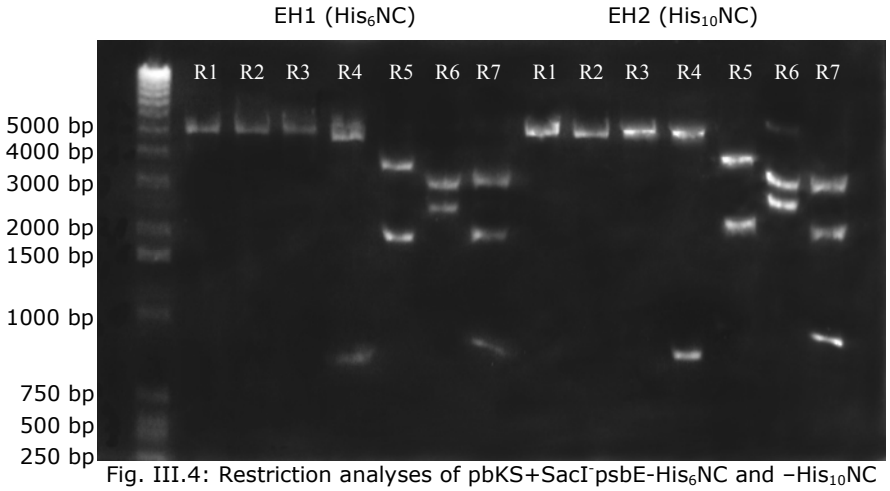

Fig. III.4: Restriction analyses of pbKS+SacI⁻psbE-His_6NC and –His_{10}NC

R1: EH1/2 single digest (SacI)	1 band, 5.3 kbp
R2: EH1/2 single digest (SpeI)	1 band, 5.3 kbp
R3: EH1/2 single digest (SalI)	1 band, 5.3 kbp
R4: EH1/2 double digest (SacI, SpeI)	2 bands, 4.7 + 0.7 kbp
R5: EH1/2 double digest (SacI, SalI)	2 bands, 3.5 + 1.8 kbp
R6: EH1/2 double digest (SpeI, SalI)	2 bands, 3.0 + 2.3 kbp
R7: EH1/2 triple digest (SpeI, SacI, SalI)	3 bands, 2.9 + 1.8 + 0.7 kbp

1.4 Inserting the resistance cassette (pbKS+SacI⁻psbE-$His_{6/10}$-aadA)

After the transformation of the chloroplasts, a resistance gene will be necessary to put a selection pressure on positively transformed plants to separate them from non-transformed plants. In this case a resistance to the antibiotics spectinomycin and streptomycin was added to the *psbE*-His gene sequence on the plasmid, in the form of the aadA cassette. Since the insertion of the resistance cassette is achieved with a so called blunt end ligation, two possible orientations of the inserted sequence may occur, of which only one can be used for the transformation procedure. To check the orientation, an additional restriction analysis is necessary after the cloning experiment. If the orientation is correct, two bands with sizes of 3.9 kbp and 2.5 kbp respectively, will appear. If the orientation is incorrect, two bands with sizes 4.7 kbp and 1.7 kbp respectively will appear, instead. Of the non-cleavable strains, only the clones EH1a/6 and EH2a/4 contained the aadA cassette in the desired orientation (Fig. III.5). The

respective control experiments were also carried out for the His-cleavable lines EH3a and EH4a. These confirmed the tobacco strains EH3a/3, EH4a/21, EH4a/26 and EH4a/28 as positive (data not shown).

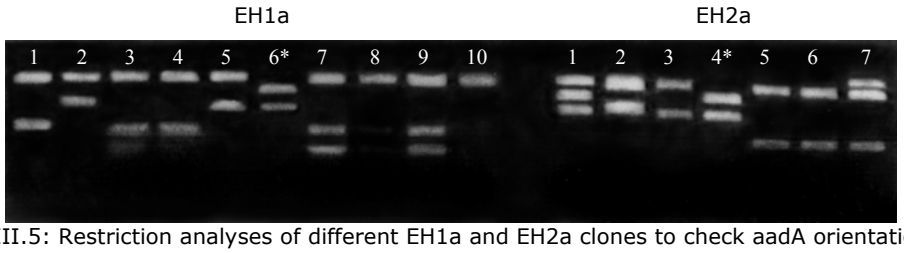

Fig. III.5: Restriction analyses of different EH1a and EH2a clones to check aadA orientation

Final constructs:

EH1a = pbKS+SacI⁻psbE-His_6NC-aadA

EH2a = pbKS+SacI⁻psbE-His_{10}NC-aadA

EH3a = pbKS+SacI⁻psbE-His_6C-aadA

EH4a = pbKS+SacI⁻psbE-His_{10}C-aadA

1.5 Biolistic transformation of tobacco chloroplasts

With the biolistic transformation method, DNA-coated gold particles are shot at leaves of tobacco. These leaves are then cut into smaller pieces and incubated under illumination on a special medium, in order to regenerate whole plants (Fig. III.6).

Fig. III.6: Regenerated tobacco plants under cell culture conditions on antibiotic-containing medium.

Through several rounds of regeneration on antibiotic-containing medium, non-transformed chloroplasts were selectively removed from the population, due to inhibition of chloroplast protein biosynthesis by spectinomycin. After four rounds of regeneration, the genomes of the chloroplasts were checked with PCR methods to confirm the loss of the wildtype form of the gene. For this test, primers are used that theoretically allow the amplification of both, the wildtype and the transgenic form of the gene in question. If only one fragment shows up after the PCR, then only transformed or non-transformed chloroplasts are present in that particular strain of plants. The plants are then called homoplasmic. Since the insertion of the His-tag is an addition to the original gene and not a substitution, a direct increase in size of the PCR fragment of the transgenic strains, compared to the wildtype, can be observed. Due to the fact that the difference in size is very small, polyacrylamide gels were used, instead of agarose gels.

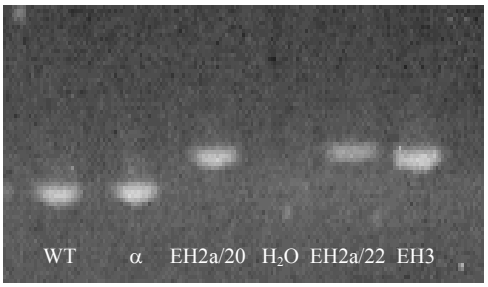

Fig. III.7: PAGE of PCR fragments to confirm His-tags in F1 generations of tobacco plants. Template DNA for the PCR was either derived from total DNA extracts of leaves (WT, 20, 22) or plasmid DNA (α1, EH3) in the case of the controls. Expected sizes for PCR products: WT, α1= 169 bp; EH2a/20, EH2a/22, EH3 = 199 bp. Samples EH2a/20 and EH2a/22 contain a His_{10}-tag. WT = wildtype; α1 = pbKS+SacI$^-$psbE; EH2a = pbKS+SacI$^-$psbE-His_{10}NC-aadA; EH3 = pbKS+SacI$^-$psbE-His_6C

In total, 8 strains (EH1a/13, EH2a/20, EH2a/22, EH2a/34, EH3a/3, EH4a/21, EH4a/26, EH4a/28) have thus been confirmed to be homoplasmic. Of these strains, plants were regenerated to full size and seeds were produced through self fertilisation of the flowers. Since the process of genetic modification with this method is based on the homologous recombination machinery of the chloroplast, it is possible that parts of the gene get lost during the production of the seeds. Therefore, F1 generation plants need to be checked again on the DNA level, to make sure no unwanted modification of the genome occurred. Figure III.7 demonstrates this exemplarily for strains EH2a/20 and EH2a/22. Plants grown from these transgenic seeds showed no differences in speed of

growth or morphology compared to wildtype plants (Fig. III.8) under the chosen culture conditions (25°C, 8 hrs light, 100–150 µE/(s·m^2), 16 hrs darkness, 50 % rel. humidity).

Fig. III.8: Transgenic (EH2a/34) and WT tobacco plants

2. Characterisation of transgenic tobacco

2.1 Chlorophyll content of tobacco leafs

The amount of chlorophyll in wildtype and transgenic tobacco leafs was determined in relation to the leaf area and the leaf fresh weight. Small disks were punched out of the leaves, the pigments extracted with acetone and the respective chlorophyll concentrations photometrically determined. The results are collected in Table III.1.

	Wildtype	EH2a/34
Chl / leaf area [µg/cm^2]	17.6	17.0
Chl / fresh weight [mg/g]	1.25	1.18

Tab. III.1: Chlorophyll content of wildtype and transgenic tobacco leafs

The chlorophyll content in relation to the leaf area as well as in relation to leaf fresh weight is very similar compared between wildtype and transgenic (EH2a/34) tobacco.

This means that under the chosen growth conditions (25°C, 8 hrs light, 100–150 µE/(s·m^2), 16 hrs darkness, 50 % rel. humidity), the addition of the His-tag appears to have no drastic effect on the leaf organisation and the photosynthetic components.

2.2 Oxygen evolution of tobacco thylakoids

Using a standard Clark-type electrode, oxygen evolution rates of preparations of thylakoids of wildtype and transgenic (EH2a/34) tobacco lines were measured at different light intensities. The total chlorophyll concentration was adjusted to 50 µg/ml. Ferricyanide ($K_3[Fe(CN)_6]$) and DCBQ (2,6-Dichloro-p-benzoquinone) were also added to the solution as electron acceptors. The combination of these two acceptors was shown to yield higher oxygen evolution rates, compared to measurements with ferricyanide as the sole electron acceptor in photoactivation experiments with RC-CP47 photosystem II complexes (Büchel *et al.*, 1999).

As can be clearly seen in Figure III.9, the oxygen evolution rates of wildtype and mutant thylakoids differ significantly in their level of saturation and from approximately 1 000 µE/(s·m^2) on, also in the slope of the curve. So, under very high light conditions, wildtype tobacco thylakoids are able to increase their rate of oxygen evolution more strongly than the transgenic tobacco line EH2a/34.

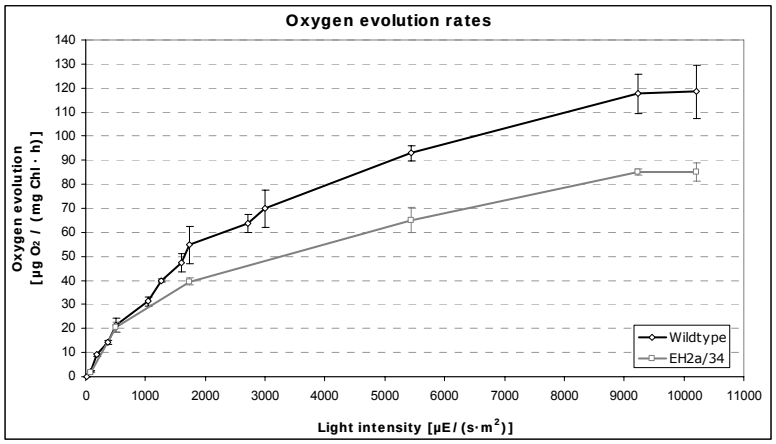

Fig. III.9: Oxygen evolution rates of wildtype and mutant (EH2a/34) tobacco thylakoids measured at different light intensities. Measurement points represent the average of 3 independent measurements; the error bars the standard deviation.

This comparison is carried out at the level of the thylakoids, because it is not possible to purify wildtype photosystem II with Ni-NTA affinity chromatography. Using wildtype tobacco photosystem II isolated with the "classical" preparation method, based on the production of "BBY" particles, would create a low degree of comparability between wildtype and transgenic tobacco samples. Nevertheless, photosystem II reaction centres isolated with Ni-NTA affinity chromatography still retain the ability to evolve oxygen (Piano, D., personal communication).

2.3 Pulse-amplitude modulated (PAM) fluorometry

In principle, chlorophyll fluorescence can function as an indicator at all levels of photosynthetic reactions. This indicator function arises from the fact that fluorescence emission is complementary to the alternative pathways of de-excitation, which are photochemistry and heat dissipation. Generally speaking, fluorescence yield is highest when the yields of photochemistry and heat dissipation are lowest. With a very strong pulse of white light the electron transport chain between the two photosystems can be quickly fully reduced, such that the acceptors in photosystem II become exhausted. Hence, during the saturation pulse, photochemical fluorescence quenching becomes zero and any remaining quenching must be non-photochemical. It is assumed that changes in non-photochemical quenching are too slow to become effective within the approximately one second duration of a saturation pulse. On the basis of these considerations so-called quenching coefficients qP and qN were defined, which can be determined by simple fluorescence measurements. For qP and qN determination it is necessary to measure the extremes of maximal (F_M) and minimal fluorescence (F_0) yield in the dark-adapted state and also the respective values in the light adapted state (F_M' & F_0').

The fluorescence measurements of wildtype and transgenic tobacco show no significant differences between both types, indicating that in both lines photosystem II is working properly. This can be seen in the curves for photochemical (qP) and non-photochemical (qN) quenching (Fig. III.10), which are almost identical. At low light

intensities photochemical quenching is high in both strains, meaning that the absorbed energy is used to drive the photosynthetic reactions and comparatively little energy needs to be dissipated as fluorescence again. With increasing light intensities, the ratio of non-photochemical to photochemical quenching gets higher, until it reaches saturation. At light intensities of 2 000 µE/(s·m^2) or higher, the photosystems are no longer able to utilise all the absorbed light energy to drive the electron transport chain, which leads to a high emission of fluorescence light to dissipate excess excitation energy.

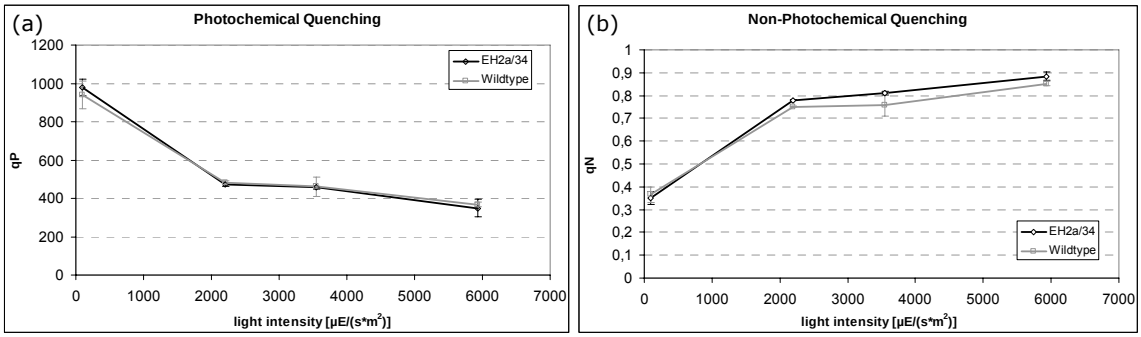

Fig. III.10: (a) Photochemical and (b) non-photochemical quenching of wildtype and transgenic (EH2a/34) tobacco thylakoids measured at different light intensities. Measurement points represent the average of 3 independent measurements; the error bars the standard deviation.

3. Preparation of photosystem II

3.1 Preparation of photosystem II from different tobacco strains

During the rather long and complicated procedure of preparing photosystem II by solubilisation and centrifugation of ground leaf material (Berthold *et al.*, 1981), especially the treatment with the detergent Triton X100 can lead to the degradation of PSII to some extent. In order to isolate PSII under milder conditions, different His-tags have been added to the α-chain of cytochrome b_{559} (*psbE*). In this work, His-tags consist of 6 or 10 consecutive histidine residues, either with or without a cleavage site for the protease "Factor Xa". Histidine residues form complex bonds with nickel ions,

even when these are immobilised on a nitrilotriacetic acid matrix (Ni-NTA). This effect can be used to preferentially attach His-tagged proteins to a Ni-NTA resin, while all other components can be washed away. After the washing, the His-tagged protein can be eluted by adding high concentrations of imidazole to the resin. The imidazole will compete with the histidine residues of the tagged protein for the binding sites on the nickel and, due to the excess of imidazole compared to the amount of protein, it will effectively displace the bound protein from the resin.

3.2 His_6-tag facilitated photosystem II preparation

After solubilisation at final concentrations of 25 mM DDM and 1 mg/ml chlorophyll, tobacco EH1a/13 thylakoids were applied to a Ni-NTA column. The *Nicotiana tabacum* strain EH1a/13 carries a non-cleavable His_6-tag on the cytochrome b_{559} α-chain of PSII. Figures III.11a and III.11b show elution profiles of such a Ni-NTA column PSII preparation.

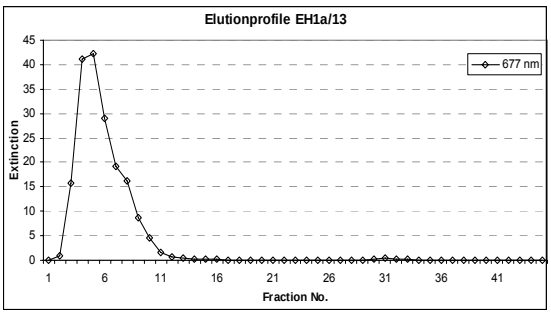

Fig. III.11a

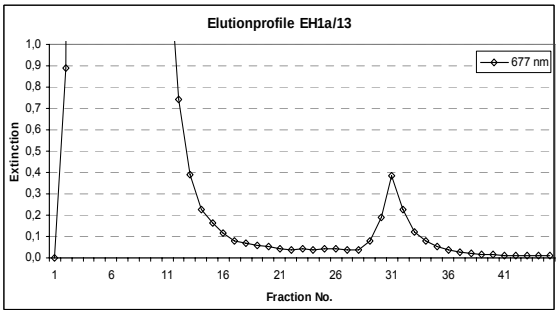

Fig. III.11b

Elution profiles of a tobacco strain EH1a/13 (His_6) Ni-NTA column PSII preparation, eluted with 150 mM imidazole. Extinction measured at 677 nm.

The majority of the solubilised thylakoid sample does not bind to the Ni-NTA matrix and is found in the first few fractions coming off the column (fractions 2–11). After washing with three column volumes of buffer, the absorption at 677 nm is almost reduced to zero (fractions 12–28), which indicates that basically no unbound components are left on the column. By the addition of two column volumes of imidazole-containing buffer (150 mM), the His-tagged proteins are released from the

resin and a peak in the absorption at 677 nm is observed (fractions 29–36). Of the total chlorophyll content detected as peaks after the column run, ~99.2 % are found in the flow through (FT) fractions, whereas ~0.8 % are found in the eluate fractions. Due to the triangular shape of the peaks, the peak area has been approximated with the formula $g \cdot h/2$, with the base width g and the peak height h.

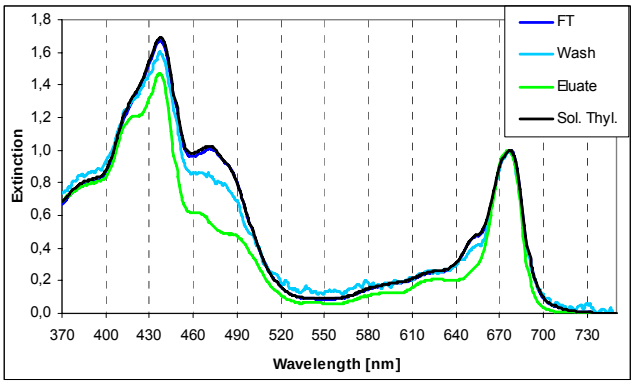

Fig. III.12: Absorption spectra of different Ni-NTA column fractions from an EH1a/13 (His_6) PSII preparation. Flow through (FT) = Fr. 2-11; Wash = Fr. 12-28; Eluate = Fr. 29-36

To characterise the content of each fraction, absorption spectra in the wavelength range from 370 to 750 nm were recorded (Fig. III.12). To achieve better comparability, all spectra were normalised in their absorption in the red peak (maximum between 600-700 nm). The spectra of the solubilised thylakoids and flow through fractions 5 and 8 are almost identical and show the characteristic peaks of the different pigment-protein complexes of the thylakoid membrane. These spectra are largely dominated by the absorption peaks of chlorophyll *a*, chlorophyll *b* and carotenoids. Chlorophyll *b* and high amounts of xanthophylls are bound by the antenna complexes of both photosystem I and photosystem II (Ben-Shem *et al.*, 2003; Liu *et al.*, 2004), but not by the respective reaction centres (Loll *et al.*, 2005). The spectra of the eluate fractions show a drastic decrease in the absorption of chlorophyll *b* and the xanthophylls of the antenna complexes (~ 480 nm). At the same time the lower wavelength shoulder of chlorophyll *a* (~ 420 nm) is more pronounced and the red maximum of the spectrum is shifted from 677 nm to 675 nm. This shift is due to the loss of photosystem I with its very high wavelength absorbing chlorophyll *a* molecules (P700) (Croce *et al.*, 2002).

3.3 His_{10}-tag facilitated photosystem II preparation

The behaviour of tobacco strain EH2a/34, which carries a non cleavable His_{10}-tag at the cytochrome b_{559} α-chain, during the Ni-NTA column preparation is very similar to that of a His_6-tagged strain. Figures III.13a and III.13b show typical elution profiles of Ni-NTA PSII preparations performed with this strain of tobacco.

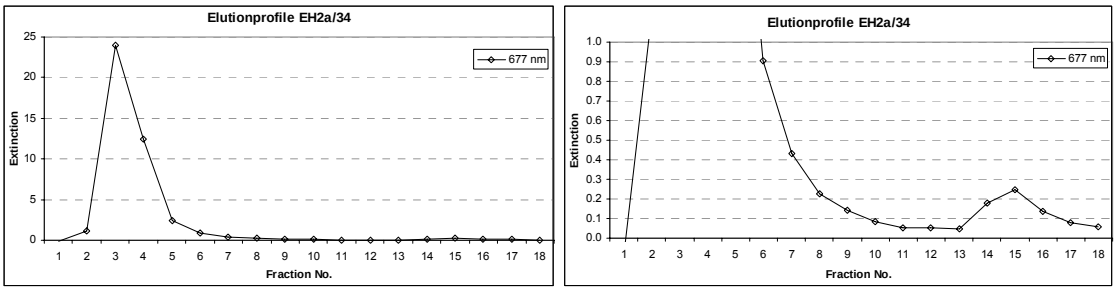

Fig. III.13a Fig. III.13b

Elution profiles of a tobacco strain EH2a/34 (His_{10}) Ni-NTA column PSII preparation, eluted with 150 mM imidazole. Extinction measured at 677 nm.

Again, the majority of the sample does not bind to the Ni-NTA resin and is found in the flow through fractions (fractions 2–6). After washing with three column volumes of buffer, the absorption at 677 nm also decreases to almost zero (fractions 7–13). Comparable to a His_6-tagged tobacco strain, PSII can be eluted from the column by adding imidazole-containing buffer (fractions 14–17). Of the total chlorophyll content detected as peaks in the elution profile, ~99.0 % was found in the flow through fractions, whereas ~1.0 % are found in the eluate fractions. The peak areas were approximated with $g \cdot h/2$.

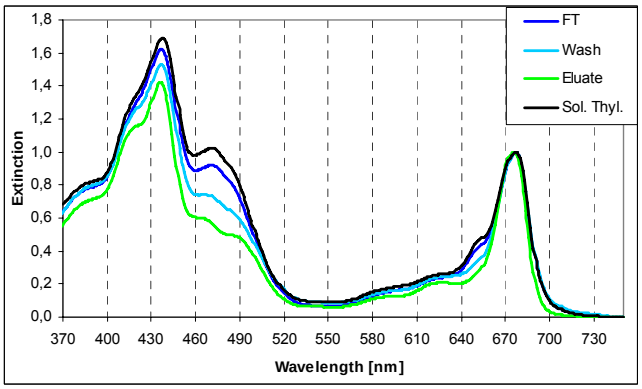

Fig. III.14: Absorption spectra of different Ni-NTA column fractions from an EH2a/34 (His_{10}) PSII preparation. Flow through (FT) = Fr. 2-6; Wash = Fr. 7-13; Eluate = Fr. 14-17

The comparison of absorption spectra of the different fractions of a His_{10}-tagged PSII preparation (Fig. III.14) displays no major differences to the respective spectra of the His_6-tag preparation. Through the binding of PSII to the column matrix, large parts of the Chl *b* and xanthophyll binding pigment-protein complexes can be removed and a fraction enriched in pigment-protein complexes binding mostly Chl *a* can be isolated.

3.4 Wildtype control photosystem II preparation

In contrast to the His-tagged tobacco strains, it is not possible to isolate PSII from wildtype tobacco in the above manner and thus confirming a specific binding to the Ni-NTA matrix in the case of the His-tagged tobacco strains. After the initial flow through fractions (fractions 2–5) and the washing (fractions 6–20), no increase in the absorption at 677 nm occurs, not even after adding the imidazole-containing elution buffer (Fig. III.15a/III.15b).

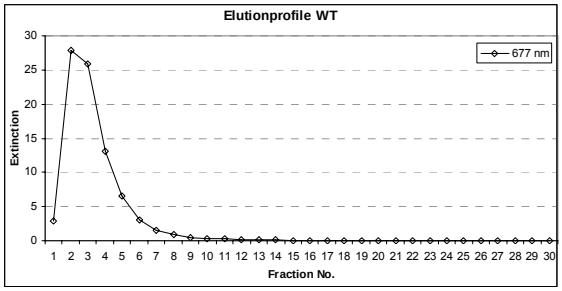

Fig. III.15a

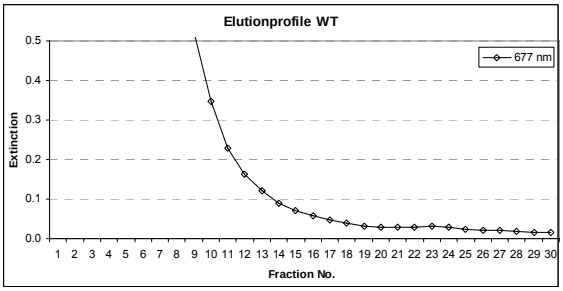

Fig. III.15b

Elution profiles of a wildtype tobacco Ni-NTA column PSII preparation, eluted with 150 mM imidazole. Extinction measured at 677 nm.

In agreement with the elution profiles, the spectra show no qualitative variation between different fractions (Fig. III.16). This means that no specific accumulation of any pigment-protein complex occurs during the column preparation of wildtype tobacco.

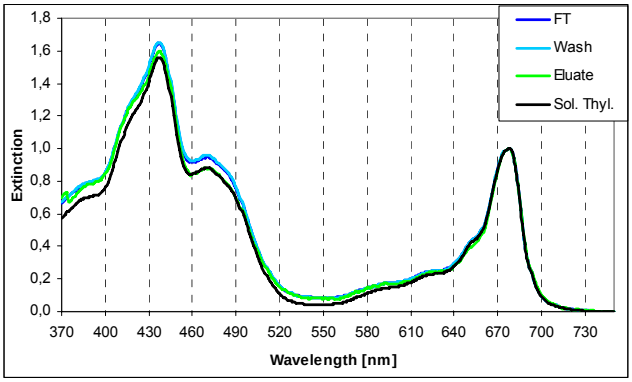

Fig. III.16: Absorption spectra of different Ni-NTA column fractions from a wildtype tobacco PSII preparation. Flow through (FT) = Fr. 2-5; Wash = Fr. 6-20; Eluate = Fr. 21-30

3.5 Protein composition of different column fractions

One method of characterising Ni-NTA column fractions is polyacrylamide gel electrophoresis (PAGE), which gives an overview of the protein composition of the respective fractions, irrespective of their pigmentation.

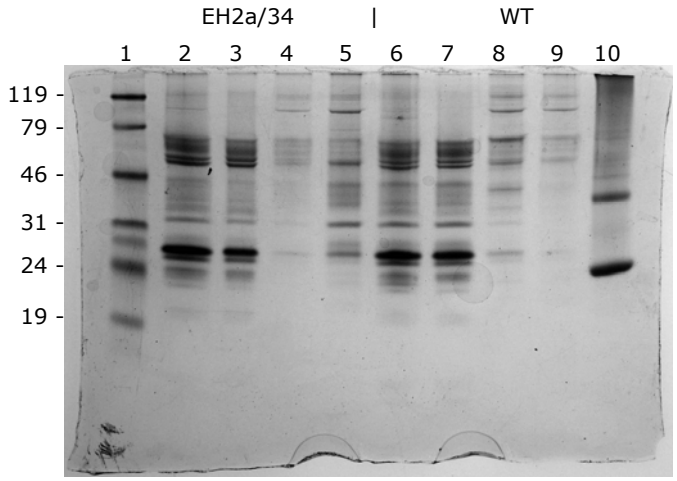

Fig. III.17: SDS-PAGE of Ni-NTA column fractions of an EH2a/34 PSII preparation and a WT control preparation. 1 = prestained protein marker; 2 = EH2a/34 solubilised thylakoids; 3 = EH2a/34 flow through, 4 = EH2a/34 wash fractions; 5 = EH2a/34 eluate fractions; 6 = WT solubilised thylakoids; 7 = WT flow through; 8 = WT wash fractions; 9 = WT eluate fractions; 10 = PsbS (His-tag control)

DDM solubilised thylakoids and the flow through fractions of the Ni-NTA column preparation are very similar in their patterns of bands on a SDS-PAGE (Fig. III.17; lanes 2 & 3 or lanes 6 & 7). Due to the fact that it is the most abundant protein of the

thylakoid membrane, both lanes have strong LHCIIb bands (~27 kDa), but also a high content of PSI (double band, ~60–66 kDa). The 33 kDa extrinsic protein of PSII (PsbO) is clearly visible in these fractions, because it forms a sharply focused band, as opposed to the D1 and D2 reaction centre proteins, which run more diffuse (expected size: D1 = 38 kDa, D2 = 39 kDa). These can be found at much smaller apparent molecular masses (~28–29 kDa) on the gel (for example: Nakazato *et al*., 1996), depending on the presence or absence of tricine in the gel. With tricine in the gel, D1 and D2 are found at higher molecular weights compared to the 33 kDa protein (for example Boekema *et al.*, 1999). Therefore the location of D1 has been determined by western blot analysis (Fig. III.19 & Fig. III.20). In the same region, the bands for the PSII core antenna, namely CP43 and CP47 appear.

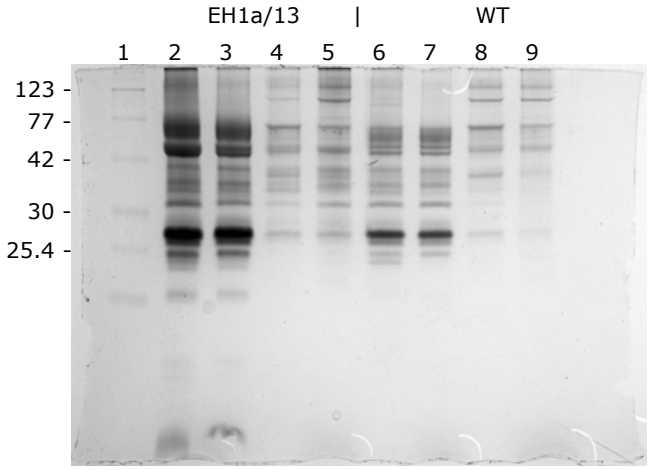

Fig. III.18: SDS-PAGE of Ni-NTA column fractions of an EH1a/13 PSII preparation and a WT control preparation. 1 = prestained protein marker; 2 = EH1a/13 solubilised thylakoids; 3 = EH1a/13 flow through, 4 = EH1a/13 wash fractions; 5 = EH1a/13 eluate fractions; 6 = WT solubilised thylakoids; 7 = WT flow through; 8 = WT wash fractions; 9 = WT eluate fractions

Compared to the flow through, the washing fractions contain the same distribution of proteins, although at much lower concentrations (Fig. III.17; lane 4 or lane 8). Even with roughly ten times concentrated samples, only very weak bands can be observed.

In contrast to the washing fractions, the eluate fractions of EH2a/34 contain only specific proteins of the solubilised thylakoids (Fig. III.17, lane 5). The amounts of PSI and LHCIIb are drastically reduced, whereas the strength of the signals for D1, D2, CP47, CP43 and the 33 kDa extrinsic protein are comparable to the respective signals of the solubilised thylakoids. The eluate fractions have also been concentrated about ten fold, before the application to the gel.

The wildtype control lane (Fig. III.17, lane 9) for the eluate fractions is very similar to the wildtype washing fractions and does not show a different band pattern, but instead only the overall protein concentration is decreased.

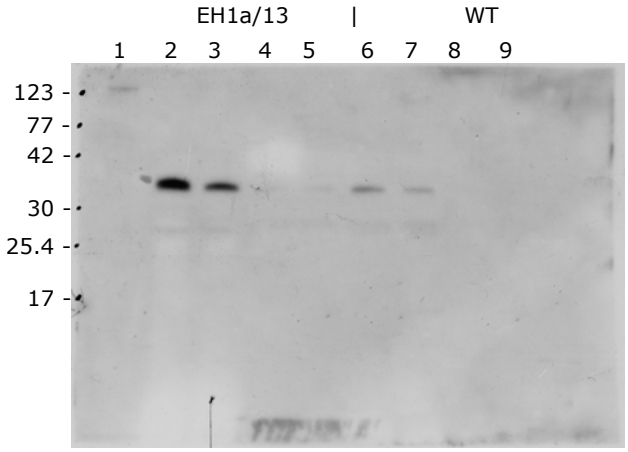

Fig. III.19: Western blot of a SDS-PAGE (Fig. III.18) of Ni-NTA column fractions of an EH1a/13 PSII preparation and a WT control preparation, treated with an antibody against D1. 1 = prestained protein marker [kDa]; 2 = EH1a/13 solubilised thylakoids; 3 = EH1a/13 flow through, 4 = EH1a/13 wash fractions; 5 = EH1a/13 eluate fractions; 6 = WT solubilised thylakoids; 7 = WT flow through; 8 = WT wash fractions; 9 = WT eluate fractions

As could already be seen in the comparison of the respective absorption spectra of the Ni-NTA column fractions, there is virtually no difference between His_6 and His_{10} purifications. This is also true for the pattern of bands in polyacrylamide gels (Fig. III.17, Fig. III.18).

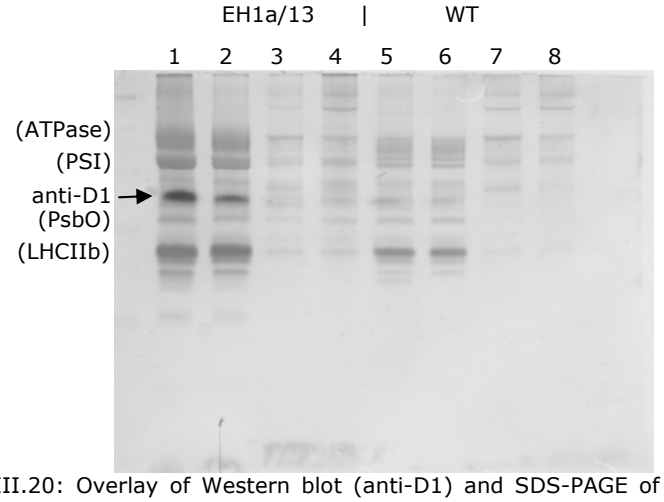

Fig. III.20: Overlay of Western blot (anti-D1) and SDS-PAGE of Ni-NTA column fractions of an EH1a/13 (His_6) PSII preparation and a WT control preparation. 1 = EH1a/13 solubilised thylakoids; 2 = EH1a/13 flow through, 3 = EH1a/13 wash fractions; 4 = EH1a/13 eluate fractions; 5 = WT solubilised thylakoids; 6 = WT flow through; 7 = WT wash fractions; 8 = WT eluate fractions. Designations in parentheses according to molecular mass.

3.6 Two-dimensional crystallisation of photosystem II

It has been shown that it is possible to form two-dimensional crystals out of purified photosystem II complexes (Nakazato *et al.*, 1996). The analysis of two-dimensional crystals also led to a three-dimensional model of the photosystem II RC-CP47 subcomplex, containing D1, D2, CP47, cytochrome b_{559} and a number of small non-pigmented subunits (Rhee *et al.*, 1997; Rhee *et al.*, 1998). Two-dimensional crystals of membrane proteins can be achieved by solubilising the protein of interest, together with certain lipids, with detergents. When the detergent is later removed, for example by dialysis, the proteins can be arranged in an orderly manner (Kühlbrandt, 2003).

15 mM KCl	- -	1.0 mM $CuCl_2$	- -
15 mM KCl	- -	2.0 mM $CuCl_2$	- -
15 mM KCl	- -	3.0 mM $CuCl_2$	- -
15 mM KCl	- -	5.0 mM $CuCl_2$	- -
15 mM KCl	- -	1.0 mM $CoCl_2$	- -
15 mM KCl	- -	2.0 mM $CoCl_2$	- -
15 mM KCl	- -	3.0 mM $CoCl_2$	- -
15 mM KCl	1.0 mM $ZnCl_2$	1.0 mM $CaCl_2$	0.1 mM $FeNO_3$
15 mM KCl	1.0 mM $ZnCl_2$	1.0 mM $CaCl_2$	0.3 mM $FeNO_3$
15 mM KCl	1.0 mM $ZnCl_2$	1.0 mM $CaCl_2$	0.6 mM $FeNO_3$
15 mM KCl	1.0 mM $ZnCl_2$	1.0 mM $CaCl_2$	0.1 mM $CoCl_2$
15 mM KCl	1.0 mM $ZnCl_2$	1.0 mM $CaCl_2$	0.3 mM $CoCl_2$
15 mM KCl	1.0 mM $ZnCl_2$	1.0 mM $CaCl_2$	0.1 mM $CuCl_2$
15 mM KCl	1.0 mM $ZnCl_2$	1.0 mM $CaCl_2$	0.3 mM $CuCl_2$
15 mM KCl	1.0 mM $ZnCl_2$	1.0 mM $CaCl_2$	0.5 mM $MnSO_4$
15 mM KCl	1.0 mM $ZnCl_2$	1.0 mM $CaCl_2$	1.0 mM $MnSO_4$
15 mM KCl	1.0 mM $ZnCl_2$	1.0 mM $CaCl_2$	1.5 mM $MnSO_4$

Tab. III.2: Salt conditions during 2D crystallisation of spinach RC-CP47 complexes

Additives in the dialysis buffer can have strong effects on the quality of 2D crystals. Therefore a series of salts was tested out for their effects on the formation of photosystem II RC-CP47 crystals (Tab. III.2). RC-CP47 complexes were isolated from spinach (*Spinachia oleracea*) with the solubilisation and centrifugation method (*see II.2.11*).

After the dialysis of the sample, crystals were harvested and evaluated with electron microscopy after negative staining with uranyl acetate. Of the different combinations of salts that have been tested, only the condition with 15 mM KCl, 1.0 mM $ZnCl_2$, 1.0 mM $CaCl_2$ and 0.3 mM $CoCl_2$ showed any improvement to the standard conditions

(15 mM KCl, 1.0 mM $ZnCl_2$, 1.0 mM $CaCl_2$), with crystals showing spots up to the 5th order after Fast Fourier Transformation (FFT) of the electron micrograph (Fig. III.21).

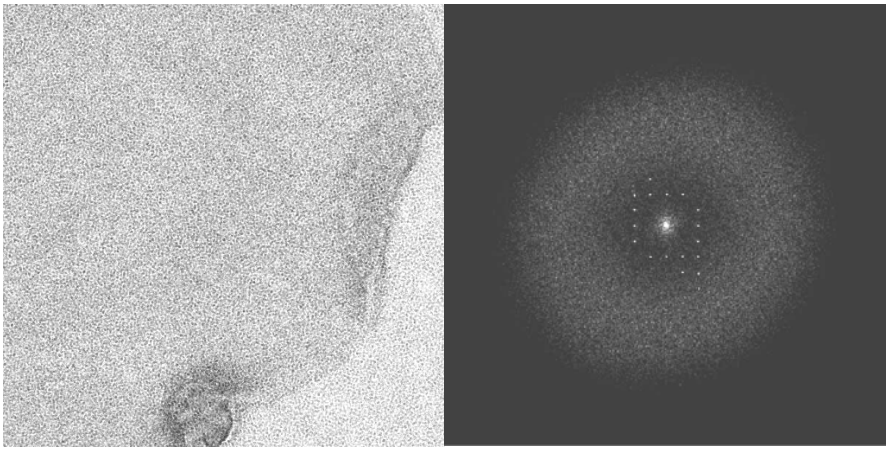

Fig. III.21: (a) Electron micrograph of a RC-CP47 2D crystal after negative staining (53 000x magnification); (b) Fast Fourier Transformation of the electron micrograph

4. Characterisation of fucoxanthin-chlorophyll-proteins

Although the light harvesting antenna proteins, the so called fucoxanthin-chlorophyll-proteins (FCPs), of diatoms show a significant protein sequence homology to the antenna proteins of higher plants (Eppard & Rhiel, 1998), very little is known about their structural and biochemical characteristics. Despite the sequence similarities, plant and diatom antenna proteins differ greatly in their pigmentation. The LHC proteins of higher plants bind Chl *a*, Chl *b*, lutein, neoxanthin and violaxanthin, whereas the FCPs of diatoms bind Chl *a*, Chl *c*, fucoxanthin, diadinoxanthin and diatoxanthin.

In order to get a more detailed picture of its pigmentation, HPLC measurements were carried out, using pigment extracts of FCP preparations. Fucoxanthin-chlorophyll-proteins were isolated from *Cyclotella meneghiniana* by sucrose gradient ultra-centrifugation after solubilisation of diatom thylakoid preparations. Band 1 of the sucrose gradient contains mostly trimers of FCP, which consist of 18 kDa peptides, together with some free pigment. Band 2 consists of a mix of trimers and higher oligomers (~50 % 18 kDa, ~50 % 19 kDa peptides). In band 3 mostly higher oligomers,

formed by 19 kDa peptides, are found (Büchel, 2003). The results of the pigment determination are collected in Table III.3. Although the bands of the sucrose gradient vary significantly in their protein composition and oligomerisation state, the pigmentation of these bands is characterised by a remarkable homogeneity.

	Chl c2	Fx	Ddx	Dtx (ca.)	Chl a (m)
band 1					
average	0,26	1,00	0,12	0,10	1
stdev	0,06	0,08	0,01	0,04	0
percentage	21,60	8,34	12,20	38,95	0
band 2					
average	0,27	0,97	0,07	0,05	1
stdev	0,06	0,11	0,03	0,03	0
percentage	20,33	10,89	37,93	50,94	0
band 3					
average	0,24	0,85	0,04	0,04	1
stdev	0,01	0,04	0,01	0,02	0
percentage	5,61	5,06	30,75	48,13	0

Tab. III.3: Pigment-pigment stoichiometries of sucrose gradient bands of solubilised *C. meneghiniana* thylakoids normalised to 1 Chl *a* molecule. Pigments extracted in 90 % acetone and subjected to HPLC. Band 1: Trimers (18 kDa peptides), some free pigment; Band 2: Trimers & higher oligomers (~50 % 18 kDa, ~50 % 19 kDa peptides); Band 3: Higher oligomers (19 kDa peptides).

The transfer of excitation energy between fucoxanthin, chlorophyll *c* and chlorophyll *a* was studied by ultra-fast transient absorption measurements (Papagiannakis *et al.*, 2005). These so called pump probe measurements were performed with an amplified Ti:sapphire laser system (Gradinaru *et al.*, 2000; Larsen *et al.*, 2004). The resulting kinetic absorption traces provide some general information about the localisation of the excitation energy in the FCP at a given time after the initial excitation. These were further evaluated with global and target analyses (Holzwart, 1996; van Stokkum *et al.*, 2004a; van Stokkum *et al.*, 2004b), which require a model of the complex of interest. One part of this model is the pigment stoichiometry of the complex. The target analysis of the measured absorption spectra led to the elucidation of parts of the excitation energy transfer network in the FCP.

After the excitation of fucoxanthin at 530 nm, efficient excitation energy transfer to chlorophyll *a*, occurring in multiple steps, was observed (Tab. III.4), but not all fucoxanthin molecules transfer energy equally efficient. The chlorophyll *c* to chlorophyll *a* excitation energy transfer is extremely fast, indicating a centrally located

position in the complex for chlorophyll *c*, but no evidence for a possible chlorophyll *c* to fucoxanthin energy transfer could be found (Papagiannakis *et al.*, 2005).

	S_2	Unrelax. S_1/ICT	S_1/ICT	Slow S_1/ICT	Chl *a*
Lifetime	75 fs	320 fs	2.6 ps	31 ps	7.5 ps, 112 ps, 3.9 ns
Efficiency [%]	40%	20%	90%	5%	

Tab. III.4: Lifetimes and the energy transfer efficiencies determined by target analysis. The first four columns correspond to the excited states of fucoxanthin and the fifth to the Chl *a* compartments. The % efficiency refers to the fraction of the population of the specific state that goes to Chl *a*. The error in estimating the lifetimes within the specific model is ± 5 % (Papagiannakis *et al.*, 2005).

IV. Discussion

1. Photosystem II

Although the process of photosynthesis is the main source of molecular oxygen in earth's atmosphere and extensive studies have been carried out over a long course of time, it is still not fully clear how the biophysical and biochemical reactions work on a molecular basis. Many of these difficulties can be attributed to the high complexity of the photosystems, which carry out the primary photosynthetic reactions, namely light-absorption, charge separation and energy conversion. One approach to gather information about the mode of operation of the photosystems is to solve their structures; the idea being that after the structure of a complex is known, its reaction mechanism can be discussed on the basis of the locations of its cofactors and the amino acid side chains. Powerful methods for structure determination are two-dimensional and three-dimensional crystallisation. Both have their respective advantages and disadvantages, but share a common problem. In order to get well ordered crystals, a prerequisite for detailed structural data, protein preparations of high concentration, high homogeneity and high purity are needed. Especially with photosystems this goal is very difficult to achieve. For example photosystem II has more than twenty different subunits (Tab. I.1), which form more or less stable supercomplexes in the thylakoid membrane (Boekema *et al.*, 1995). Nevertheless, good crystals have been produced with photosystem II preparations from cyanobacteria, which led to very good models with almost complete cofactor assignment and tracing of most amino acid side chains (Fig. IV.1) (Ferreira *et al.*, 2004; Loll *et al.*, 2005). The photosystem II core complexes, which were used for these crystallisation experiments, were isolated from the thermophilic cyanobacterium *Thermosynechoccocus elongatus* by solubilisation of the membranes with β-dodecylmaltoside, followed by two anion exchange column chromatographies (Kern *et al.*, 2005). The advantage of working with thermophilic organisms like *T. elongatus* is the relative high stability that can be expected of the important enzyme complexes, due to the ecological niches the organisms occupy.

Obviously this is not the case for higher plants. In order to achieve the higher stability, there have to be some differences between the photosystem structures of thermophilic cyanobacteria and plants. Therefore finding a way of isolating plant photosystem II in a quicker and milder procedure could prove very valuable for future crystallisation experiments or studies that require pure and intact photosystem preparations in general. To this end, four different His-tags were added to one of the subunits of photosystem II. The His-tags, which were used in this work, consist of six or ten consecutive histidine residues, either with or without a cleavage site for the protease "Factor Xa". A His-tagged protein opens up the possibility to perform Ni-NTA affinity chromatography, which generally yields fractions of purified protein after only one isolation step.

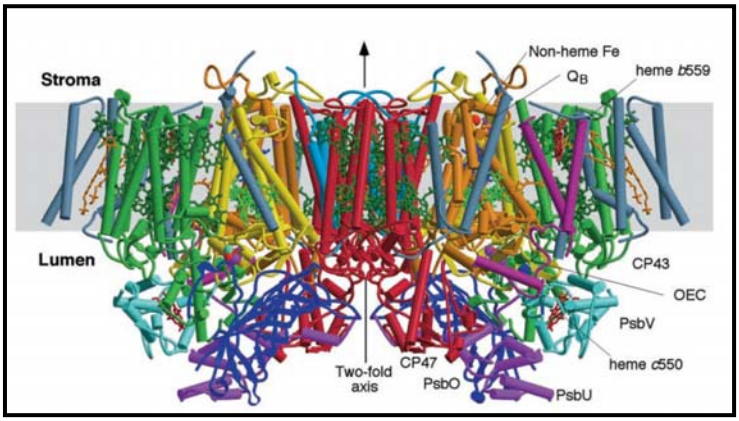

Fig. IV.1: View of the PSII dimer perpendicular to the membrane normal. Helices are represented as cylinders with D1 in yellow; D2 in orange; CP47 in red; CP43 in green; Cyt b_{559} in wine red; PsbL, PsbM, and PsbT in medium blue; and PsbH, PsbI, PsbJ, PsbK, PsbX, PsbZ, and the putative PsbN in grey. The extrinsic proteins are PsbO in blue, PsbU in magenta, and PsbV in cyan. Chlorophylls of the D1/D2 reaction centre are light green, pheophytins are blue, chlorophylls of the antenna complexes are dark green, β-carotenes are in orange, hemes are in red, non-heme Fe is red, Q_A and Q_B are purple. The oxygen-evolving centre (OEC) is shown as the red (oxygen atoms), magenta (Mn ions), and cyan (Ca^{2+}) balls (Ferreira *et al.*, 2004).

In the past, His-tags have been added to photosynthetic complexes of prokaryotic organisms, like purple bacteria and cyanobacteria, but also in eukaryotic organisms, like green algae.

With this approach it was possible to purify *Rhodobacter sphaeroides* (purple bacteria) reaction centres, after fusing a His-tag to the C-terminus of the M-protein, which is homologous to the D2 protein of oxygenic photosynthetic organisms. The isolated reaction centres showed no differences to wildtype reaction centres in room temperature absorption spectra, 77 K absorption spectra and $P^+Q_A^-$ charge recom-

bination rate and yield, suggesting that in this case the newly inserted poly-histidine sequence had no negative effect on the photosynthetic reactions (Goldsmith & Boxer, 1996).

By adding a His-tag to the photosystem II core antenna protein CP47 in *Synechocystis* PCC 6803 (cyanobacteria), highly active PSII complexes could be isolated with Ni-NTA chromatography, which were almost indistinguishable from wildtype PSII complexes. One major difference was found between the respective isolates, the His-tagged photosystem II preparation had a significantly higher cytochrome c_{550} (PsbV) content, compared to the wildtype preparations. The cytochrome c_{550} content of these preparations was comparable to that of photosystem II preparations by anion exchange chromatography of the thermophilic organism *Synechococcus lividus*. In this way it could be confirmed that by using a His-tag, PSII preparations can be obtained from non-thermophilic organisms, which retain high amounts of the extrinsic proteins of the oxygen evolving complex. Electron paramagnetic resonance (EPR) spectra of the His-tagged *Synechocystis* photosystem II preparations suggest not only a structural, but also a functional homology between the cytochrome c_{550} of cyanobacteria and the 17 kDa (PsbQ) and 23 kDa (PsbP) extrinsic proteins of the higher plant oxygen evolving complex (Lakshmi *et al.*, 2002).

In a different mutational study, a His-tag has been fused to the C-terminus of the core antenna protein CP47 of the green alga *Chlamydomonas reinhardtii* (Suzuki *et al.*, 2003). The reaction centre particles isolated with Ni-NTA chromatography from these transgenic green algae strains also yielded oxygen evolving photosystem II complexes. The oxygen evolution rates of these particles were the highest, if ferricyanide was used as artificial electron acceptor when $CaCl_2$ was also present. On the other hand, oxygen evolution rates could not be increased by the addition of calcium, when DCBQ or other quinine-type compounds were used as electron acceptors. In both cases DCMU did not significantly inhibit the oxygen evolution of the PSII particles. This suggests a disturbance of the Q_B binding site in these transgenic photosystem II particles (Suzuki *et al.*, 2003). Both, the C-terminus of CP47 and the Q_B binding site are located on the stromal side of the thylakoid membrane, i.e. the His-tag might lead to an actual disturbance of the quinone and DCMU binding capacity of the reaction centre. It appears that less interference with the photosynthetic reactions occurs, when the His-

tag is somewhat further removed from the reaction centre proteins. For example, $P680^+$ reduction kinetics studies of photosystem II preparations from *C. reinhardtii*, carrying a His-tag on the C-terminus of the PsbH protein, displayed no differences to the kinetics of wildtype spinach "BBY" particle preparations (Jeans *et al.*, 2002). The PsbH protein is located a bit more in the periphery of PSII, on one side of CP47, adjacent to cytochrome b_{559} (Büchel *et al.*, 2001; Loll *et al.*, 2005), with its C-terminus exposed on the lumenal side of the membrane.

In some cases the genetically engineered organisms showed either a distinctive phenotype compared to the respective wildtype or lost their ability to grow photo-autotrophically all together. The latter was the case for a *C. reinhardtii* strain, which carried an N-terminal His_6-tag on the D1 reaction centre protein, although the N-terminus of D1 is located on the stromal side of the thylakoid membrane and the particles were still capable of oxygen evolution, albeit only up to 30 % the amount of the wildtype algae. Even though the C-terminus of D2 lies on the very crowded lumenal side of the reaction centre (Fig. IV.1), photosystem II particles could be isolated by introducing a His_6-tag at this location. The maximal oxygen evolution rates of this strain were reduced to about 80 % of the capacity of wildtype *Chlamydomonas reinhardtii*, although measurements of thermoluminescence glow curves, which are used to characterise S_2-Q_B^- charge recombination events, were basically identical between transgenic and wildtype cells, thus giving an indication for the intactness of photosystem II (Sugiura *et al.*, 1998). These findings are comparable to the situation in this work. Not only are the band patterns for the proteins of the reaction centre (D1, D2, CP43, CP47, PsbO) in polyacrylamide gel electrophoresis of this work (Fig. III.17 & Fig. III.18) very similar, when compared to those in Sugiura *et al.* (1998), but also maximal oxygen evolution rates of thylakoid membranes isolated from transgenic tobacco strains are lower when compared to wildtype tobacco. At the same time, pulse amplitude modulated (PAM) fluorescence measurements displayed no significant alterations between transgenic and wildtype plants, so that it can be safely assumed, that photosystem II is intact in both cases. It is rather the ratio of photosystem II to the other pigmented components of the thylakoid membrane which appears to be reduced in the transgenic tobacco strains. This would lead to diminished maximal oxygen evolution rates in relation to the amount of chlorophyll in the thylakoid samples. The

reduced amount of photosystem II could be ascribed to a reduction of available PsbE. In PsbE deletion mutants of *Chlamydomonas reinhardtii* no photosystem II activity could be detected, neither in oxygen evolution assays nor by measuring variable chlorophyll fluorescence. Western blot analyses of light adapted cells of these mutants, using antibodies against D1 and D2 revealed the absence of both proteins. Dark adapted cells, which were tested with antibodies against D1, D2, cytochrome b_{559} and CP47 yielded no signal for any of these subunits (Morais *et al.*, 1998). Furthermore, mutational studies of the cyanobacterium *Synechocystis* PCC 6803 demonstrated a dependency of the amount of D2 in thylakoid preparations on the presence of cytochrome b_{559} (Shukla *et al.*, 1992). So if the addition of the His-tag to the N-terminus of PsbE has any detrimental effects on the translation, correct folding or membrane-insertion of PsbE, then this would result in a correlated reduction of the number of assembled photosystem II complexes. In general, some of the smaller subunits of photosystem II seem to be important for the assembly of the complex. For example, PsbJ deletion mutants of *Nicotiana tabacum* could not grow photoautotrophically, due to defects in the oxygen evolving complex and hypersensitivity to light (Hager *et al.*, 2002). Since PsbE and PsbJ are encoded in the same operon (EFLJ-operon) (Pakrasi *et al.*, 1991), it is also imaginable that a mutation of the *psbE* gene could negatively influence the transcription of *psbJ*, which in turn could lead to the observed reduction in photosystem II complexes in the thylakoid membrane.

Overall, the effects on the structure and function of photosystem II caused by mutations of cytochrome b_{559} are difficult to judge, since the role this cytochrome plays is not yet fully investigated. Cytochrome b_{559} is a crucial component of photosystem II and is capable of displaying photooxidation and photoreduction of its heme group. Furthermore, it is attributed a role in protecting photosystem II from photoinhibition by re-reducing chlorophylls, after they have been oxidised by $P680^+$ (Thompson & Brudvig, 1988) and – more importantly – by donating electrons to $P680^+$, if it is not quickly reduced by Y_Z. This flow of electrons is mediated by a membrane embedded β-carotene molecule, which acts as a molecular wire (Faller *et al.*, 2001). Another possible reaction of cytochrome b_{559} in its low-potential form is the re-oxidation of plastohydroquinones of the plastoquinone pool in the dark (Kruk & Strzalka, 1999;

Bondarava *et al.*, 2003), to prevent a lack of available plastoquinone once the photosynthetic electron flow is started again by illumination.

After the transformation of tobacco chloroplasts, it is now possible to isolate His-tagged higher plant photosystem II by Ni-NTA chromatography (*see III.3*). The comparison of the absorption spectra of the different column fractions (Fig. III.12 & Fig. III.14) shows the loss of large amounts of chlorophyll *b* binding proteins and a shift of the red chlorophyll absorption maximum (Q_y), which can be attributed to the removal of photosystem I. The major light-harvesting complex II (LHCIIb) is the most abundant pigment-protein complex of the thylakoid membrane (Peter & Thornber, 1991) and binds large amounts of not only xanthophylls and chlorophyll *a*, but also chlorophyll *b*, in contrast to the reaction centre complex, which does not bind chlorophyll *b* at all. So, a reduction of the amount of chlorophyll *b* corresponds to a removal of the peripheral antenna proteins (Lhcb1-Lhcb6) from the sample.

The high amount of LHCIIb in the thylakoid preparations is also reflected in the band pattern after gel electrophoresis (Fig. III.17 & Fig. III.18), although it has to be pointed out that the assignment of bands for photosystem II and thylakoid samples is rather difficult. The sequence of the bands can vary quite dramatically with the chosen electrophoresis assay. This is especially true for the reaction centre proteins D1 and D2 ('D' stands for diffuse in electrophoresis), which can be found either at higher apparent molecular mass (Boekema *et al.*, 1999) or lower apparent molecular mass than the 33 kDa extrinsic protein (PsbO) band (Nakazato *et al.*, 1996; Hankamer *et al.*, 1997; Morris *et al.*, 1997), depending on the presence or absence of tricine in the gel. Therefore the actual assignment of the bands to certain subunits of the photosystems remains somewhat preliminary unless it is verified by other methods, like western blotting (Fig. III.20) or MALDI TOF mass spectrometry.

Due to the high degree of complexity and adaptability of the thylakoid membrane, the yield of the PSII purification procedure is difficult to assess. A yield, evaluated on the basis of chlorophyll, of around 1 % appears to be very low, but it has to be taken into consideration that a large number of chlorophylls are bound to photosystem I, the light-harvesting complexes of PSI and the light-harvesting complexes of PSII. All these components are supposed to be removed during the purification procedure; i.e. these chlorophylls should not be found in the purified photosystem II fraction. In the

thylakoid membrane the ratio of chlorophylls per reaction centre is around 400:1 for photosystem I and around 590:1 for photosystem II (Wild *et al.*, 1986). Of these chlorophylls, only 42 are bound to the photosystem II reaction centre core proteins (D1, D2, CP47, CP43) (Ferreira *et al.*, 2004). This means the maximum theoretical yield for pure photosystem II cores, isolated from thylakoid membranes is around $^{42}/_{590}$ = 7.1 %. Taking this as the maximum, the actual yield of the purification reaches a value of ~14 %. Of course the significance of this number depends on the growth conditions of the plants and the related light adaptations of the photosynthesis apparatus, as well as the purity of the preparation.

In respect to the yield, the PSII purity and the growth of the plants, no significant differences between the different His-tagged plant strains were observed; i.e. using a considerably longer His_{10}-tag compared to a His_6-tag on cytochrome b_{559}, did not lead to an improvement of the yield or the purity of the photosystem II preparation.

Another advantage of isolating photosystem II with the His-tag method is the opportunity to find the most suitable detergent for subsequent experiments, like for example, 2D crystallisation. The formation of 2D crystals occurs after the solubilisation of the protein with detergent and later removal of the detergent by dialysis, which energetically forces the solubilised membrane proteins to form ordered arrays (Kühlbrandt, 2003). Therefore the choice of detergent is critical for successful crystallisation, because the duration of dialysis, the size of the micelles and the ability to solubilise membrane proteins are characteristic for each detergent. Besides, especially in 2D crystallisation experiments the choice of detergent is not only critical for the formation of crystals in the first place, but also plays a decisive role for the shape the crystalline membranes can adopt. The most common shapes of two-dimensional crystals are single layer membrane sheets, tubular crystals or vesicular crystals. The advantage of tubes and sheets is the possibility to grow crystals without being confined to a limited area, like it is the case for vesicles, i.e. it is desirable to grow 2D crystals as sheets or tubes. Since the His-tag purification method is not dependent on a specific detergent and its related solubilisation characteristics, as opposed to, for example, the "BBY" protocol by Berthold *et al.* (1981), where in a first step grana particles are formed by partial detergent solubilisation of the thylakoid membrane, no systematic limitation for the formation of 2D crystals caused by the

purification method exists. Another important factor for the quality and size of 2D crystals are additives in the dialysis buffer. Although these substances are only present in low concentrations, they can have strong effects on the crystallisation process. In the case of salts as additives, these effects are for example based on the neutralisation of charges, which would repulse each other if they were brought in close proximity to each other, either on the protein or on bound lipid or detergent molecules. Divalent ions can also function as a connecting element, when two charges on adjacent proteins are neutralised by one ion. Therefore, preliminary experiments concerning the effects of ionic additives on the crystallisation of photosystem II, isolated from spinach by the solubilisation and centrifugation method, were carried out. In these, the addition of 0.3 mM $CoCl_2$ to the standard dialysis buffer, led to an improvement of the crystals. The quality of the crystals was evaluated by Fast Fourier Transformation of digital electron micrographs. Crystallisation trials of spinach PSII with $CoCl_2$ in the dialysis buffer, showed spots of up to two orders higher, compared to the standard conditions.

2. Energy transfer in fucoxanthin-chlorophyll-proteins

Pigment analyses of fucoxanthin-chlorophyll-protein preparations of the diatom *Cyclotella meneghiniana* (Tab. III.3) have shown a much higher carotenoid to chlorophyll ratio for FCPs compared to the LHCs of higher plants, implying an important role for carotenoids as light-harvesting pigments in FCP. FCPs were isolated by detergent solubilisation of *C. meneghiniana* thylakoids and subsequent sucrose-gradient ultra-centrifugation, which yielded three FCP-containing bands. For band 1 of the sucrose gradient, which consists mostly of trimers of 18 kDa proteins (Büchel, 2003), the pigment to pigment stoichiometry was determined to be ~1.0 fucoxanthin, 0.12 ~diadinoxanthin and ~0.25 Chl *c* molecules per Chl *a*. The amount of diatoxanthin was estimated on the basis of the diadinoxanthin extinction coefficient to be ~0.1 molecules per Chl *a*. The stoichiometries for band 2, which contains a mix of trimers and higher oligomers with a ratio of ~50 % 18 kDa and ~50 % 19 kDa peptides, are ~0.97 Fx, ~0.07 Ddx, (~0.05 Dtx) and ~0.27 Chl *c* per Chl *a*. Band 3, which is made up

predominantly of higher oligomers of the 19 kDa peptide, is mostly comparable to band 1 and band 2 (Tab. III.3), but displays an overall diminished amount of carotenoids in relation to the chlorophylls, with ~0.85 Fx, ~0.04 Ddx, (~0.04 Dtx) and ~0.24 Chl *c* per Chl *a*. These results are in stark contrast to the LHC pigment-protein complexes of higher plants, which are characterised by a strong diversity in their pigmentation (Tab. IV.1), which is most likely caused by structural requirements for fulfilling the light-harvesting and energy transfer functions of the antenna complexes. Compared to this, the different FCPs exhibit a remarkable homogeneity.

Complex	Chl *a*	Chl *b*	Car	References
LHCI-730	8.6	2.9	1.94	Schmid *et al.*, 2002
LHCI-680	6.4	2.6	1.76	Schmid *et al.*, 2002
LHCIIb	8	6	3-4	Liu *et al.*, 2004
CP29	6	2	2	Bassi *et al.*, 1999
CP26	6.8	2.3	1.8	Dainese & Bassi, 1991
CP24	2.7-3.1	2.0-2.3	1	Dainese *et al.*, 1991; Pagano *et al.*, 1998

Tab. IV.1: Overview of LHC pigment stoichiometries per monomer

The actual pigment to protein stoichiometry of FCP is most likely 4:4:1 (Chl *a*:Fx:Chl *c*) per monomer, with substoichiometric amounts of diadinoxanthin and diatoxanthin. If the stoichiometry were 8:8:2, the chlorophyll *a* Q_y-absorption band at 670 nm should be red-shifted due to excitonic interactions of the pigments (van Amerongen & van Grondelle, 2001; Novoderezhkin *et al.*, 2004). Moreover, it seems highly unlikely the apoprotein could accommodate eight fucoxanthin molecules in addition to the chlorophylls (Fig. IV.3). Due to the finding of substoichiometric amounts of diadinoxanthin and diatoxanthin, either one carotenoid binding site with mixed occupancy in FCP has to be expected or purification artefacts contaminate the measurement. The fact that binding sites are not exclusive for certain pigments could be demonstrated in LHCIIb not only for carotenoids (Hobe *et al.*, 2000), but also for chlorophylls (Hobe *et al.*, 2003). The occurrence of different carotenoid species in substoichiometric amounts in preparations of light-harvesting complexes can also be attributed to the xanthophyll cycle, which is a mechanism of excess energy dissipation.

Cyclic xanthophyll epoxidation and de-epoxidation, which results in an increased energy dissipation as heat, has been described for the LHCIIb carotenoids violaxanthin, antheraxanthin and zeaxanthin (Demmig *et al.*, 1987), as well as for diadinoxanthin and diatoxanthin in diatoms (Hager & Stransky, 1970). This possibly leads to a copurification of a mixture of different carotenoids during the isolation of the respective antenna complexes.

Fluorescence-excitation measurements, carried out with FCPs found in band 2 of the sucrose gradient described above, have shown that the energy transfer from chlorophyll *c* to chlorophyll *a* is 100 % efficient and extremely fast (Papagiannakis *et al.*, 2005), which hints at a centrally located position, close to chlorophyll *a*, for chlorophyll *c* in the FCP structure. A sequence alignment of FCP and LHCIIb demonstrates that five of the chlorophyll binding sites in LHCIIb are conserved in FCP: a1, a2, a3, a4 and a5 (Eppard & Rhiel, 1998; nomenclature as in Kühlbrandt *et al.*, 1994). These binding sites form the essential core of chlorophylls in LHCIIb (a1, a2, a4 and a5).

Time-resolved transient absorption measurements of FCP, after excitation of fucoxanthin to its highest excited state, the so-called S_2 state, at 530 nm and subsequent modelling of the kinetic traces, were used to characterise the energy transfer network of FCP. After the initial excitation, efficient energy transfer to chlorophyll *a* can be observed, but not equally efficient by all the fucoxanthin molecules of the complex. Furthermore, the chlorophylls in the FCP are not excitonically coupled, like it is the case in LHCIIb (Papagiannakis *et al.*, 2005).

Target analysis of the kinetic absorption traces (Holzwart, 1996; van Stokkum *et al.*, 2004a&b) allowed the characterisation of four different energy transfer pathways following the excitation of fucoxanthin. Eight different compartments were needed to model the populations of electronic states observed (Fig. IV.2). From the S_2 state of fucoxanthin, which has a lifetime of ~75 fs, energy is transferred with 40 % efficiency directly to chlorophyll *a*, giving an indication for at least one fucoxanthin molecule being closely positioned to the central cluster of chlorophylls. This resembles the situation in LHCIIb, where one carotenoid was found to be very well coupled to the central chlorophyll cluster (Gradinaru *et al.*, 2000). The remaining 60 % of the population of fucoxanthin S_2 states decay to an unrelaxed or so-called 'hot' S_1/ICT state through internal conversion mechanisms. This state has a lifetime of ~320 fs and

transfers its energy with an efficiency of 20 % to chlorophyll *a*. A sub-picosecond energy transfer step from an unrelaxed S_1/ICT state was also observed in the peridinin-chlorophyll *a*-protein (PCP) of the dinoflagellate *Amphidinium carterae* (Zigmantas *et al.*, 2002). Although structurally very different, PCP is comparable to FCP in the respect that carotenoids are important light-harvesting pigments, which is reflected by its very high carotenoid to chlorophyll ratio of 4:1 (Hofmann *et al.*, 1996). Another trait fucoxanthin and peridinin have in common, is the occurrence of a conjugated carbonyl group in the isoprenoid chain. This carbonyl group is responsible for distinctive effects on the energetics and dynamics of these carotenoids, like for example a considerable narrowing of the S_1/ICT–S_2 gap. Apart from this, both, fucoxanthin and peridinin display an unusually strong bathochromic shift upon binding to the apoprotein (Zigmantas *et al.*, 2004).

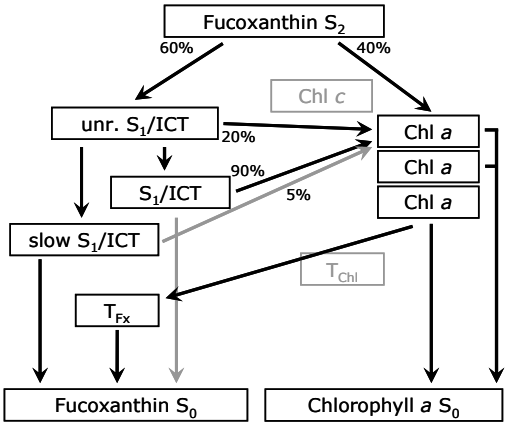

Fig. IV.2: The compartmental scheme that was used to model the energy transfer network in FCP. The grey arrows depict the least efficient pathways of energy flow. The Chl *a* compartments describe the continuous decay observed in the signal and not necessarily different molecules. No contribution of Chl *c* or of the Chl *a* triplet state was observed. For the sake of completeness the corresponding compartments are included in light grey (Papagiannakis *et al.*, 2005). S_0 = ground state; S_1/S_2 = singlet excited states; T = triplet state; ICT = intra molecular charge-transfer state

After further decay of the unrelaxed S_1/ICT state in the FCP, the excitation reaches the S_1/ICT state, which has a lifetime of ~2.6 ps and transfers most of its energy to chlorophyll *a* (90 % efficiency). The final state that could be characterised by target analysis is a slow S_1/ICT state, which transfers energy rather poorly (5 % efficiency) and has comparably long lifetimes of ~31 ps (Papagiannakis *et al.*, 2005). On the one hand, this split energy transfer network, with direct transfer from the S_2 state of the carotenoids to chlorophyll, and the decay to lower electronic states before energy

transfer occurs, is comparable to the one found in LHCIIb and CP29 (Gradinaru *et al.*, 2000). On the other hand, FCP follows a similar strategy to achieve efficient excitation energy transfer like PCP. In PCP and FCP, a significant portion of the excitation energy transfer is mediated on an extremely short time-scale and occurs to a large extent via the S_1/ICT state. Following the decay of the S_2 state, part of the excitation decays to the lower singlet excited states of the respective carotenoids, which then perform efficient energy transfer to chlorophyll *a*. This is demonstrated by the significantly shorter lifetimes of these electronic states, compared to the respective lifetimes for fucoxanthin in organic solvent (Zigmantas *et al.*, 2004).

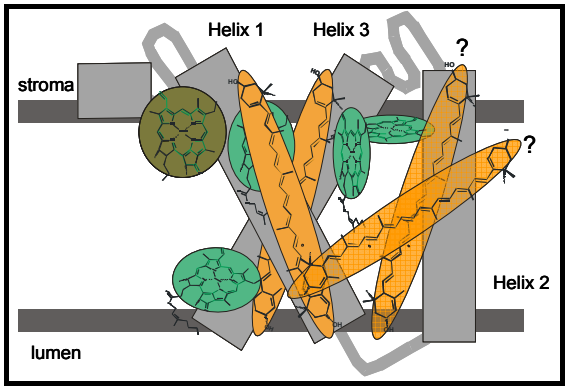

Fig. IV.3: Hypothetical FCP structure model. Adapted from the LHCIIb model by Kühlbrandt *et al.* (1994) and modified according to Eppard & Rhiel (1998) and Papagiannakis *et al.* (2005). Chl *a* in light green, Chl *c* in dark green, Fx in orange, α-helices in grey. *Explanation see text*.

Since FCP binds a small number of chlorophylls, but high amounts of carotenoids compared to LHCIIb, it is to be expected that some of the chlorophyll binding sites found in LHCIIb are filled with fucoxanthin instead in FCP. This would likely result in at least one fucoxanthin not being bound near any chlorophyll molecules; i.e. this fucoxanthin would be energetically disconnected from the cluster of chlorophylls at the centre of the complex (Fig. IV.3). This hypothesis is supported by the determination of the slow S_1/ICT state which transfers energy poorly. Furthermore, there was no evidence for an excitation energy transfer from fucoxanthin to chlorophyll *c*, which means it is unlikely that any of the fucoxanthin molecules are located close to chlorophyll *c* in the FCP structure. The total rate of excitation energy transfer from fucoxanthin to chlorophyll *a* in FCP approaches ~80 %, which is similar to the energy

transfer efficiency of carotenoids in LHCIIb and CP29 (Gradinaru *et al.*, 2000). Taking all this information together, a hypothetical model for the structure of FCP can be constructed. Comparable to the two lutein molecules in LHCIIb, two carotenoids are placed centrally to support the structure of the complex and reside in close proximity to the chlorophylls. The positions of the two additionally placed carotenoids are largely hypothetical. The chlorophylls are arranged according to the conserved chlorophyll binding sites between LHCIIb and FCP, with the chlorophyll *c* in the central cluster (Fig. IV.3).

3. Outlook

The addition of the His-tag to the cytochrome b_{559} complex in *Nicotiana tabacum* opens up various possibilities for working with purified higher plant photosystem II. As has been pointed out earlier, up to now, a major part of the structural work on photosystem II has been carried out with thermophilic organisms like the cyano-bacterium *Thermosynechococcus elongatus*, but the higher PSII stability inherent to these organisms, is based on differences in the protein structures between thermophiles and higher plants. In order to investigate these differences and improve the resolution of the currently available higher plant photosystem II structures, which is around 8-10 Å (Rhee *et al.*, 1998; Hankamer *et al.*, 2001a), good preparations of higher plant PSII are needed, no matter which kind of structural studies are to be employed. Protein structures are often investigated with the methods of single particle analysis of electron micrographs, two-dimensional or three-dimensional crystallisation, all of which benefit greatly from homogenous preparations of intact protein. As the His-tag purification procedure allows for a tight control of protein solubilisation, the isolation of photosystem II-LHCII supercomplexes is also a possibility. These supercomplexes might in turn also be submitted to structural studies. Apart from this, photosystem II fractions, which contain only low amounts of contaminations by other pigment-protein complexes, also serve as good samples for several spectroscopic techniques. For example, more accurate ultra-fast transient absorption spectroscopic measurements

could be carried out with these photosystem II preparations. These could be used to model the excitation energy transfer pathways in the complexes and lead to a characterisation of the pigments and the electronic states involved, including the lifetimes of the excited states and their efficiency of energy transfer, similar to the measurements that have been carried out with FCP.

V. Summary

Today the structure of photosystem II, which is the enzyme responsible for the evolution of molecular oxygen by plants, algae and cyanobacteria, is known up to a resolution of about 3.0 Å in cyanobacteria (Loll *et al.*, 2005). Photosystem II of higher plants, which shows some differences compared to the photosystem II of cyanobacteria, is not resolved in such high detail, yet (8-10 Å) (Rhee *et al.*, 1998; Hankamer *et al.*, 2001a). Therefore, the molecular structure of PSII of higher plants and its adjacent antenna complexes remains in the focus of the current research.

One of the major problems when working with photosystem II is its relative instability during isolation. Together with the antenna proteins and several other proteins, some of which still have an unclear function, PSII forms a huge multi-protein-complex, which tends to fall apart during classical preparation methods. In order to achieve a faster and milder method of purification for PSII, four different His-tags have been added to one of the subunits of PSII. The gene targeted in this study is called *psbE* and codes for the α-chain of cytochrome b_{559}, an integral part of PSII. The gene for PsbE is encoded in the chloroplast genome. The His-tags, which were employed in this work, consist of six or ten consecutive histidine aminoacid residues, which were fused to the N-terminus of the protein, either with or without a cleavage site for the protease "Factor Xa". The N-terminus of PsbE is located on the more accessible stromal side of the thylakoid membrane.

After inserting the *psbE* gene in a vector plasmid, in which the recognition site for the restriction endonuclease SacI had been eliminated, the different His-tags were generated by PCR with purposefully altered primers. In a final cloning step, a gene, which confers resistance to the antibiotics spectinomycin and streptomycin, was added to the DNA construct. Subsequently, the so-called biolistic transformation method ("*gene gun*") was applied to introduce this genetically engineered plasmid DNA to *Nicotiana tabacum* chloroplasts (Bock & Hagemann, 2000). Through the processes of homologous recombination that take place in the chloroplast, the plastid encoded wildtype *psbE* gene was replaced by its His-tag containing counterparts.

After several rounds of regenerating plants on antibiotic-containing medium, successful transformation was confirmed through PCR methods. By self fertilisation of fully regenerated plants, seeds were produced from tobacco strains, which carried only the mutated *psbE* gene. Plants cultivated from these seeds showed no distinctive phenotype under the chosen growth conditions, in respect to wildtype plants. The presence of the His-tag in this F1 generation was again confirmed with PCR methods.

Measurements of oxygen evolution and pulse amplitude modulated fluorescence (PAM), carried out with preparations of wildtype and transgenic tobacco strains, revealed no differences for photochemical or non-photochemical quenching between both types. However, the oxygen evolution capacity of transgenic tobacco thylakoids compared to the wildtype was significantly reduced, although the chlorophyll content in relation to the leaf area was almost identical. This hints at a reduced amount of photosystem II complexes in the thylakoid membranes of transgenic tobacco. This alteration could be related to the mutation of cytochrome b_{559}, because, amongst other functions, this subunit was shown to be important for the assembly of photosystem II (Morais *et al.*, 1998).

If solubilised thylakoid preparations of His-tagged plant strains were applied to a Ni-NTA column, photosystem II was selectively bound to the matrix. After washing away most of the contaminations, photosystem II core complexes could be eluted with imidazole-containing buffer. Photosystem II prepared in this way, displayed a drastic reduction of the peripheral light-harvesting complexes (LHCI & LHCII) and photosystem I reaction centres. This could be demonstrated by the loss of chlorophyll *b* and xanthophyll bands (LHCs) in absorption spectra, a small blue-shift of the chlorophyll *a* Q_y absorption (PSI) and the respective band patterns in polyacrylamide gel electrophoresis. The photosystem II complexes prepared in this way can now be put to use in different structural studies, like two-dimensional or three-dimensional crystallisation and spectroscopic measurements.

Another photosynthetic pigment-protein complex of interest is the fucoxanthin-chlorophyll *a*/*c*-binding protein of diatoms, because eukaryotic algae, like diatoms, are important factors of oceanic ecosystems and account for a large part of marine biomass production. In order to facilitate ultra-fast time-resolved transient absorption spectroscopy and subsequent modelling of the kinetic traces, FCPs were prepared by

sucrose-gradient ultra-centrifugation and their pigment stoichiometries determined by HPLC. Combining the spectroscopic data (Papagiannakis *et al.*, 2005) with protein sequence alignments (Eppard & Rhiel, 1998) and the structure of the homologous higher plant LHCIIb (Kühlbrandt *et al.*, 1994), a hypothetical model for the structure of FCP could be proposed (Fig. IV.3).

VI. Zusammenfassung

In höheren Pflanzen, Algen und Cyanobakterien ist das Photosystem II der Pigment-Protein-Komplex, der für die Freisetzung von molekularem Sauerstoff verantwortlich ist. Seine räumliche Struktur wurde kürzlich für Cyanobakterien mit einer Auflösung von circa 3,0 Ångstrom bestimmt (Loll *et al.*, 2005). Das Photosystem II höherer Pflanzen, welches einige Unterschiede zu cyanobakteriellem PSII aufweist, konnte bisher nicht so detailliert aufgelöst werden (8-10 Å) (Rhee *et al.*, 1998; Hankamer *et al.*, 2001a). Aus diesem Grund stehen das Photosystem II höherer Pflanzen und die dazugehörigen Antennenkomplexe weiterhin im Mittelpunkt des Forschungsinteresses.

Eines der größten Probleme bei der Arbeit mit Photosystem II ist seine relativ geringe Stabilität während des Aufreinigungsprozesses. Zusammen mit den Antennenkomplexen und einigen anderen Proteinen, deren Funktion zum Teil noch nicht geklärt werden konnte, liegt Photosystem II als ausgedehnter Multiproteinkomplex in der Membran vor, der dazu neigt, während der Präparation einige seiner Untereinheiten zu verlieren. Um nun eine schnellere und schonendere Aufreinigung durchführen zu können, wurde eine Untereinheit von Photosystem II mit vier verschiedenen His-tags versehen. Das Gen, welches für die vorliegende Arbeit ausgewählt wurde, heißt *psbE* und kodiert für die α-Untereinheit des Cytochrom b_{559}, welches einen integralen Bestandteil des Photosystems II darstellt. Das PsbE Protein ist im Chloroplastengenom kodiert. Die His-tags, die verwendet wurden, bestehen aus einer Folge von sechs beziehungsweise zehn Histidin-Aminosäureseitenketten, die an den N-Terminus des Proteins angehängt wurden, sowohl mit als auch ohne Spaltstelle für die Protease „Faktor Xa“. Der N-Terminus von PsbE befindet sich auf der leichter zugänglichen stromalen Seite der Thylakoidmembran.

Um im weiteren Verlauf die Chloroplasten wie gewünscht transformieren zu können, mussten zunächst vier verschiedene Plasmid-DNA-Konstrukte erstellt werden, welche das jeweilige veränderte *psbE* Gen, sowie umfangreiche flankierende Sequenzbereiche und ein Resistenzgen beinhalteten. Die flankierenden Bereiche müssen dabei möglichst identisch zu den Sequenzabschnitten des Chloroplastengenoms sein, die während der Transformation ausgetauscht werden sollen, da dies die Austauschrate der ent-

sprechenden DNA-Abschnitte durch die homologe Rekombinationsmaschinerie erhöht (Bock & Hagemann, 2000).

Bevor das *psbE* Gen, das zusammen mit den flankierenden Sequenzen eine Länge von ~2300 bp aufweist, in den Plasmidvektor (~3.0 kbp) inseriert werden konnte, musste in diesem durch PCR mit gezielt veränderten Primern eine Erkennungsstelle für die Restriktionsendonuklease SacI eliminiert werden, da es durch diese bei späteren Modifikationsschritten zu einer ungewollten Spaltung des Plasmids gekommen wäre. Die so entstandenen PCR-Produkte von ~3000 bp Länge, wurden mit Hilfe einer DNA Ligase wieder in ihre ringförmige Form gebracht, um in *E. coli* amplifiziert werden zu können. Sobald dies geschehen war und sich das *psbE* Gen in dem modifizierten Vektor befand, wurden wiederum durch PCR mit gezielt veränderten Primern die verschiedenen His-tags erzeugt. Die entstandenen PCR-Produkte wurden dann im Anschluss mit den entsprechenden Restriktionsendonukleasen (AgeI, SacI) zugeschnitten und in das Vektorplasmid eingefügt. In einem letzten Klonierungsschritt wurde ein Gen, welches Resistenz gegenüber den Antibiotika Spectinomycin und Streptomycin verleiht, in die Sequenz eingefügt. Mit Hilfe der so genannten biolistischen Transformationsmethode („*Genkanone*“) wurden schließlich die fertigen DNA-Konstrukte in Chloroplasten von *Nicotiana tabacum* eingebracht (Bock & Hagemann, 2000). Durch die homologen Rekombinationsprozesse, die in den Chloroplasten ablaufen, wurde das Wildtyp *psbE* Gen durch sein His-tag tragendes Gegenstück ersetzt.

Nach mehreren Runden der Regeneration und Selektion der Pflanzen auf Antibiotikum enthaltendem Medium, wurde die erfolgreiche Transformation mit Hilfe von PCR-Methoden überprüft. Aus den Tabaklinien, die nur noch Chloroplasten mit dem mutierten *psbE* Gen besaßen, die also homoplasmisch waren, wurden Samen hergestellt, indem vollständig regenerierte Pflanzen mit ihren eigenen Pollen befruchtet wurden. Die verschiedenen transgenen Tabaklinien, die mit Hilfe dieser Samen angezogen wurden, zeigten unter den gewählten Anzuchtsbedingungen (25°C, 8 h Licht, 100–150 µE/(s·m^2), 16 h Dunkelheit, 50 % relative Luftfeuchtigkeit) keinerlei auffällige phänotypische Abweichung gegenüber den Wildtyppflanzen. Das Vorhandensein des His-tags in der entstandenen F1 Generation wurde anschließend erneut durch PCR überprüft.

Die Messungen der Sauerstoffbildungsraten und PAM-Fluoreszenz, die an Thylakoidpräparationen von Wildtyptabak und transgenem Tabak durchgeführt wurden, ergaben keine Unterschiede im photochemischen und nicht-photochemischen Quenching. Dies lässt darauf schließen, dass das Photosystem II der transgenen Tabaklinien intakt ist. Transgene Tabakthylakoide produzierten allerdings im Vergleich zum Wildtyp deutlich weniger Sauerstoff, obwohl der Chlorophyllgehalt der Blätter, bezogen auf die Blattfläche oder das Frischgewicht des Blattes, von Wildtyptabak und transgenen Pflanzen praktisch identisch war. Dabei erreichte Wildtyptabak eine maximale Sauerstoffbildungsrate von ca. 120 µg O_2 / (mg Chl·h), während die maximale Sauerstoffbildungsrate für die transgene Tabaklinie EH2a/34 (His_{10}) nur bei ca. 85 µg O_2 / (mg Chl·h) lag. Dies deutete darauf hin, dass in den Thylakoidmembranen der untersuchten transgenen Tabaklinien weniger Photosystem II Komplexe vorhanden waren. Ein vergleichbarer Sachverhalt wurde bereits durch Sauerstoffmessungen an *Chlamydomonas reinhardtii* Photosystem II Partikeln, welche einen His-tag am C-terminalen Ende des Reaktionszentrumsproteins D2 trugen, beobachtet (Sugiura *et al.*, 1998). Die verminderte Menge an Photosystem II, wie sie in der vorliegenden Arbeit beschrieben wurde, könnte auf die Mutation des Cytochrom b_{559} zurückzuführen sein, welches, neben diversen anderen Funktionen, auch eine wichtige Rolle in der Assemblierung des Photosystems II spielt (Morais *et al.*, 1998). Sollte also die Menge an korrekt gefaltetem PsbE in der Thylakoidmembran gegenüber dem Wildtyp verringert sein, so würde dies auch zu einer Verringerung der vorhandenen Photosystem II Komplexe führen. Ein weiteres Genprodukt, welches für die korrekte Assemblierung von PSII wichtig ist, ist PsbJ (Hager *et al.*, 2002). PsbJ ist mit PsbE in einem Operon (EFLJ-Operon) im Chloroplastengenom kodiert (Pakrasi *et al.*, 1991). Das heißt, dass Mutationen innerhalb des EFLJ-Operons, wie im vorliegenden Fall an *psbE*, zu einer Störung der Transskription von *psbJ* führen können, was sich wiederum in einer Reduktion der PSII Mengen in der Thylakoidmembran niederschlagen könnte.

Gab man Präparationen von solubilisierten Thylakoiden aus Tabaklinien, die einen His-tag enthalten, auf eine Ni-NTA Säule, so wurde Photosystem II gezielt an die Säulenmatrix gebunden. Nachdem ein Großteil der Verunreinigungen von der Säule gewaschen war, konnten durch Verwendung von imidazolhaltigem Puffer aufgereinigte Photosystem II Komplexe von der Säule eluiert werden. Photosystem II

Präparationen, die auf diese Art hergestellt wurden, zeichneten sich durch eine starke Abreicherung der peripheren Lichtsammelkomplexe (LHCI & LHCII) und einem Verlust des Photosystems I aus. Dies wurde durch die Verringerung der Chlorophyll *b* und Xanthophyll (LHCs) Banden in Absorptionsspektren, durch eine Blauverschiebung der Chlorophyll *a* Q_y Absorption (PSI) und durch die entsprechenden Bandenmuster in Polyacrylamidgelen nachgewiesen. Die Position des D1 Proteins im Gel wurde darüber hinaus durch Western-Blot-Analyse bestimmt. In den entsprechenden Kontrollexperimenten mit Wildtyptabak, konnte durch die Säulenchromatographie keinerlei Anreicherung von bestimmten Pigment-Protein-Komplexen erzielt werden, da Photosystem II ohne His-tag nicht an die Säulenmatrix binden kann, was dazu führte, dass in allen Fraktionen dieselbe Proteinverteilung zu finden war. Die mittels Ni-NTA Chromatographie gewonnen His-tag-Photosystem II Komplexe können nun weiteren strukturellen Untersuchungen, wie zum Beispiel zweidimensionaler oder dreidimensionaler Kristallisation zugeführt werden oder darüber hinaus für spektroskopische Methoden verwendet werden. Sollte es sich herausstellen, dass bei diesen Experimenten der His-tag einen störenden Einfluss hat, so besteht die Möglichkeit diesen in den Tabaklinien EH3a (His_6) und EH4a (His_{10}) mit Hilfe der Protease „Faktor Xa“ nachträglich zu entfernen. Generell konnten keine signifikanten Abweichungen zwischen den verschiedenen His-tag Tabaklinien, weder in Bezug auf die Ausbeute während der Ni-NTA Chromatographie, die bei ca. 14 % bezogen auf den Chlorophyllgehalt liegt, noch in Bezug auf die Reinheit der gewonnen Photosystem II Fraktionen, festgestellt werden.

Ein weiterer interessanter Pigment-Protein-Komplex der Photosynthese ist das Fucoxanthin-Chlorophyll *a*/*c*-bindende Protein aus Kieselalgen. Eukaryotische Algen, wie Kieselalgen, sind wichtige Bestandteile der Ökosysteme der Ozeane und stellen einen großen Anteil der marinen Biomasseproduktion dar. Um ultraschnelle zeitaufgelöste transiente Absorptionsspektroskopie durchführen zu können, wurden FCPs mittels Saccharose-Dichtegradienten Ultrazentrifugation isoliert und die Pigmentstöchiometrie der einzelnen Banden durch HPLC-Messungen bestimmt. Zum einen zeigte sich hier, dass FCP über ein sehr hohes Xanthophyll zu Chlorophyllverhältnis verfügt, was auf eine wichtige Lichtsammelfunktion der Xanthophylle schließen lässt, und zum anderen waren nur geringe Unterschiede in der Pigmentierung der ver-

schiedenen FCP Banden des Saccharosegradienten zu beobachten, obwohl sich diese deutlich in ihrem Oligomerisierungsgrad unterscheiden (Büchel, 2003). Für Bande 1 des Saccharosegradienten, die sich hauptsächlich aus Trimeren des 18 kDa FCPs zusammensetzt, wurden pro Molekül Chlorophyll *a*, ~1,0 Moleküle Fucoxanthin, ~0,12 Diadinoxanthin und ~0,25 Chlorophyll *c* ermittelt. Bande 2, in der eine Mischung aus Trimeren und höheren Oligomeren (~50 % 18 kDa, ~50 % 19 kDa Proteine) von FCPs zu finden ist, ergab pro Molekül Chl *a*, ~0,97 Fx, ~0,07 Ddx und ~0,27 Chl *c*. Bande 3, in der hauptsächlich höhere Oligomere des 19 kDa FCPs zu finden sind, zeichnete sich durch eine leichte Verminderung des Xanthophyllgehalts gegenüber den beiden anderen Banden aus. Die Pigmentverhältnisse betrugen ~0,85 Fx, ~0,04 Ddx und ~0,24 Chl *c* pro Chl *a*. Diese Ergebnisse stehen in starkem Kontrast zu der Situation in den Lichtsammelkomplexen aus höheren Pflanzen, die deutlich in ihrer Pigmentierung voneinander abweichen (Tab. IV.1).

Des Weiteren gingen die Pigmentdaten in die Definition des Grundmodells, welches zur Auswertung („target analysis“) der ultraschnellen spektroskopischen Messungen nötig war, mit ein (Holzwart, 1996; van Stokkum *et al.*, 2004a&b). Unter der Annahme von acht verschiedenen Kompartimenten im FCP, wurden die Lebenszeiten und Energietransferraten (Tab. III.4) für eine Reihe von Energieniveaus der beteiligten Pigmente berechnet, um den Weg der Anregungsenergie von Fucoxanthin zu Chlorophyll *a* nachvollziehen zu können (Fig. IV.2). Vom S_2 Zustand des Fucoxanthin, der eine Lebensdauer von ~75 fs hat und 40 % seiner Energie direkt auf Chl *a* überträgt, wird als nächstes ein energiereicher (engl. „hot“ oder „unrelaxed“) S_1/ICT Zustand erreicht, der eine Lebensdauer von ~320 fs hat und 20 % seiner Energie auf Chl *a* überträgt. Nach weiteren internen Konversionsprozessen, befindet sich Fucoxanthin im S_1/ICT Zustand, der seine Energie praktisch vollständig auf Chl *a* überträgt (90 %, Lebensdauer: ~2,6 ps). Der letzte energetische Zustand, der bestimmt werden konnte, ist ein vergleichsweise langlebiger S_1/ICT Zustand mit niedriger Übertragungseffizienz (5 %, Lebensdauer: ~31 ps) (Papagiannakis *et al.*, 2005). Hierbei zeigte sich, dass die Energietransferstrategie von FCP auf der einen Seite vergleichbar ist, mit der der Lichtsammelkomplexe LHCIIb und CP29 aus höheren Pflanzen (Gradinaru *et al.*, 2000), aber auf der anderen Seite auch Ähnlichkeiten zum Peridinin-Chlorophyll-Protein (PCP) des Dinoflagellaten *Amphidinium carterae* aufweist, welches ebenfalls

durch ein sehr hohes Xanthophyll zu Chlorophyllverhältnis charakterisiert ist (Hofmann *et al.*, 1996). Sowohl in FCP als auch in PCP wird ein substantieller Anteil der Anregungsenergie in weniger als einer Picosekunde über einen energiereichen S_1/ICT Zustand von Xanthophyllen auf Chlorophyll übertragen (Papagiannakis *et al.*, 2005; Zigmantas *et al.*, 2002).

Durch die Interpretation von Sequenzvergleichen (Eppard & Rhiel, 1998), den spektroskopischen Daten (Papagiannakis *et al.*, 2005) und unter zu Hilfenahme der Struktur des zu FCP homologen LHCIIb aus höheren Pflanzen (Kühlbrandt *et al.*, 1994) konnte ein hypothetisches Modell für die Struktur des FCP erstellt werden. Dieses Modell beinhaltet vier Moleküle Chlorophyll *a*, ein Chlorophyll *c* und zwei Moleküle Fucoxanthin, deren Positionierung aus den entsprechenden Daten abgeleitet wurde. Die Platzierung der beiden übrigen Fucoxanthinmoleküle ist dagegen noch weitestgehend hypothetisch (Fig. IV.3).

VII. References

Allen, J. **(1995)** Thylakoid protein phosphorylation, state 1-state 2 transitions, and photosystem stoichiometry adjustment: Redox control at multiple levels of gene expression, *Physiologia Plantarum* **93**, 196-205

Baena-Gonzalez, E., Aro, E. M. **(2002)** Biogenesis, assembly and turnover of photosystem II units, *Phil. Trans. R. Soc. Lond. B* **357**, 1451-1459

Barber, J., Nield, J., Morris, E.P., Zheleva, D., Hankamer, B. **(1997)** The structure, function and dynamics of photosystem two, *Physiologia Plantarum* **100**, 817-827

Barber, J. **(2002)** P680: what is it and where is it? *Bioelectrochemistry* **55**, 135-138.

Barter, L. M. C., Durrant, J. R., Klug, D. R. **(2003)** A quantitative structure-function relationship for the photosystem II reaction center: Supermolecular behaviour in natural photosynthesis, *Proc. Natl. Acad. Sci. USA* **100**, 946-951.

Bassi, R., Croce, R., Cugini, D., Sandonà, D. **(1999)** Mutational analysis of a higher plant antenna protein provides identification of chromophores bound into multiple sites, *Proc. Natl. Acad. Sci. USA* **96**, 10056-10061

Ben-Shem, A., Frolow, F., Nelson, N. **(2003)** Crystal structure of plant photosystem I, *Nature* **426 (6967)**, 630-635

Berthold, D. A., Babcock, G. T., Yocum, C. F. **(1981)** A highly resolved, oxygen evolving photosystem II preparation from spinach thylakoid membranes, *FEBS Letters* **134/II**, 231-234

Blankenship, R. **(1992)** Origin and early evolution of photosynthesis, *Photosynthesis Research* **33**, 91-111

Bock, R., Kössel, H., Maliga, P. **(1994)** Introduction of a heterologous editing site into the tobacco plastid genome – The lack of RNA editing leads to a mutant phenotype, *The EMBO Journal* **13 (19)**, 4623-4628

Bock, R., Hagemann, R. **(2000)** Extranuclear inheritance: Plastid genetics: Manipulation of plastid genomes and biotechnological applications, *Progress in Botany* **61**, 76-90

Boekema, E., Hankamer, B., Bald, D., Kruip, J., Nield, J., Boonstra, A., Barber, J., Rögner, M. **(1995)** Supramolecular structure of the photosystem II complex from green plants and cyanobacteria, *Proc. Natl. Acad. Sci. USA* **92**, 175-179

Boekema, E., van Roon, H., Calkoen, F., Bassi, R., Dekker, J. P. **(1999)** Multiple types of association of photosystem II and its light-harvesting antenna in partially solubilized photosystem II membranes, *Biochemistry* **38 (8)**, 2233-2239

Bondarava, N., de Pascalis, L., Al-Babili, S., Goussias, C., Golecki, J. R., Beyer, P., Bock, R., Krieger-Liszkay, A. **(2003)** Evidence that cytochrome b_{559} mediates the oxidation of reduced plastoquinone in the dark, *The Journal of Biological Chemistry* **278 (15)**, 13554-13560

Bricker, T. M. **(1990)** The structure and function of CPa-1 and CPa-2 in photosystem II, *Photosynthesis Research* **24 (1)**, 1-13

Buchannan, B., Gruissem, W., Jones, R. **(2000)** Biochemistry & molecular biology of plants, Part 3 "Energy flow", pp 567, *The American Society Of Plant Physiologists*

Büchel C., Wilhelm, C. **(1993)** Isolation and characterization of a photosystem-I-associated antenna (LHC-I) and a photosystem-I core complex from the chlorophyll-c-containing alga *Pleurochloris-meiringensis* (Xanthophyceae), *The Journal of Photochemistry and Photobiology B - Biology* **20 (2-3)**, 87-93

Büchel, C., Barber, J., Ananyev, G., Eshagi, S., Watt, R., Dismukes, C. **(1999)** Photoassembly of the manganese cluster and oxygen evolution from monomeric and dimeric CP47 reaction center photosystem II complexes, *Proc. Natl. Acad. Sci. USA* **96 (25)**, 14288-14293

Büchel, C., Morris, E., Orlova, E., Barber, J. **(2001)** Localisation of the PsbH subunit in photosystem II: a new approach using labelling of His-tags with a Ni^{2+}-NTA gold cluster and single particle analysis; *The Journal of Molecular Biology* **312**, 371-379

Büchel, C., Kühlbrandt, W. **(2005)** Structural differences in the inner part of photosystem II between higher plants and cyanobacteria, *Photosynthesis Research* **85**, 3-13

Butt, H. J., Wang, D. N., Hansma, P. K. Kühlbrandt, W. **(1991)** Effect of surface-roughness of carbon support films on high-resolution electron-diffraction of 2-dimensional protein crystals, *Ultramicroscopy* **36 (4)**, 307-318

Croce, R., Morosinotto, T., Castelletti, S., Breton, J., Bassi, R. **(2002)** The Lhca antenna complexes of higher plant photosystem I, *Biochimica et Biophysica Acta – Bioenergetics*, **1556**, 29-40

Dainese, P., Bassi, R. **(1991)** Subunit stoichiometry of the chloroplast photosystem II antenna system and aggregation state of the component chlorophyll *a*/*b*-binding proteins, *The Journal of Biological Chemistry* **266 (13)**, 8136-8142

Damjanović, A., Ritz, T., Schulten, K. **(2000)** Excitation energy trapping by the reaction center of *Rhodobacter sphaeroides*, *International Journal of Quantum Chemistry* **77**, 139-151

Deisenhofer, J., Epp, O., Miki, K., Huber, R., Michel, H. **(1985)** Structure of the protein subunits in the photosynthetic reaction centre of *Rhodopseudomonas viridis* at 3Å resolution, *Nature* **318**, 618-624

Deisenhofer, J., Michel, H. **(1991)** Structures of bacterial photosynthetic reaction centers, *Annual Reviews in Cell Biology* **7**, 1-23

Demmig, B., Winter, K., Krüger, A., Czygan, F. C. **(1987)** Photoinhibition and zeaxanthin formation in intact leaves, *Plant Physiology* **82 (2)**, 218-224

Dismukes, G. C. **(2001)** Photosynthesis: Splitting water, *Science* **292**, 447-448

Eppard, M, Rhiel, E. **(1998)** The genes encoding light-harvesting subunits of *Cyclotella cryptica* (Bacillariophyceae) constitute a complex and heterogeneous family, *Molecular and General Genetics* **260**, 335-345

Eppard, M., Rhiel, E. **(2000)** Investigations on gene copy number, introns, and chromosomal arrangement of genes encoding the fucoxanthin chlorophyll *a*/*c* binding proteins of the centric diatom *Cyclotella cryptica*, *Protist* **151**, 27-29

Eppard, M., Krumbein, W. E., von Haesler, A., Rhiel, E. **(2000)** Characterization of fcp4 and fcp12, two additional genes encoding light-harvesting proteins of *Cyclotella cryptica* (*Bacillariophyceae*) and phylogenetic analysis of this complex gene family, *Plant Biology* **2**, 283-289

Ermler, U., Fritzsch, G., Buchanan, S., Michel, H. **(1994)** Structure of the photosynthetic reaction centre from *Rhodobacter sphaeroides* at 2.65Å resolution: cofactors and protein-cofactor interactions, *Structure* **15 (2)**, 925-936

Faller, P., Pascal, A., Rutherford, A. W. **(2001)** β-Carotene redox reactions in photosystem II: electron transfer pathway, *Biochemistry* **40**, 6431-6440

Falkowski, P. G., Katz, M. E., Knoll, A. H., Quigg, A., Raven, J. A., Schofield, O., Taylor, F. J. R. **(2004)** The evolution of modern eukaryotic phytoplankton, *Science* **305**, 354-360

Ferreira, K. N., Iverson, T. M., Maghlaoui, K., Barber, J., Iwata, S. **(2004)** Architecture of the photosynthetic oxygen-evolving center, *Science* **303**, 1831-1838

Goldsmith, J., Boxer, S. **(1996)** Rapid isolation of bacterial photosynthetic reaction centers with an engineered poly-histidine tag, *Biochimica et Biophysica Acta* **1276**, 171-175

Gradinaru, C. C., van Stokkum, I. H. M., Pascal, A. A., van Grondelle, R., van Amerongen, H. **(2000)** Identifying the pathways of energy transfer between carotenoids and chlorophylls in LHCII and CP29. A multicolour, femtosecond pump-probe study, *The Journal of Biophysical Chemistry B* **104**, 9330-9342

Green, B. R., Kühlbrandt, W. **(1995)** Sequence conservation of light-harvesting and stress-response proteins in relation to the three-dimensional molecular structure of LHCII, *Photosynthesis Research* **44**, 139-148

Green, B. R., Durnford, D. G. **(1996)** The chlorophyll-carotenoid proteins of oxygenic photosynthesis, *Annual Reviews in Plant Physiology and Plant Molecular Biology* **47**, 685-714

Grossman, A., Schaefer, M., Chiang, G., Collier, J. **(1993)** The phycobilisome, a light-harvesting complex responsive to environmental conditions, *Microbiological Reviews* **57 (3)**, 725-749

Hager, A., Stransky, H. **(1970)** Das Carotinoidmuster und die Verbreitung des lichtinduzierten Xanthophyllcyclus in verschiedenen Algenklassen, *Archiv für Mikrobiologie* **73**, 77-89

Hager, M., Hermann, M., Biehler, K., Krieger-Liszkay, A., Bock, R. **(2002)** Lack of the small plastid-encoded PsbJ polypeptide results in a defective water-splitting apparatus of photosystem II, reduced photosystem I levels, and hypersensitivity to light, *The Journal of Biological Chemistry* **277 (16)**, 14031-14039

Hankamer, B., Nield, J., Zheleva, D., Boekema, E., Jansson, S., Barber, J. **(1997)** Isolation and biochemical characterisation of monomeric and dimeric photosystem II complex from spinach and their relevance to the organisation of photosystem II *in vivo*, *The European Journal of Biochemistry* **243**, 422-429

Hankamer, B., Morris, E., Nield, J., Gerle, C., Barber, J. **(2001a)** Three-dimensional structure of the photosystem II core dimer of higher plants determined by electron microscopy, *The Journal of Structural Biology* **135**, 262-269

Hankamer, B., Morris, E., Nield, J., Carne, A., Barber, J. **(2001b)** Subunit positioning and transmembrane helix organisation in the core dimer of photosystem II, *FEBS Letters* **504**, 142-151

Haugan, J. A., Englert, G., Glinz, E. and Liaaen-Jensen, S. **(1992)** Algal carotenoids. 48. Structural assignments of geometrical isomers of fucoxanthin, *Acta Chemica Scandinavica* **46**, 389-395

Heathcote, P. **(2001)** Type I photosynthetic reaction centres, *Biochimica et Biophysica Acta – Bioenergetics* **1507**, 1-2

Hobe, S., Niemeier, H., Bender, A., Paulsen, H. **(2000)** Carotenoid binding sites in LHCIIb. Relative affinities towards major xanthophylls of higher plants, *The European Journal of Biochemistry* **267**, 616-624

Hobe, S., Fey, H., Rogl, H., Paulsen, H. **(2003)** Determination of relative chlorophyll binding affinities in the major light-harvesting chlorophyll *a*/*b* complex, *The Journal of Biological Chemistry* **278 (8)**, 5912-5919

Hofmann, E., Wrench, P. M., Sharples, F. P., Hiller, R. G., Welte, W., Diederichs, K. **(1996)** Structural basis of light harvesting by carotenoids: peridinin-chlorophyll-protein from *Amphidinium carterae*, *Science* **272**, 1788-1791

Holzwart, A. R. **(1996)** Data analysis of time-resolved measurements. In: Amesz, J. & Hoff, A. J. (eds) Biophysical techniques in photosynthesis, pp. 75-92. *Kluwer Academic Publishers*, Dordrecht, The Netherlands

Jansson, S. **(1994)** The light-harvesting chlorophyll *a*/*b* binding proteins, *Biochimica et Biophysica Acta – Bioenergetics* **1184**, 1-19

Jeans, C., Schilstra, M. J., Ray, N., Husain, S., Minagawa, J., Nugent, J. H. A., Klug, D. R. **(2002)** Replacement of Tyrosine D with phenylalanine affects the normal proton transfer pathways for the reduction of $P680^+$ in oxygen-evolving photosystem II particles from *Chlamydomonas*, *Biochemistry* **41**, 15754-15761

Jeffrey, S.W. **(1972)** Preparation and some properties of crystalline chlorophyll c1 and c2 from marine algae, *Biochimica et Biophysica Acta* **279**, 15-33

Jeffrey, S. W., Humphrey, G. F. **(1975)** New spectrometric equations for determining chlorophyll a, b, c1 and c2 in higher plants, algae and natural phytoplankton, *Biochem. Physiol. Pflanzen* **167**, 191-194

Johansen, J. E., Svec, W. A., Liaaen-Jensen, S. **(1974)** Carotenoids of the Dinophyceae, *Phytochemistry* **13**, 2261-2271

Kamiya, N., Shen, J. R. **(2003)** Crystal structure of oxygen-evolving photosystem II from *Thermosynechococcus vulcanus* at 3.7-Å resolution, *Proc. Natl. Acad. Sci. USA* **100**, 98-103

Kashino, Y., Lauber, W. M., Carroll, J. A., Wang, Q. J., Whitmarsh, J., Satoh, K., Pakrasi, H. B. **(2002)** Proteomic analysis of a highly active photosystem II preparation from the cyanobacterium *Synechocystis* sp PCC 6803 reveals the presence of novel polypeptides, *Biochemistry* **41**, 8004-8012

Kern, J., Loll, B., Lüneberg, C., DiFiore, D., Biesiadka, J., Irrgang, K. D., Zouni, A. **(2005)** Purification, characterisation and crystallisation of photosystem II from *Thermosynechococcus elongatus* in a new type of photobioreactor, *Biochimica et Biophysica Acta* **1706**, 147-157

Kok, B., Forbush, B., McGloin, M. **(1970)** Cooperation of charges in photosynthetic oxygen evolution. A linear four step mechanism, *Photochemistry and Photobiology* **11**, 457-475

Kühlbrandt, W., Wang, D. N., Fujiyoshi, Y. **(1994)** Atomic model of plant light-harvesting complex by electron microscopy, *Nature* **367**, 614-621

Kühlbrandt, W. **(2003)** Two-dimensional crystallization of membrane proteins: A practical guide in Membrane protein purification and crystallization, Second edition, pp. 253-284, Hunte, C., von Jagow, G., Schägger, H. (Editors), *Academic Press, San Diego*, California, USA

Kuhl, H., Rögner, M., van Breemen, J. F., Boekema, E. J. **(1999)** Localization of cyanobacterial photosystem II donor-side subunits by electron microscopy and the supramolecular organization of photosystem II in the thylakoid membrane, *The European Journal of Biochemistry* **266**, 453-459

Kuhl, H., Kruip, J., Seidler, A., Krieger-Liszkay, A., Bunker, M., Bald, D., Scheidig, A. J., Rögner, M. **(2000)** Towards structural determination of the water-splitting enzyme. Purification, crystallization, and preliminary crystallographic studies of photosystem II from a thermophilic cyanobacterium, *The Journal of Biological Chemistry* **275**, 20652-20659.

Krauss, N., Schubert, W. D., Klukas, O., Fromme, P., Witt, H. T., Saenger, W. **(1996)** Photosystem I at 4 Å resolution represents the first structural model of a joint photosynthetic reaction centre and core antenna system, *Nature Structural Biology* **3**, 965-973

Kruk, J., Strzalka, K. **(1999)** Dark reoxidation of the plastoquinone-pool is mediated by the low-potential form of cytochrome b-559 in spinach thylakoids, *Photosynthesis Research* **62**, 273-279

Lakshmi, K. V., Reifler, M. J., Chisholm, D. A., Wang, J. Y., Diner, B. A., Brudvig, G. W. **(2002)** Correlation of the cytochrome c_{550} content of cyanobacterial photosystem II with the EPR properties of the oxygen-evolving complex, *Photosynthesis Research* **72**, 175-189

Larsen, D. S., Vengris, M., van Stokkum, I. H. M., van der Horst, M., de Weerd, F. L., Hellingwerf, K. J., van Grondelle, R. **(2004)** Photoisomerization and photoionization of the photoactive yellow protein chromophores in solution, *The Biophysical Journal* **86**, 2538-2550

Lichtenthaler, H. K. **(1987)** Chlorophylls and carotenoids – pigments of photosynthetic biomembranes, *Methods in Enzymology* **148**, 350-382

Liu, Z., Yan, H., Wang, K., Kuang, T., Zhang, J., Gui, L., An, X., Chang, W. **(2004)** Crystal structure of spinach major light-harvesting complex at 2.72 Å resolution, *Nature* **428**, 287-292

Loll, B., Kern, J., Saenger, W., Zouni, A., Biesiadka, J. **(2005)** Towards complete cofactor arrangement in the 3.0 Å resolution structure of photosystem II, *Nature* **438 (7070)**, 1040-1044

McFadden, G. I. **(2001)** Primary and secondary endosymbiosis and the origin of plastids, *The Journal of Phycology* **37**, 951-959

Mitchell, P. **(1976)** Possible molecular mechanisms of the protonmotive function of cytochrome systems, *The Journal of Theoretical Biology.* **62**, 327-367

Morais, F., Barber, J., Nixon, P. J. **(1998)** The chloroplast-encoded α subunit of cytochrome b-559 is required for assembly of the photosystem two complex in both the light and the dark in *Chlamydomonas reinhardtii*, *The Journal of Biological Chemistry* **273 (45)**, 29315-29320

Morris, E., Hankamer, B., Zheleva, D., Friso, G., Barber, J. **(1997)** The three-dimensional structure of a photosystem II core complex determined by electron crystallography, *Structure* **5 (6)**, 837-849

Nakamura, Y., Kaneko, T., Sato, S., Mimuro, M., Miyashita, H., Tsuchiya, T., Sasamoto, S., Watanabe, A., Kawashima, K., Kishida, Y., Kiyokawa, C., Kohara, M., Matsumoto, M., Matsuno, A., Nakazaki, N., Shimpo, S., Takeuchi, C., Yamada, M., Tabata, S. **(2003)** Complete genome structure of *Gloebacter violaceus* PCC 7421, a cyanobacterium that lacks thylakoids, *DNA Research* **10**, 137-145.

Nakazato, K., Toyoshima, C., Enami, I., Inoue, Y. **(1996)** Two-dimensional crystallisation and cryo-electron microscopy of photosystem II, *The Journal of Molecular Biology* **257**, 225-232

Nield, J., Orlova, E., Morris, E., Gowen, B., van Heel, M., Barber, J. **(2000)** 3D map of the plant photosystem II supercomplex obtained by cryoelectron microscopy and single particle analysis, *Nature Structural Biology* **7 (1)**, 44-47

Novoderezhkin, V. I., Palacios, M. A., van Amerongen, H., van Grondelle, R. **(2004)** Energy-transfer dynamics in the LHCII complex of higher plants: modified redfield approach, *The Journal of Physical Chemistry B* **108**, 10363-10375

Olson, J. M. **(1998)** Chlorophyll organization and function in green photosynthetic bacteria, *Photochemistry and Photobiology* **67 (1)**, 61-75

Pagano, A., Cinque, G., Bassi, R. **(1998)** *In vitro* reconstitution of the recombinant PSII light-harvesting complex CP24 and its spectroscopic characterization, *The Journal of Biological Chemistry* **273**, 17154-17165

Pakrasi, H. B., De Ciechi, P., Whitmarsh, J. **(1991)** Site directed mutagenesis of the heme axial ligands of cytochrome b559 affects the stability of the photosystem II complex, *The EMBO Journal* **10 (7)**, 1619-1627

Papagiannakis, E., van Stokkum, I. H. M., Fey, H., Büchel, C., van Grondelle, R. **(2005)** Spectroscopic characterization of the excitation energy transfer in the fucoxanthin-chlorophyll protein of diatoms, *Photosynthesis Research* **86**, 241-250

Peter, G. F., Thornber, J. P. **(1991)** Biochemical composition and organization of higher plant photosystem II light-harvesting pigment-proteins, *The Journal of Biological Chemistry* **266**, 16745-16754

Porra, R. J., Thompson, W. A., Kriedmann, P. E. **(1989)** Determination of accurate extinction coefficients and simultaneous equations for assaying chlorophylls *a* and *b* with four different solvents: verifications of the concentration of chlorophyll standards by atomic absorption spectroscopy, *Biochimica et Biophysica Acta* **975**, 384-394

Provasoli, L., McLaughlin, J. J. A., Droop, M. R. **(1957)** The development of artificial media for marine algae, *Archiv für Mikrobiologie* **25**, 392-428.

Rhee, K-H., Morris, E. P., Zheleva, D., Hankamer, B., Kühlbrandt, W., Barber, J. **(1997)** Two dimensional structure of plant photosystem II at 8 Å resolution, *Nature* **389**, 522-526

Rhee, K-H., Morris, E. P., Barber, J., Kühlbrandt, W. **(1998)** Three dimensional structure of the photosystem II reaction centre at 8 Å, *Nature* **396**, 283-286

Richter, G. **(1988)** Stoffwechselphysiologie der Pflanzen, 5. Aufl., *Georg Thieme* Verlag

Rivas, J. D., Balsera, M., Barber, J. **(2004)** Evolution of oxygenic photosynthesis: genome-wide analysis of the OEC extrinsic proteins, *Trends in Plant Science* **9**, 18-25

Schägger H., v. Jagow, G. **(1987)** Tricine sodium dodecyl-sulfate polyacrylamide-gel electrophoresis for the separation of proteins in the range from 1-kDa to 100-kDa, *Analytical Biochemistry* **166 (2)**, 368-379

Schmid, V., Potthast, S., Wiener, M., Bergauer, V., Paulsen, H., Storf, S. **(2002)** Pigment binding of photosystem I light-harvesting proteins, *The Journal of Biological Chemistry* **277 (40)**, 37307-37314

Schönknecht, G., Althoff, G., Junge, W. **(1990)** The electric unit size of thylakoid membranes, *FEBS Letters* **277**, 65-68

Shen, J. R., Kamiya, N. **(2000)** Crystallization and the crystal properties of the oxygen-evolving photosystem II from *Synechococcus vulcanus*, *Biochemistry* **39**, 14739-14744.

Siegbahn, P. **(2002)** Quantum chemical studies of manganese centers in biology, *Current Opinion in Chemical Biology* **6**, 227-235

Shukla, V. K., Stanbekova, G. E., Shestakov, S. V., Pakrasi, H. B. **(1992)** The D1 protein of the photosystem-II reaction-center complex accumulates in the absence of D2 – Analysis of a mutant of the cyanobacterium *Synechocystis* SP PCC-6803 lacking cytochrome b559, *Molecular Microbiology* **6 (7)**, 947-956

Sugiura, M., Inoue, Y., Minagawa, J. **(1998)** Rapid and discrete isolation of oxygen-evolving His-tagged photosystem II core complex from *Chlamydomonas reinhardtii* by Ni^{2+} affinity column chromatography, *FEBS Letters* **426**, 140-144

Suzuki, T., Minagawa, J., Tatsuya, T., Sonoike, K., Ohta, H., Enami, I. **(2003)** Binding and functional properties of the extrinsic proteins in oxygen-evolving photosystem II particle from a green alga, *Chlamydomonas reinhardtii* having His-tagged CP47, *Plant Cell Physiology* **44 (1)**, 76-84

Svensson, B., Etchebest, C., Tuffery, P., van Kan, P., Smith, J., Styring, S. **(1996)** A model for the photosystem II reaction center core including the structure of the primary donor P_{680}, *Biochemistry* **35**, 14486-14502

Taiz, L. & Zeiger, E. **(2002)** Plant Physiology, Third Edition, *Sinauer Associates*, Inc.

Thompson, L. K., Brudvig, G. W. **(1988)** Cytochrome b-559 may function to protect photosystem II from photoinhibition, *Biochemistry* **27**, 6653-6658

Tommos, C., Babcock, G. **(2000)** Proton and hydrogen currents in photosynthetic water oxidation, *Biochimica et Biophysica Acta – Bioenergetics* **1458**, 199-219

van Amerongen, H., van Grondelle, R. **(2001)** Understanding the energy transfer function of LHCII, the major light-harvesting complex of green plants, *The Journal of Physical Chemistry B* **105**, 604-617

van den Hoek, C., Jahns, H. M., Mann, D. G. **(1993)** Algen, *Georg Thieme* Verlag, New York

van Stokkum, I. H. M., Larsen, D. S., van Grondelle, R. **(2004a)** Global and target analysis of time resolved spectra, *Biochimica et Biophysica Acta* **1657**, 82-104

van Stokkum, I. H. M., Larsen, D. S., van Grondelle, R. **(2004b)** Erratum to: Global and target analysis of time resolved spectra, *Biochimica et Biophysica Acta* **1658**, 82-104

Voet, D., Voet J. G. **(1995)** Biochemistry, Second Edition, *John Wiley & Sons*, Inc.

Wang, J. H. **(1969)** Synthesis of a model system for the primary energy conversion reactions in photosynthesis, *Proc. Natl. Acad. Sci. USA* **62 (3)**, 653-660

Wild, A., Höpfner, M., Rühle, W., Richter, M. **(1986)** Changes in the stoichiometry of photosystem II components as an adaptive response to high-light and low-light conditions during growth, *Zeitschrift für Naturforschung C* **41 (5-6)**, 597-603

Yang, C., Kosemund, K., Cornet, C., Paulsen, H. **(1999)** Exchange of pigment-binding amino acids in light-harvesting chlorophyll *a*/*b* protein, *Biochemistry* **38**, 16205-16212

Ye, G. N., Daniell, H., Sanford, J. C. **(1990)** Optimization of delivery of foreign DNA into higher-plant chloroplasts, *Plant Molecular Biology* **15 (6)**, 809-819

Zigmantas, D., Hiller, R. G., Sundström, V., Polívka, T. **(2002)** Carotenoid to chlorophyll energy transfer in the peridinin-chlorophyll-a-protein complex involves an intramolecular charge transfer state, *Proc. Natl. Acad. Sci. USA* **99 (26)**, 16760-16765

Zigmantas, D., Hiller, R. G., Sharples, F. P., Frank, H. A., Sundström, V., Polívka, T. **(2004)** Effect of a conjugated carbonyl group on the photophysical properties of carotenoids, *Phys. Chem. Chem. Phys.* **6**, 3009-3016

Zouni, A., Witt, H. T., Kern, J., Fromme, P., Krauss, N., Saenger, W., Orth, P. **(2001)** Crystal structure of photosystem II from *Synechococcus elongatus* at 3.8 angstrom resolution, *Nature* **409**, 739-743

VIII. Appendix

1. Equipment and chemicals

1.1 Equipment

- *Minispin* table top centrifuge, Eppendorf, Hamburg (Germany)
- *ZK401* centrifuge with *A8.24* (8 x 50 ml) and *AS4.13* (6 x 250 ml) rotors, Hermle, Wehingen (Germany)
- *Biofuge fresco* table top centrifuge, Heraeus, Hanau (Germany)
- *Biofuge primo R*, Heraeus, Hanau (Germany)
- Sorvall *Discovery 90 SE* ultra centrifuge with Sorvall *AH-629* rotor
- Heidolph magnetic stirrer *MR 80*, Labotec, Wiesbaden (Germany)
- Heidolph vortexer *Reax 1DR*, Labotec, Wiesbaden (Germany)
- Pharmacia *LKB pump 1* peristaltic pump, Pfizer Pharma (Germany)
- Pharmacia *Frac-100* fraction collector, Pfizer Pharma (Germany)
- Pharmacia Biotech *Ultrospec 4000* UV/visible spectrophotometer, Pfizer Pharma (Germany)
- *Mighty Small* SE245 gel casting system (0.75 mm, 2 gels), Hoefer Scientific Instruments, San Francisco, CA (USA)
- *Trans-Blot SD* semi dry transfer cell, Bio-Rad, Hercules, CA (USA)
- *Desatronic 3x500/100* power supply, Desaga, Heidelberg (Germany)
- Blender, Waring, New Hartford, Conn. (USA)
- Savant SpeedVac concentrator
- Cell Disrupter, Constant Cell Systems, Daventry, Northants (UK)
- Multiporator, Eppendorf, Hamburg (Germany)
- Mini-PAM, Walz Mess- und Regeltechnik, Effeltrich (Germany)

- Oxygen electrode setup: *Perkeo Soft* slide projector, Zeiss Ikon, Oberkochen (Germany); *Servogor 310* recorder, BBC Goerz, Nürnberg (Germany); Bachofer control unit and measuring cell, Reutlingen (Germany)
- EM setup: *Auto 306 Turbo* carbon evaporator, Edwards High Vacuum (UK); *CM12 transmission electron microscope*, Philips, Eindhoven (The Netherlands); *CCD camera*, Gatan GmbH, München (Germany); *EM Copper grids (3.05 mm/400 mesh)*, Plano, Wetzlar (Germany); *Mica (75 x 25 mm)*, Plano, Wetzlar (Germany)

1.2 Chemicals

Acetic acid	Merck, Darmstadt (Germany)
Acetone, HPLC grade	Merck, Darmstadt (Germany)
Agar (M1002)	Duchefa (The Netherlands)
Agarose	Carl Roth, Karlsruhe (Germany)
$AgNO_3$	Carl Roth, Karlsruhe (Germany)
Ammoniumpersulfat	Serva, Heidelberg (Germany)
Ampicillin	Sigma-Aldrich, St. Louis, MO (USA)
Ascorbic acid	Merck, Darmstadt (Germany)
BAP (6-Benzylaminopurine)	Carl Roth, Karlsruhe (Germany)
Boric acid	Serva, Heidelberg (Germany)
Bromphenole blue	Merck, Darmstadt (Germany)
BSA (Bovine serum albumin)	Carl Roth, Karlsruhe (Germany)
Butylated hydroxytoluene (BHT)	Carl Roth, Karlsruhe (Germany)
$CaCl_2$ x 2 H_2O	Merck, Darmstadt (Germany)
Chlorophyll *a*	provided by S. Hobe, Mainz (Germany)
Chlorophyll *c*	DHI Water and Environment (Denmark)
$CoCl_2$ x 6 H_2O	Carl Roth, Karlsruhe (Germany)
Coomassie Brilliant Blue G-250	Serva, Heidelberg (Germany)
p-Coumaric acid	Fluka, Buchs (Switzerland)

$CuSO_4$ x 5 H_2O	Merck, Darmstadt (Germany)
Diadinoxanthin	DHI Water and Environment (Denmark)
DCBQ (2,6-Dichloro-p-benzoquinone)	Sigma-Aldrich, St. Louis, MO (USA)
o-Dianisidin	Sigma-Aldrich, St. Louis, MO (USA)
2,4-D (2,4-Dichlorophenoxyacetic acid)	Merck, Darmstadt (Germany)
Dimethylsulfoxid (DMSO)	Carl Roth, Karlsruhe (Germany)
β-dodecylmaltoside (DDM)	Glycon, Luckenwalde (Germany)
Ethylenediaminetetraacetic acid (EDTA)	Merck, Darmstadt (Germany)
Ethanol	Carl Roth, Karlsruhe (Germany)
Ethidium bromide	Sigma-Aldrich, St. Louis, MO (USA)
FeNaEDTA (E6760)	Sigma-Aldrich, St. Louis, MO (USA)
Fucoxanthin	DHI Water and Environment (Denmark)
GFX PCR DNA & Gel Band Purification Kit	Amersham-Biosciences, Freiburg (Germany)
Gibberellic acid (GA3)	Carl Roth, Karlsruhe (Germany)
Glucose	Carl Roth, Karlsruhe (Germany)
Glycerol	Carl Roth, Karlsruhe (Germany)
Glycine	Carl Roth, Karlsruhe (Germany)
Gold particles (0.6 μm)	Bio-Rad, Hercules, CA (USA)
H_2O_2	Carl Roth, Karlsruhe (Germany)
HCl	JTBaker, Deventer (The Netherlands)
HEPES (N-(2-hydroxyethyl)piperazine-N'-(2-ethanesulfonic acid))	Carl Roth, Karlsruhe (Germany)
n-heptyl-β-D-thioglucoside (HTG)	Sigma-Aldrich, St. Louis, MO (USA)
Hygromycin B	Carl Roth, Karlsruhe (Germany)
Imidazole	Carl Roth, Karlsruhe (Germany)
Indole-3-acetic acid (IAA)	Carl Roth, Karlsruhe (Germany)
Isopropanol	Riedel-de Haën, Hannover (Germany)
Kanamycin	Sigma-Aldrich, St. Louis, MO (USA)
KCl	Carl Roth, Karlsruhe (Germany)

$K_3[Fe(CN)_6]$	Merck, Darmstadt (Germany)
KH_2PO_4	Carl Roth, Karlsruhe (Germany)
KJ	Carl Roth, Karlsruhe (Germany)
KNO_3	Carl Roth, Karlsruhe (Germany)
LB-Medium	Carl Roth, Karlsruhe (Germany)
LB-Agar	Carl Roth, Karlsruhe (Germany)
Luminol	Fluka, Buchs (Switzerland)
Lysozyme	Carl Roth, Karlsruhe (Germany)
β-mercaptoethanol	Carl Roth, Karlsruhe (Germany)
MES (2-[N-Morpholino]ethanesulfonic acid)	Sigma-Aldrich, St. Louis, MO (USA)
Methanol, HPLC grade	Carl Roth, Karlsruhe (Germany)
$MgCl_2$ x 6 H_2O	Carl Roth, Karlsruhe (Germany)
$MgSO_4$ x 7 H_2O	Carl Roth, Karlsruhe (Germany)
Milk powder	Carl Roth, Karlsruhe (Germany)
$MnSO_4$ x 1 H_2O	Carl Roth, Karlsruhe (Germany)
Na_2HPO_4 7x H_2O	Carl Roth, Karlsruhe (Germany)
Na_2MoO_4 x 2 H_2O	Carl Roth, Karlsruhe (Germany)
NaCl	Carl Roth, Karlsruhe (Germany)
NaOH	Carl Roth, Karlsruhe (Germany)
NH_4NO_3	Merck, Darmstadt (Germany)
$NiCl_2$	Merck, Darmstadt (Germany)
Nicotinic acid	Merck, Darmstadt (Germany)
Potassium acetate	Carl Roth, Karlsruhe (Germany)
Pyridoxine•HCl	Carl Roth, Karlsruhe (Germany)
Midiprep Plasmid DNA purification Kit	QIAgen, Hilden (Germany)
PCR product purification Kit	QIAgen, Hilden (Germany)
Miniprep Plasmid DNA purification Kit	QIAgen, Hilden (Germany)
RNase A	Sigma-Aldrich, St. Louis, MO (USA)
Rotiphorese 40 (40 %)	Carl Roth, Karlsruhe (Germany)
Rotiphorese Gel B (2 %)	Carl Roth, Karlsruhe (Germany)
Sodium acetate x 3 H_2O	Carl Roth, Karlsruhe (Germany)
Sodium azide	Merck, Darmstadt (Germany)

Sodium dodecylsulphate (SDS)	Carl Roth, Karlsruhe (Germany)
Spectinomycin	Sigma-Aldrich, St. Louis, MO (USA)
Streptomycin	Sigma-Aldrich, St. Louis, MO (USA)
TEMED (Tetramethylethylenediamine)	Carl Roth, Karlsruhe (Germany)
Thiamine•HCl	Carl Roth, Karlsruhe (Germany)
Tricine	Carl Roth, Karlsruhe (Germany)
Tris	Carl Roth, Karlsruhe (Germany)
Tryptone	Carl Roth, Karlsruhe (Germany)
Uranyl acetate	Riedel-de Haën, Hannover (Germany)
Urea	Carl Roth, Karlsruhe (Germany)
Xylene cyanol	Carl Roth, Karlsruhe (Germany)
Yeast extract	Carl Roth, Karlsruhe (Germany)
$ZnSO_4$ x 7 H_2O	Carl Roth, Karlsruhe (Germany)

Liquid fertiliser Wuxal Top N:

Substance	Weight proportion (g/kg)	Volume proportion (g/l)
N	120	140
P_2O_5	40	45
K_2O	60	70
B (boron)	0.1	0.11
Cu	0.07	0.08
Fe	0.15	0.18
Mn	0.13	0.15
Mo	0.01	0.011
Zn	0.05	0.055

Cu, Fe, Mn and Zn fully chelated by EDTA

2. Sequences

Colour code and abbreviations:

GTCGAC SalI recognition site

ActagT SpeI recognition site

Gagctc SacI recognition site (starting point of forward primers (EH1 – EH4))

Accggt AgeI recognition site

Aagattctcttagctcattcgg complementary to reverse primer (P7652)

ATG – Start codon

CAT/CAC – His codons

ATT GAT GGA CGA – Factor Xa cleavage site (= Ile-Asp-Gly-Arg)

2.1 pbKS+SacI-psbE-His$_6$NC (EH1)

The following is the sequence of the antisense strand, reading 5' to 3'. Lower case: flanking region, upper case: *psbE* coding sequence, lower case: flanking region

ActagTaatttctattaggttccacattttatctttccctactgccccatccttgtagctagatcaagaa
agaacctttggatcgagatccacaacaatgcatcacaactatggattccaattattcgatttttctttc
ctcgaatatgatctactactcttatttcttactcgaccattaacttcttctttaaaaaaaggattccaac
aacaaaactgcttccacaactacgaaaagcaaatttctatatctcgcatctacttaaattgtgtgaatat
gagaatctctttcgttgaattgaaagaattttctattgaatggaagatgattttacatcaacaagtaaag
gaaaaaagaaattatttagtacttacttttgatactatttcaaattgcgttgctgtgtcagaagaaggat
agctatactgattcggtatactctaaagacgccttcggtacaatattgacgatctcacaaagatgaaatt
tcagtgaattgtcatttactgatctcatcttttacggaatcgatcttctttgactgtacaagaatatgtg
gagctCAGCATGCATCATCACCATCACCATTCTGGAAGCACAGGAGAACGTTCGTTTGCTGATATTATTA
CCAGTATTCGATACTGGGTCATTCATAGCATTACTATACCTTCCCTATTCATTGCGGGTTGGTTATTTGT
CAGCAccggttagcttacgatgtgtttggaagccctcggccaaacgagtattttacagagagccgacaa
ggaattccattaataactggccgttttgatcctttggaacaactcgatgaatttagtagatcgttttagg
aggccctaatgactatagatcgaacctatccaatttttacagtacgatggttggctgttcacggcctagc
tgtacctaccgtctttttttttgggatcaatatcagcaatgcagttcatccaacgataaacttaatccgaa
ttatagagctacgacacaatcaaacccgaacgaacaaaatgttgaattgaatcgtaccagtctctactgg
gggttattactcatttttgtacttgctgttttatttccaattatttcttcaattaagaaaacgaaagag
aatcaatAAGATTCTCTTAGCTCATTCGGaaggatctcataatttaattatccatgactgtttatgtctc
tagcatgaccacttgatgaaatctggagggaagtggggtaaatggccgatactactggaaggattcctct
ttggataataggtactgtagctggtattcttgtaatcggtttaataggtattttcttttatggttcatat
tccggattgggttcatccctctagtaatcgaatgaattgagtcgtcaacatgaaagcgtaagaactcaac
ggaattcccttctttgtttgtttgattcgaaggggaagggcccgttgagttcttaagaatcataatattt
ttttcgtctaaatgataaaatggatttctttttctttttcaaaaactccatttttctcatttttctgatca
tgtttttgaaaaattcactattcggaccacctcttctttttctatgatagtatctatcggtactttcaaa
gttggaagaaagaaggaatcactcaatttcttggctgctataatatattagatatcgtgcaaatcctttc
tatactaatctaatgtagaaccttactctctctattacattactctatttatttttttattgttttcatat
ttcatcatcaaattttgtataagataagttgattgaagaagttttatttaattaataaaatttcctctct
ttttttgttttgtttgtccaccacttagtatattatacgtaaaggggtgggggtaaggtaaagggtttc
tgatacatctggaaaaatcgaaaccaagactaggaatttttaacaaacaggatcaagaatcattactctt
tcgtttcgacacaagaaaaaaggatttttctacacccctttcttgtgtcgaagactaggaagacaaataa
tccctcctagaatttttgttccccgcatttatcccctgcttccttatgtctagtatttagacaaatttg
actttctttctatttagaatagaaaactattgatacgtcttatggcattgaaatctgtcaatagtaacat
agtcacactactccaattttaaaaaacgaaataaaaataatgaaagtcaaatactcttcttcaaattcta
cattacatactctttttctacgagatgctgggaatcccttgtaccacatagtatgtagattttgaagaag
agtataaataagacaaaggagttttcagaatttcatttttttgatcataaataatcgccaacaagaattt
ggttctttttacgaacttgatgTCGAC

2.2 pbKS+SacI⁻psbE-His$_{10}$NC (EH2)

The following is the sequence of the antisense strand, reading 5' to 3'. Lower case: flanking region, upper case: *psbE* coding sequence, lower case: flanking region

ActagTaatttctattaggttccacattttatctttccctactgccccatccttgtagctagatcaagaa
agaacctttggatcgagatccacaacaatgcatcacaactatggattccaattattcgatttttctttc
ctcgaatatgatctactactcttatttcttactcgaccattaacttcttctttaaaaaaaggattccaac
aacaaaactgcttccacaactacgaaaagcaaatttctatatctcgcatctacttaaattgtgtgaatat
gagaatctctttcgttgaattgaaagaattttctattgaatggaagatgattttacatcaacaagtaaag
gaaaaaagaaattatttagtacttacttttgatactatttcaaattgcgttgctgtgtcagaagaaggat
agctatactgattcggtatactctaaagacgccttcggtacaatattgacgatctcacaaagatgaaatt
tcagtgaattgtcatttactgatctcatctttacggaatcgatcttctttgactgtacaagaatatgtg
gagctCAGCATGCATCATCACCATCACCATCACCATCACCATTCTGGAAGCACAGGAGAACGTTCGTTTG
CTGATATTATTACCAGTATTCGATACTGGGTCATTCATAGCATTACTATACCTTCCCTATTCATTGCGGG
TTGGTTATTTGTCAGCAccggttagcttacgatgtgtttggaagccctcggccaaacgagtattttaca
gagagccgacaaggaattccattaataactggccgttttgatcctttggaacaactcgatgaatttagta
gatcgttttaggaggccctaatgactatagatcgaacctatccaatttttacagtacgatggttggctgt
tcacggcctagctgtacctaccgtctttttttgggatcaatatcagcaatgcagttcatccaacgataa
acttaatccgaattatagagctacgacacaatcaaacccgaacgaacaaaatgttgaattgaatcgtacc
agtctctactgggggttattactcatttttgtacttgctgttttatttccaattatttcttcaattaag
aaaacgaaagagaatcaatAAGATTCTCTTAGCTCATTCGGaaggatctcataatttaattatccatgac
tgtttatgtctctagcatgaccacttgatgaaatctggagggaagtggggtaaatggccgatactactgg
aaggattcctctttggataataggtactgtagctggtattcttgtaatcggtttataggtattttcttt
tatggttcatattccggattgggttcatccctctagtaatcgaatgaattgagtcgtcaacatgaaagcg
taagaactcaacggaattcccttctttgtttgtttgattcgaaggggaagggcccgttgagttcttaaga
atcataatatttttttcgtctaaatgataaaatggatttctttttctttttcaaaaactccatttttctca
tttttctgatcatgtttttgaaaaattcactattcggaccacctcttctttttctatgatagtatctatc
ggtactttcaaagttggaagaaagaaggaatcactcaatttcttggctgctataatatattagatatcgt
gcaaatcctttctatactaatctaatgtagaaccttactctctctattacattactctatttatttttta
ttgttttcatatttcatcatcaaatttgtataagataagttgattgaagaagttttatttaattaataa
aatttcctctctttttttgttttgtttgtccaccacttagtatattatacgtaaaggggtgggggtaag
gtaaagggtttctgatacatctggaaaaatcgaaaccaagactaggaatttttaacaaacaggatcaaga
atcattactctttcgtttcgacacaagaaaaaaggatttttctacacccctttcttgtgtcgaagactag
gaagacaaataatccctcctagaatttttgttccccgcatttatcccctgcttccttatgtctagtatt
tagacaaatttgactttctttctatttagaatagaaaactattgatacgtcttatggcattgaaatctgt
caatagtaacatagtcacactactccaattttaaaaaacgaaataaaaataatgaaagtcaaatactctt
cttcaaattctacattacatactctttttctacgagatgctgggaatcccttgtaccacatagtatgtag
attttgaagaagagtataaataagacaaaggagttttcagaatttcatttttttgatcataaataatcgc
caacaagaatttggttctttttacgaacttgatgTCGAC

2.3 pbKS+SacI⁻psbE-His$_6$C (EH3)

The following is the sequence of the antisense strand, reading 5' to 3'. Lower case: flanking region, upper case: *psbE* coding sequence, lower case: flanking region

ActagTaatttctattaggttccacattttatctttccctactgccccatccttgtagctagatcaagaa
agaacctttggatcgagatccacaacaatgcatcacaactatggattccaattattcgatttttctttc
ctcgaatatgatctactactcttatttcttactcgaccattaacttcttctttaaaaaaaggattccaac
aacaaaactgcttccacaactacgaaaagcaaatttctatatctcgcatctacttaaattgtgtgaatat
gagaatctctttcgttgaattgaaagaattttctattgaatggaagatgattttacatcaacaagtaaag
gaaaaaagaaattatttagtacttacttttgatactatttcaaattgcgttgctgtgtcagaagaaggat
agctatactgattcggtatactctaaagacgccttcggtacaatattgacgatctcacaaagatgaaatt
tcagtgaattgtcatttactgatctcatctttacggaatcgatcttctttgactgtacaagaatatgtg
gagctCAGCATGCATCATCACCATCACCATATTGATGGACGATCTGGAAGCACAGGAGAACGTTCGTTTG
CTGATATTATTACCAGTATTCGATACTGGGTCATTCATAGCATTACTATACCTTCCCTATTCATTGCGGG
TTGGTTATTTGTCAGCAccggttagcttacgatgtgtttggaagccctcggccaaacgagtattttaca
gagagccgacaaggaattccattaataactggccgttttgatcctttggaacaactcgatgaatttagta
gatcgttttaggaggccctaatgactatagatcgaacctatccaatttttacagtacgatggttggctgt
tcacggcctagctgtacctaccgtctttttttgggatcaatatcagcaatgcagttcatccaacgataa
acttaatccgaattatagagctacgacacaatcaaacccgaacgaacaaaatgttgaattgaatcgtacc
agtctctactgggggttattactcatttttgtacttgctgttttatttccaattatttcttcaattaag
aaaacgaaagagaatcaatAAGATTCTCTTAGCTCATTCGGaaggatctcataatttaattatccatgac
tgtttatgtctctagcatgaccacttgatgaaatctggagggaagtggggtaaatggccgatactactgg
aaggattcctctttggataataggtactgtagctggtattcttgtaatcggtttataggtattttcttt
tatggttcatattccggattgggttcatccctctagtaatcgaatgaattgagtcgtcaacatgaaagcg
taagaactcaacggaattcccttctttgtttgtttgattcgaaggggaagggcccgttgagttcttaaga
atcataatatttttttcgtctaaatgataaaatggatttctttttctttttcaaaaactccatttttctca
tttttctgatcatgtttttgaaaaattcactattcggaccacctcttctttttctatgatagtatctatc
ggtactttcaaagttggaagaaagaaggaatcactcaatttcttggctgctataatatattagatatcgt
gcaaatcctttctatactaatctaatgtagaaccttactctctctattacattactctatttatttttta
ttgttttcatatttcatcatcaaattttgtataagataagttgattgaagaagttttatttaattaataa
aatttcctctctttttttgttttgtttgtccaccacttagtatattatacgtaaaggggtgggggtaag
gtaaagggtttctgatacatctggaaaaatcgaaaccaagactaggaatttttaacaaacaggatcaaga
atcattactctttcgtttcgacacaagaaaaaaggatttttctacacccctttcttgtgtcgaagactag
gaagacaaataatccctcctagaatttttgttccccgcatttatcccctgcttccttatgtctagtatt
tagacaaatttgactttctttctatttagaatagaaaactattgatacgtcttatggcattgaaatctgt
caatagtaacatagtcacactactccaattttaaaaaacgaaataaaaataatgaaagtcaaatactctt
cttcaaattctacattacatactctttttctacgagatgctgggaatcccttgtaccacatagtatgtag
attttgaagaagagtataaataagacaaaggagttttcagaatttcatttttttgatcataaataatcgc
caacaagaatttggttctttttacgaacttgatgTCGAC

2.4 pbKS+SacI-psbE-His$_{10}$C (EH4)

The following is the sequence of the antisense strand, reading 5' to 3'. Lower case: flanking region, upper case: *psbE* coding sequence, lower case: flanking region

ActagTaatttctattaggttccacattttatctttccctactgccccatccttgtagctagatcaagaa
agaacctttggatcgagatccacaacaatgcatcacaactatggattccaattattcgatttttctttc
ctcgaatatgatctactactcttatttcttactcgaccattaacttcttctttaaaaaaaggattccaac
aacaaaactgcttccacaactacgaaaagcaaatttctatatctcgcatctacttaaattgtgtgaatat
gagaatctctttcgttgaattgaaagaattttctattgaatggaagatgattttacatcaacaagtaaag
gaaaaaagaaattatttagtacttacttttgatactatttcaaattgcgttgctgtgtcagaagaaggat
agctatactgattcggtatactctaaagacgccttcggtacaatattgacgatctcacaaagatgaaatt
tcagtgaattgtcatttactgatctcatctttacggaatcgatcttctttgactgtacaagaatatgtg
gagctCAGCATGCATCATCACCATCACCATCACCATCACCATATTGATGGACGATCTGGAAGCACAGGAG
AACGTTCGTTTGCTGATATTATTACCAGTATTCGATACTGGGTCATTCATAGCATTACTATACCTTCCCT
ATTCATTGCGGGTTGGTTATTTGTCAGCAccggttagcttacgatgtgtttggaagccctcggccaaac
gagtattttacagagagccgacaaggaattccattaataactggccgttttgatcctttggaacaactcg
atgaatttagtagatcgttttaggaggccctaatgactatagatcgaacctatccaatttttacagtacg
atggttggctgttcacggcctagctgtacctaccgtctttttttgggatcaatatcagcaatgcagttc
atccaacgataaacttaatccgaattatagagctacgacacaatcaaacccgaacgaacaaaatgttgaa
ttgaatcgtaccagtctctactgggggttattactcatttttgtacttgctgttttatttccaattatt
tcttcaattaagaaaacgaaagagaatcaatAAGATTCTCTTAGCTCATTCGGaaggatctcataattta
attatccatgactgtttatgtctctagcatgaccacttgatgaaatctggagggaagtggggtaaatggc
cgatactactggaaggattcctctttggataataggtactgtagctggtattcttgtaatcggtttaata
ggtattttcttttatggttcatattccggattgggttcatccctctagtaatcgaatgaattgagtcgtc
aacatgaaagcgtaagaactcaacggaattcccttctttgtttgtttgattcgaaggggaagggcccgtt
gagttcttaagaatcataatatttttttcgtctaaatgataaaatggatttctttttctttttcaaaaact
ccatttttctcatttttctgatcatgtttttgaaaaattcactattcggaccacctcttctttttctatg
atagtatctatcggtactttcaaagttggaagaaagaaggaatcactcaatttcttggctgctataatat
attagatatcgtgcaaatcctttctatactaatctaatgtagaaccttactctctctattacattactct
atttatttttattgttttcatatttcatcatcaaattttgtataagataagttgattgaagaagtttta
tttaattaataaaatttcctctctttttttgttttgtttgtccaccacttagtatattatacgtaaaggg
ggtgggggtaaggtaaagggtttctgatacatctggaaaaatcgaaaccaagactaggaatttttaacaa
acaggatcaagaatcattactctttcgtttcgacacaagaaaaaaggatttttctacacccctttcttgt
gtcgaagactaggaagacaaataatccctcctagaatttttgttccccgcatttatcccctgcttcctt
atgtctagtatttagacaaatttgactttctttctatttagaatagaaaactattgatacgtcttatggc
attgaaatctgtcaatagtaacatagtcacactactccaatttaaaaaacgaaataaaaataatgaaag
tcaaatactcttcttcaaattctacattacatactctttttctacgagatgctgggaatcccttgtacca
catagtatgtagattttgaagaagagtataaataagacaaaggagttttcagaatttcatttttttgatc
ataaataatcgccaacaagaatttggttctttttacgaacttgatgTCGAC

3. HPLC parameters

3.1 HPLC retention times

	main peak		side peak	
	start	end	start	end
Chlorophyll *c*	13.3 ± 0.2	16.2 ± 0.2	na	na
Fucoxanthin	17.2 ±0.6	17.8 ± 0.6	18.3 ± 0.5	19.0 ± 0.5
Diadinoxanthin	18.9 ± 0.3	19.5 ± 0.1	19.5 ± 0.1	20.0 ± 0.1
Chlorophyll *a*	22.5 ± 0.2	23.0 ± 0.2	23.0 ± 0.2	23.3 ± 0.2

Tab. VIII.1: HPLC retention times of FCP pigments in minutes

3.2 HPLC calibration factors and calibration limits

		Calibration factor	
	Wavelength	for ng/µL	for pmol/µL
Chlorophyll *c*	450 nm	$4.49479 * 10^{-6}$	$7.38109 * 10^{-6}$
Fucoxanthin	445 nm	$7.72738 * 10^{-6}$	$1.17273 * 10^{-5}$
Diadinoxanthin	445 nm	$5.34131 * 10^{-6}$	$9.16381 * 10^{-6}$
Chlorophyll *a*	432 nm	$1.36277 * 10^{-5}$	$1.52517 * 10^{-5}$

Tab. VIII.2: HPLC calibration factors

	Calibration limits		
	[ng/µL]	[pmol/µL]	[ng per run]
Chlorophyll *c*	0.21 -> 5.50	0.35 -> 9.03	4.25 -> 109.95
Fucoxanthin	0.21 -> 3.87	0.32 -> 5.87	4.2 -> 77.4
Diadinoxanthin	0.41 -> 9.00	0.70 -> 15.44	8.16 -> 179.96
Chlorophyll *a*	2.01 -> 39.11	2.24 -> 43.77	40.11 -> 782.18

Tab. VIII.3: HPLC calibration limits

3.3 Spectral data of FCP pigments

	Solvent	Wavelength	Extinction coeff.	Mol. Mass
Chlorophyll *c*	90% acetone	444 nm	374.00 $lg^{-1}cm^{-1}$	608.96 g/mol
Fucoxanthin	100% acetone	448 nm	166.00 $lg^{-1}cm^{-1}$	658.92 g/mol
Diadinoxanthin	100% acetone	448 nm	223.00 $lg^{-1}cm^{-1}$	582.87 g/mol
Chlorophyll *a*	80% acetone	431 nm	95.82 $lg^{-1}cm^{-1}$	893.52 g/mol

Tab. VIII.4: Extinction coefficients (ε) of pigments in the respective solvent, which were used for HPLC calibration. (Lichtenthaler, 1987; Jeffrey, 1972; Haugan, *et al.*, 1992; Johansen *et al.*, 1974)

3.4 Spectra of FCP pigments

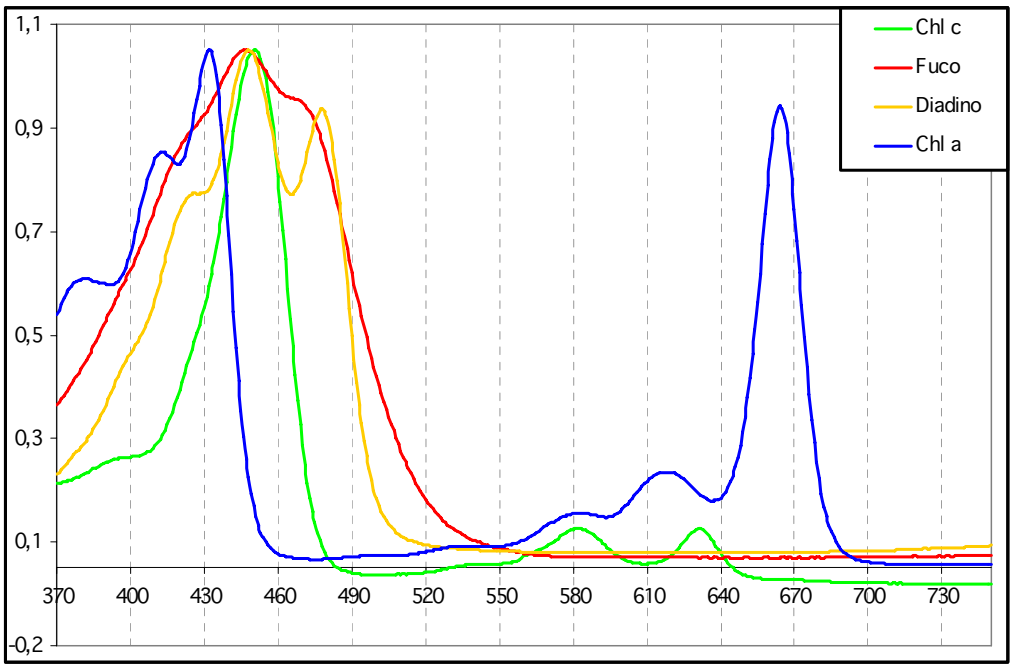

Fig. VIII.1: Normalised spectra of FCP pigments in organic solvents

Publications

Diploma thesis:

Fey, H. **(2001)** Klassifizierung von Chlorophyll-Bindungsstellen des rekombinanten Lichtsammlerkomplexes LHCII hinsichtlich ihrer Affinitäten gegenüber Chlorophyll *a* und Chlorophyll *b*, *Johannes-Gutenberg-Universität*, Mainz

Articles:

Hobe, S., Fey, H., Rogl, H., Paulsen, H. **(2003)** Determination of relative chlorophyll binding affinities in the major light-harvesting chlorophyll *a*/*b* complex, *The Journal of Biological Chemistry* **278 (8)**, 5912-5919

Papagiannakis, E., van Stokkum, I. H. M., Fey, H., Büchel, C., van Grondelle, R. **(2005)** Spectroscopic characterization of the excitation energy transfer in the fucoxanthin-chlorophyll protein of diatoms, *Photosynthesis Research* **86**, 241-250

Poster:

Hobe, S., Fey, H., Rogl, H., Paulsen, H. **(2002)** Chlorophyll binding sites in the major light-harvesting chlorophyll *a*/*b* complex (LHCIIb) exhibit differential affinities towards chlorophylls *a* and *b*, *Tagung der Deutschen Botanischen Gesellschaft*, Freiburg

Fey, H., Hermann, M., Bock, R., Büchel, C. **(2005)** His-tagging cytochrome b_{559}, a subunit of photosystem II, *18. Tagung Molekularbiologie der Pflanzen*, Dabringhausen

Lebenslauf (Curriculum vitae)

Persönliche Daten

Holger Fey, geboren am 30.03.1974 in Pirmasens
ledig
Fischerstr. 10, 67069 Ludwigshafen am Rhein
0177 / 689 41 44
fey_holger@web.de

Schulische Ausbildung

08/1980 – 07/1984	Bärenbach Grundschule, *Stadtallendorf*
08/1984 – 11/1985	Stiftsschule St. Johann, *Amöneburg*
12/1985 – 06/1993	Theodor-Heuss-Gymnasium, *Ludwigshafen / Rhein*

Zivildienst

10/1993 – 06/1994	Naturfreundehaus Rahnenhof, *Hertlingshausen*
06/1994 – 12/1994	Sonderkindergarten des Zweckverbandes Kinderzentrum *Ludwigshafen / Rhein*

Studium

04/1995 – 01/2001	Studium der Biologie mit Abschluss Diplom Diplomarbeit bei Prof. H. Paulsen *Institut für Allgemeine Botanik* *Johannes-Gutenberg-Universität, Mainz*

Promotion

10/2001 – 12/2004	Wissenschaftlicher Mitarbeiter bei PD Dr. habil. C. Büchel *Abteilung für Strukturbiologie* *Max-Planck-Institut für Biophysik, Frankfurt / Main*
01/2005 – 06/2006	Wissenschaftlicher Mitarbeiter bei Prof. C. Büchel *Institut für Molekulare Biowissenschaften* *Johann-Wolfgang-Goethe Universität*, *Frankfurt / Main*

Berufserfahrung

09/1996 – 09/2001	Bühnenhilfskraft, *Theater im Pfalzbau, Ludwigshafen / Rhein*
05/2000 – 07/2000	Wissenschaftliche Hilfskraft, *Johannes-Gutenberg-Universität, Mainz*
03/2001 – 09/2001	Studentische Hilfskraft im DNA-Labor, *ID-Labor GmbH, Wiesbaden*

Acknowledgements

First and foremost I want to thank Prof. Claudia Büchel, not only for giving me the opportunity to do my PhD-work in her group, but also for the excellent support at all stages of my thesis. Without her knowledge, encouragement and supervision this thesis would never have developed into what it is now.

I also want to thank Prof. Gerhard Sandmann for accepting to review this thesis on such short notice.

Furthermore, I wish to express my gratitude to Prof. Ralph Bock and his co-workers Marita Hermann and Stephanie Ruf for the great collaboration on the tobacco chloroplast transformation project.

I'm also greatly indebted to Kerstin Pieper, Christel van Oijen and Matthias Schmidt for keeping everything up and running and well organised, especially during the times of refurbishment of the lab. And, who knows, maybe one of these days Kerstin will really get her cake…

Of course, I also need to mention my office colleagues Anja, Tom and Dario here, who were responsible for a great deal of rarely unwelcome diversions from work and who always bore the musical torment I inflicted upon them with a smile. Mille grazie, Dario, your mouse…eh YOU were a great help in finishing my thesis!

Naturally, I also want to thank the remaining people of the group – Regina, Kathi, Simone, Nadine, Gudrun, Marion, Janet and Zena - for creating such a nice and enjoyable atmosphere for working and beyond.

Last and definitely not least, my gratitude goes to my family and friends for backing me at all possible turns of my PhD time and helping me to clear my vision at regular intervals in order to focus on the really important things. Above all, I want to thank Nathalie, who had the enormous patience to put up with my evil moods and always found a way to keep me going, when my batteries were empty.

E R K L Ä R U N G

Ich erkläre hiermit, dass ich mich bisher keiner Doktorprüfung unterzogen habe.

Frankfurt am Main, den……

……..
(Unterschrift)

Eidesstattliche Versicherung

Ich erkläre hiermit an Eides Statt, dass ich die vorliegende Dissertation über

……
……
……

selbständig angefertigt und mich anderer Hilfsmittel als der in ihr angegebenen nicht bedient habe, insbesondere, dass aus Schriften Entlehnungen, soweit sie in der Dissertation nicht ausdrücklich als solche mit Angabe der betreffenden Schrift bezeichnet sind, nicht stattgefunden haben.

Frankfurt am Main, den……. ……...
(Unterschrift)